8-8-2014 12:00 AM

Laser-Assisted Surface Modification of Hybrid Hydrogels to Prevent Bacterial Contamination and Protein Fouling

Guobang Huang
The University of Western Ontario

Supervisor
Jin Zhang
The University of Western Ontario

Graduate Program in Chemical and Biochemical Engineering
A thesis submitted in partial fulfillment of the requirements for the degree in Master of Engineering Science

LASER-ASSISTED SURFACE MODIFICATION OF HYBRID HYDROGELS TO PREVENT BACTERIAL CONTAMINATION AND PROTEIN FOULING

(Thesis format: Integrated Article)

by

Guobang Huang

Graduate Program in Engineering Science
Department of Chemical and Biochemical Engineering

A thesis submitted in partial fulfillment
of the requirements for the degree of
Master of Engineering Science

The School of Graduate and Postdoctoral Studies
The University of Western Ontario
London, Ontario, Canada

Abstract

Silicone hydrogels have been extensively studied in the fields of contact lenses, tissue engineering, and drug delivery due to their good biocompatibility, high oxygen permeability, and proper light transmission. However, their applications in biomedical devices are limited by protein adsorption and bacterial contamination because of the hydrophobic surface of silicone, which will cause more irreversible protein adsorption. Several physical methods can be applied to create a hydrophilic surface on hydrogels, such as spin coating, physical vapor deposition, dip coating, drop casting, etc. Compared to the conventional methods, the matrix assisted pulsed laser evaporation (MAPLE) is suitable to produce biopolymer/polymer film with a contamination-free manner. In this thesis, hydrophilic polymer, polyethylene glycol (PEG) and polyvinylpyrrolidone (PVP), were deposited by MAPLE with a pulsed Nd:YAG 532 nm laser for the surface hydrophilicity modification. The polymer coatings were characterized by Fourier transform infrared spectroscopy (FTIR) and atomic force microscopy (AFM). Our results demonstrate that protein adsorption decreases 28.2% and 18.7% with the surface modifications by PEG and PVP, respectively. In addition, the polymer coated silicone hydrogels do not impose toxic effect on mouse NIH/3T3 cells.

Normally, protein fouling can lead to biofilm contamination caused by the growth of bacteria. Therefore, we further deposit hybrid nanocomposite on silicone hydrogels to inhibit the growth of bacteria. Silver nanoparticles incorporating with PVP (Ag-PVP NPs) were developed through a photochemical method without addition of reductive reagents. On the other hand, sol-gel method was applied to incorporate ZnO nanoparticles into PEG (ZnO-PEG NPs). MAPLE process was applied to deposit the two different nanocomposites on the silicone hydrogels, respectively. Our results indicate that the silicone hydrogels with Ag-PVP nanocomposite coating can reduce 28.2% of the protein adsorption compared to silicone hydrogels without coating, while ZnO-PEG coating is able to reduce 30% protein adsorption. The cytotoxicity study shows that the nanocomposite coated silicone hydrogels do not impose toxic effect on mouse NIH/3T3 cells. In addition, MAPLE-deposited Ag-PVP and ZnO-PEG nanocomposite coatings can inhibit bacterial growth significantly. Our result show that Ag-PVP nanocomposite coating can eliminate almost all the *E.coli* after 8 hours' culturing; the relative numbers of *E.coli* on the ZnO-PEG coated silicone hydrogel approach

to zero when the culturing time is 4 hours. In addition, the thickness and roughness of Ag-PVP film over time were measured by AFM. The result shows that MAPLE process is a time dependent (linear) deposition, and it is able to create homogenous thin films (roughness is lower than 30 nm). MAPLE shows good ability to control the thickness in the deposition of organic molecules and nanoparticles, which maintains the chemical backbone of polymers, and prevents contamination.

Keywords

Silicone hydrogel; Polyethylene glycol (PEG); Polyvinylpyrrolidone (PVP); Silver nanoparticles; Zinc oxide nanoparticles; Surface coating; Matrix assisted pulsed laser evaporation (MAPLE); protein adsorption; Antibacterial property.

Co-Authorship Statement

Chapter 1 (Introduction), Chapter 2 (Background and literature review) and Chapter 3 (Experiment Procedures) were written by Guobang Huang with the suggestion of Dr. Jin Zhang. Chapter 4 and 5 include the research studies, which have been published or under preparing. The ZnO-PEG nanoparticles were synthesized under Dr. Yi Chen's help. The experiment work of Ag-PVP nanoparticles were accomplished with the help of Dr. Lingyun Hao. The cytotoxicity test was achieved by Andrew Tse. The other invaluable help for my thesis are named in the acknowledge section.

Acknowledgments

This thesis would not have been written without the help and guidance from several people. I would like to gratefully acknowledge all of them.

I would like to extend my heartfelt appreciation and gratitude to my supervisor Dr. Jin Zhang, for her continuous encouragement, constructive criticism, enthusiastic guidance, support, trust and understanding throughout my program. The encouragement and support she has provided me over the past two years have been and will continue to be fundamental for my development.

I would like to thank my examination committee: Dr. Anand Prakash, Dr. Chunbao Charles Xu and Dr. Clara Wren for their guidance and feedback throughout the course of my project. I would like to thank Dr. Richard Gardiner and Mrs. Nygard Karen in Biotron center for their assistants in using the facilities. I would like to thank Dr. Jun Yang and Dr. Qiuquan Guo for the AFM measurement. Special gratitude is extended to all of my current and previous colleagues at Multifunctional Nanocomposite Lab, Dr. Yi Chen, Andrew Tse, Longyi Chen, Dr. Longyan Chen, Pei Yin, Dr. Yueqi Bi, Dr. Lingyun Hao and Dr. Hong Hai for their continuous support, encouragement, and nice time that we have had together. Finally, I would dearly like to thank my family for the support they provided me through my entire life and in particular, I must acknowledge my wife, Lianlian, without whose love, encouragement and assistance, I would not have finished this thesis.

This work has been supported by funding from Natural Science and Engineering Research Council of Canada (NSERC) through a Discovery Grant and Western Engineering Graduate Scholarship.

Table of Contents

List of Tables

List of Figures

List of Abbreviations

AFM	−	Atomic force microscopy
BSA	−	Bovine serum albumin
CFU	−	Colony forming unit
CVD	−	Chemical vapor deposition
DMA	−	N,N-Dimethylacrylamide
DMSO	−	Dimethyl sulfoxide
E. coli	−	Escherichia coli
EDX	−	Energy-dispersive X-ray spectroscopy
EG	−	Ethylene glycol
EGDMA	−	Ethylene glycol dimethacrylate
MAPLE	−	Matrix assisted pulsed laser evaporation
NPs	−	Nanoparticles
NVP	−	N-vinylpyrolidinone xi
PBS	−	Phosphate buffer saline
PDMS	−	bis-alpha,omega-(methacryloxypropyl) polydimethylsiloxane
PEG	−	Polyethylene glycol
PHEMA	−	2-Hydroxyethyl methacrylate
PLD	−	Pulsed laser deposition

PMMA	−	Polymethylmethacrylate
PVD	−	Physical vapor deposition
PVP	−	Polyvinylpyrrolidone
TEM	−	Transmission electron microscopy
TRIS	−	3-methacryloxypropyl tris (trimethylsiloxy) silane
UV	−	Ultraviolet
XRD	−	X-ray Diffraction

Chapter 1

1 Introduction

1.1 Biocompatible hydrogel

Hydrogels have been one of the best choice materials for biomedical applications because of their unique biocompatibility, large extent on their bulk structure, flexible methods of synthesis, high water content, wide range of constituents, and desirable physical characteristics [1,2]. Hydrogels can be divided into two groups. The first is synthetic hydrogels (PHEMA [3], PEG [4], PVA [5] and silicone [6]), and the second is biological hydrogels (collagen [7], hyaluronic acid (HA) [8], fibrin [9]). Synthetic hydrogels can be synthesized using various chemical methods (such as photo-initiated and thermal-initiated polymerization). Photo-polymerization can minimize the invasive effect during synthesis, which is an important issue for biomedical material. Therefore, a number of hydrogels are free radical photo-polymerized *in vivo* and *in vitro* with the help of photo-initiators under visible or ultraviolet (UV) light [10]. Hydrogels have been extensively used in tissue engineering [11], controlled drug delivery [12], medical and biological sensors [13], and contact lenses [6].

For contact lens, there are several types of hydrogels that have been used in the past fifty years, such as PMMA, PHEMA and silicone hydrogels. For now, PHEMA and silicone are still the most commonly used lens materials. Comparing to PHEMA hydrogels, silicone hydrogels show higher oxygen permeability because of its different oxygen transport mechanism which is transported through siloxane-phase rather than water [14]. Therefore, silicone-based hydrogels have been used for the studies of topical ocular drug delivery and implanting medical devices.

1.2 Challenges of silicone hydrogels used as contact lens material

Silicone hydrogels are polymers consisting of silicon-oxygen bonds (siloxane), which can lead to higher oxygen permeability than other conventional hydrogel [15]. As a result, silicone hydrogel can fulfill the requirements of wearing lenses under open, closed eye

conditions and even long-term [16]. However, silicone hydrogel contains lots of siloxane, which is relatively hydrophobic, and different from amine and hydroxyl groups, which are hydrophilic. Hydrophobic surface will cause irreversible protein adsorption to form protein film, which will cause that microbial colonization and subsequent biofilm formation [17–19]. To be used as implant materials/devices, suitable hydrophilic surface is the key. Consequently, the surface treatment of silicone hydrogels is very important to allow them to be used for biomedical devices, especially for contact lenses.

1.3 Surface modification methods

Surface modification can be divided into physical and chemical methods. Chemical vapor deposition (CVD) [20] and wet chemical methods [21] have been applied for converting hydrophobic surfaces to hydrophilic surfaces by chemically adding suitable functional groups or coatings. Unfortunately, CVD process normally requires the use of toxic, corrosive, flammable and/or explosive precursor gases, and high temperature, which will decompose the structure of biomaterial [22]. Furthermore, wet chemical method introduces additional chemical agents, which normally incur adverse results such as the toxic effects. In addition, chemical methods rely on the use of surface-specific chemistries, which means they are not general and cannot be applied to a wide range of surfaces or substrates [23].

Physical methods have been applied for hydrogel surface modification recently, including spin coating [24], dip coating [25] and physical vapor deposition (PVD) [26]. Although spin coating and dip coating are much more environmentally-friendly compared to chemical methods, they all need to make direct contact with solvents. It is hard to control the thickness of films compared to PVD. PVD can prevent solvent contamination to produce highly pure coating with controllable thickness at atomic level or nanometer level, and it can be divided into four categories such as vacuum evaporation, sputter deposition, arc vapor deposition and ion plating [22,27]. However, traditional PVD method needs high temperature, electron beam or high voltage, which will break the structure of the polymers or nanoparticles. The methods mentioned above have their own advantages and drawbacks, and all can only be applied for specific range of materials. The ability to deposit a wide class of materials and protect the target material structures would be a great advantage for silicone hydrogel surface modification.

Matrix assisted pulsed laser evaporation (MAPLE) is a laser assisted physical vapor deposition technique that derives from the pulsed laser deposition (PLD) [28]. It offers an alternative and proper method to deposit polymer, biomaterial and nanocomposite films onto substrate, especially for fragile compounds such as carbohydrates and biological materials [29]. Actually, MAPLE provides a gentle mechanism to obtain homogeneous films of high molecular weight organic materials whose thickness can be accurately controlled, and also maintain their functions without laser induced damage [30]. Moreover, MAPLE is a non-contact deposition technique, and thus eliminates a major source of contamination and can be integrated with other sterile processes [31].

The mechanism of MAPLE process is shown in Figure 1.1. The target material is diluted into a highly volatile non-interacting light-adsorbing solvent with the weight concentration lower than 5% normally. Liquid nitrogen is used to freeze the target solution to liquid nitrogen temperature. The frozen target is irradiated by pulsed laser beam with fluence of 50-300 mJ/cm^2 under vacuum of $1x10^{-6}$ Torr that was achieved by turbo pump. Each laser pulse produces a plume containing both the volatile solvent and the heavier polymer molecules or nanocomposite. The solvents are pumped away while the polymer or nanocomposite is deposited onto the substrate [30,32,33].

1.4 Desired materials to promote surface property for contact lens

Polyethylene glycol (PEG) based polymers [34], polyvinylpyrrolidone (PVP) [35,36], zwitterionic materials [37], carbohydrates [38] and peptide-like polymers [39] are able to provide a hydrophilic surface, as a result they are commonly used to modify biomaterials' surface to obtain a protein resistance surface. PEG and PVP are the most commonly used polymers for hydrophilic surface modification due to their good biocompatibility, high ratio hydrophilic chemical group, stable chemical structure and inexpensive price.

Microbial contamination will increase the risk of infection, which is one of the most serious complications in body implants and contact lenses. Ag NPs and ZnO NPs have been used to coat biomedical products to inhibit bacteria growth [40,41]. PEG and PVP could also be used biocompatible stabilizers which can introduce functional groups on the surface of nanoparticles to provide them with water-soluble ability so as to meet the various biological

and biomedical needs [42,43]. Moreover, Ag-PVP and ZnO-PEG nanocomposite films on hydrogel can produce hydrophilic surfaces, which are also important as introduced.

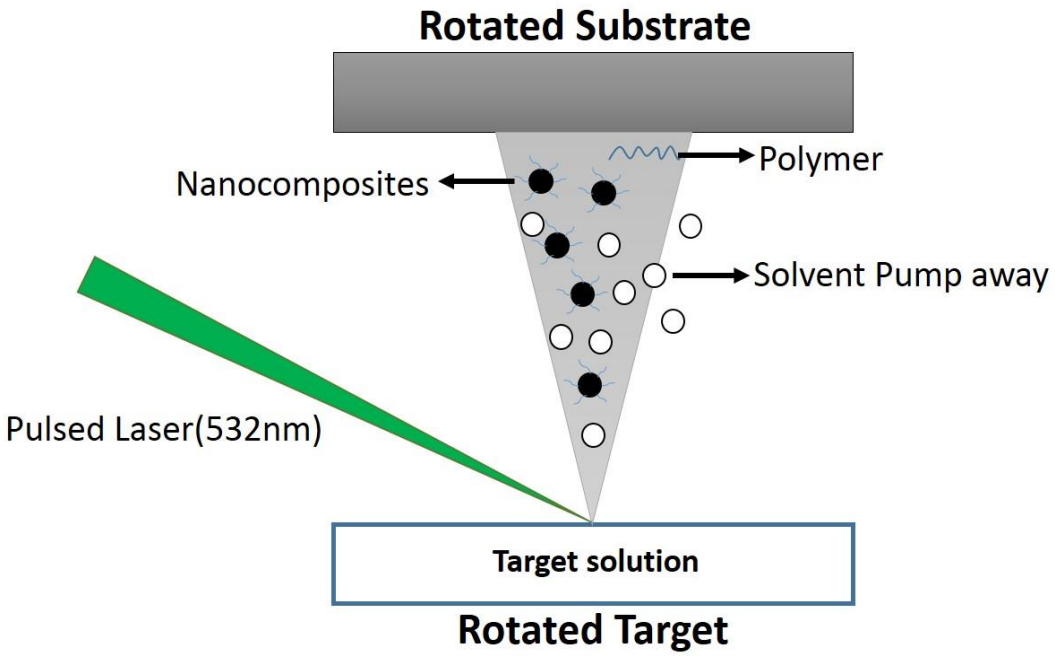

Figure 1.1 Scheme of MAPLE deposition mechanism

1.5 Thesis objectives

According to the current development of hydrogel contact lenses, high oxygen permeability is an essential factor for long-term wearing contact lenses. But silicone hydrogels with high oxygen permeability very easily cause irreversible protein adsorption due to its relatively hydrophobic properties. Irreversible protein adsorption will cause adverse clinical events and even lead to bacteria adhesion. Consequently, this thesis focuses on development of suitable coatings by using MAPLE deposition. The detailed objectives are listed as follows:

(1) Design and deposit polymers on silicone hydrogels using MAPLE to minimize the protein absorption.
(2) Design and deposit nanoparticles on silicone hydrogels using MAPLE to enhance their anti-microbial efficiency.
(3) Understand the effects of MAPLE process on the deposition of polymers and nanoparticles through different characterizations.

1.6 Thesis overview

An overview of my thesis is presented as follows:

Chapter 2: This chapter reviews the general applications of hydrogel especially for the contact lenses. Silicone hydrogel used for contact lenses has several advantages, for instance, high oxygen permeability and good mechanical properties. However, protein fouling and microbial contamination of silicone hydrogel are two major challenges for its application in contact lenses and other biomedical devices. Thus, surface modification is a solution to solve these problems. In this chapter, different surface modification techniques are described and compared, including spin coating, dip coating and laser assisted coating (PLD and MAPLE). A detailed literature review on MAPLE process is included this chapter.

Chapter 3: This chapter describes all experimental procedures for synthesizing silicone hydrogel, Ag-PVP nanoparticles, and ZnO-PEG nanoparticles. Meanwhile, MAPLE deposition parameters corresponding to polymers and nanoparticles used in my research work are introduced in this chapter. Furthermore, different characterization methods, protein adsorption protocol and antimicrobial assay are also presented.

Chapter 4: Two different types of polymers, PEG and PVP are deposited onto the surface of silicone hydrogel by MAPLE deposition in this chapter. FTIR and AFM were carried out to measure the samples after MAPLE deposition. In addition, protein adsorption tests indicate that both polymers could reduce non-specific protein adsorption and slightly improve mechanical at the same time. Cytotoxicity tests were applied to test the biocompatibility.

Chapter 5: This chapter focuses on synthesizing, characterization and depositing two different nanoparticles, Ag-PVP NPs and ZnO-PEG NPs as well as their nanocomposite films. MAPLE technique was used to deposit these nanocomposites onto silicone hydrogel. Protein adsorption and antimicrobial assay were carried out to measure the improvement. The results show that nanocomposite coated silicone hydrogels can inhibit bacterial growth and reduce protein adsorption. Meanwhile, the cytotoxicity results show that all samples' cell viability are above 80 %.

Chapter 6: This chapter gives a summary and conclusions of the research project. Future work on MAPLE system and nanocomposite synthesis are introduced and discussed as well.

1.7 Reference

[1] Slaughter B V, Khurshid SS, Fisher OZ, Khademhosseini A, Peppas N a. Hydrogels in regenerative medicine. Adv Mater 2009;21:3307–29.

[2] Peppas N a., Hilt JZ, Khademhosseini a., Langer R. Hydrogels in Biology and Medicine: From Molecular Principles to Bionanotechnology. Adv Mater 2006;18:1345–60.

[3] Baek C-H, Moon B-C, Lee W-E, Kwak G. Charge transfer dye-based PHEMA hydrogel sensor: its fluorescence responses to pH, metal ion, and humidity. Polym Bull 2012;70:71–9.

[4] Jiang G, Sun J, Ding F. PEG-g-chitosan thermosensitive hydrogel for implant drug delivery: cytotoxicity, in vivo degradation and drug release. J Biomater Sci Polym Ed 2014;25:241–56.

[5] Lian Z, Ye L. Structure and properties of PVA/PEO hydrogel prepared by freezing/thawing method. J Thermoplast Compos Mater 2011;26:912–22.

[6] Pozuelo J, Compañ V, González-Méijome JM, González M, Mollá S. Oxygen and ionic transport in hydrogel and silicone-hydrogel contact lens materials: An experimental and theoretical study. J Memb Sci 2014;452:62–72.

[7] Coyac BR, Chicatun F, Hoac B, Nelea VN, Chaussain C, Nazhat SN, et al. DENSE COLLAGEN HYDROGEL SCAFFOLDS MINERALIZATION REGULATED BY HUMAN PULP STEM CELLS. WOUND REPAIR Regen 2013;21:A62–A62.

[8] Zhang L-M, Wu C-X, Huang J-Y, Peng X-H, Chen P, Tang S-Q. Synthesis and characterization of a degradable composite agarose/HA hydrogel. Carbohydr Polym 2012;88:1445–52.

[9] Ma T, Wang Y, Qi F, Zhu S, Huang L, Liu Z, et al. The effect of synthetic oxygen carrier-enriched fibrin hydrogel on Schwann cells under hypoxia condition in vitro. Biomaterials 2013;34:10016–27.

[10] Nguyen KT, West JL. Photopolymerizable hydrogels for tissue engineering applications. Biomaterials 2002;23:4307–14.

[11] Yu F, Cao X, Li Y, Zeng L, Yuan B, Chen X. An injectable hyaluronic acid/PEG hydrogel for cartilage tissue engineering formed by integrating enzymatic crosslinking and Diels–Alder "click chemistry." Polym Chem 2014;5:1082.

[12] Awadallah-F A. Synergistic effect of poly(acrylamide)-incorporated poly(L-ascorbic acid) hydrogels in controlled release and wound dressings. Des Monomers Polym 2014;17:466–80.

[13] Zhai D, Liu B, Shi Y, Pan L, Wang Y, Li W, et al. Highly Sensitive Glucose Sensor Based on Pt Nanoparticle/Polyaniline Hydrogel Heterostructures. ACS Nano 2013;7:3540–6.

[14] Nicolson PC. Continuous wear contact lens surface chemistry and wearability. Eye Contact Lens 2003;29:S30–2; discussion S57–9, S192–4.

[15] Pozuelo J, Compan V, Gonzalez-Meijome JM, Gonzalez M, Molla S. Oxygen and ionic transport in hydrogel and silicone-hydrogel contact lens materials: An experimental and theoretical study. J Memb Sci 2014;452:62–72.

[16] López-Alemany A, Compañ V, Refojo MF. Porous structure of Purevision versus Focus Night&Day and conventional hydrogel contact lenses. J Biomed Mater Res 2002;63:319–25.

[17] Vandenbulcke K, Horvat L-IL, De Mil M, Slegers G, Beele H. Evaluation of the antibacterial activity and toxicity of 2 new hydrogels: a pilot study. Int J Low Extrem Wounds 2006;5:109–14.

[18] Banerjee I, Pangule RC, Kane RS. Antifouling coatings: recent developments in the design of surfaces that prevent fouling by proteins, bacteria, and marine organisms. Adv Mater 2011;23:690–718.

[19] Luensmann D, Jones L. Protein deposition on contact lenses: the past, the present, and the future. Cont Lens Anterior Eye 2012;35:53–64.

[20] Montero L, Gabriel G, Guimerà A, Villa R, Gleason KK, Borrós S. Increasing biosensor response through hydrogel thin film deposition: Influence of hydrogel thickness. Vacuum 2012;86:2102–4.

[21] Fan R, Deng X, Zhou L, Gao X, Fan M, Wang Y, et al. Injectable thermosensitive hydrogel composite with surface-functionalized calcium phosphate as raw materials. Int J Nanomedicine 2014;9:615–26.

[22] Choy K. Chemical vapour deposition of coatings. Prog Mater Sci 2003;48:57–170.

[23] Ryu DY, Shin K, Drockenmuller E, Hawker CJ, Russell TP. A generalized approach to the modification of solid surfaces. Science 2005;308:236–9.

[24] Nash ME, Carroll WM, Foley PJ, Maguire G, Connell CO, Gorelov A V., et al. Ultra-thin spin coated crosslinkable hydrogels for use in cell sheet recovery—synthesis, characterisation to application. Soft Matter 2012;8:3889.

[25] Hume PS, Bowman CN, Anseth KS. Functionalized PEG hydrogels through reactive dip-coating for the formation of immunoactive barriers. Biomaterials 2011;32:6204–12.

[26] Ma J, Sahai Y. A Direct Borohydride Fuel Cell with Thin Film Anode and Polymer Hydrogel Membrane. ECS Electrochem Lett 2012;1:F41–F43.

[27] Mattox DM. Physical vapor deposition (PVD) processes. Prod Finish 2001;99:72–81.

[28] Stokker-Cheregi F, Matei A, Dinescu M, Secu CE, Secu M. Photoluminescence of Eu-doped LiYF 4 thin films grown by pulsed laser deposition and matrix-assisted pulsed laser evaporation. J Phys D Appl Phys 2014;47:045304.

[29] GUTIERREZLLORENTE A. Growth of polyalkylthiophene films by matrix assisted pulsed laser evaporation. Org Electron 2004;5:29–34.

[30] Caricato a. P, Lomascolo M, Luches a., Mandoj F, Manera MG, Mastroianni M, et al. MAPLE deposition of methoxy Ge triphenylcorrole thin films. Appl Phys A 2008;93:651–4.

[31] Cristescu R, Kocourek T, Moldovan a., Stamatin L, Mihaiescu D, Jelinek M, et al. Laser deposition of cryoglobulin blood proteins thin films by matrix assisted pulsed laser evaporation. Appl Surf Sci 2006;252:4652–5.

[32] Califano V, Bloisi F, Vicari LRM, Yunos DM, Chatzistavrou X, Boccaccini AR. Matrix Assisted Pulsed Laser Evaporation (MAPLE) of Poly(D,L lactide) (PDLLA) on Three Dimensional Bioglass® Structures. Adv Eng Mater 2009;11:685–9.

[33] Caricato a P, Epifani M, Martino M, Romano F, Rella R, Taurino a, et al. MAPLE deposition and characterization of SnO 2 colloidal nanoparticle thin films. J Phys D Appl Phys 2009;42:095105.

[34] Huang R, Ferhan AR, Guo L, Qiu B, Lin Z, Kim D-H, et al. In situ synthesis of protein-resistant poly(oligo(ethylene glycol)methacrylate) films in capillary for protein separation. RSC Adv 2014;4:4883.

[35] Jiang J, Zhu L, Zhu L, Zhang H, Zhu B, Xu Y. Antifouling and antimicrobial polymer membranes based on bioinspired polydopamine and strong hydrogen-bonded poly(N-vinyl pyrrolidone). ACS Appl Mater Interfaces 2013;5:12895–904.

[36] Wu Z, Chen H, Liu X, Zhang Y, Li D, Huang H. Protein adsorption on poly(N-vinylpyrrolidone)-modified silicon surfaces prepared by surface-initiated atom transfer radical polymerization. Langmuir 2009;25:2900–6.

[37] Zhou Q, Lei X-P, Li J-H, Yan B-F, Zhang Q-Q. Antifouling, adsorption and reversible flux properties of zwitterionic grafted PVDF membrane prepared via physisorbed free radical polymerization. Desalination 2014;337:6–15.

[38] Jayasundara DR, Duff T, Angione MD, Bourke J, Murphy DM, Scanlan EM, et al. Carbohydrate Coatings via Aryldiazonium Chemistry for Surface Biomimicry. Chem Mater 2013;25:4122–8.

[39] Konradi R, Pidhatika B, Mühlebach A, Textor M. Poly-2-methyl-2-oxazoline: a peptide-like polymer for protein-repellent surfaces. Langmuir 2008;24:613–6.

[40] Eby DM, Luckarift HR, Johnson GR. Hybrid antimicrobial enzyme and silver nanoparticle coatings for medical instruments. ACS Appl Mater Interfaces 2009;1:1553–60.

[41] Jan T, Iqbal J, Ismail M, Badshah N, Mansoor Q, Arshad A, et al. Synthesis, physical properties and antibacterial activity of metal oxides nanostructures. Mater Sci Semicond Process 2014;21:154–60.

[42] Zhang Y, Jiang D, He Z, Yu Y, Zhang H, Jiang Z. Hydrothermal synthesis of PEG-capped ZnS:Mn2+ quantum dots nanocomposites. Chem Res Chinese Univ 2013;30:176–80.

[43] Borodko Y, Ercius P, Zherebetskyy D, Wang Y, Sun Y, Somorjai G. From Single Atoms to Nanocrystals: Photoreduction of [PtCl 6] 2– in Aqueous and Tetrahydrofuran Solutions of PVP. J Phys Chem C 2013;117:26667–74.

Chapter 2

2 Background and literature review

There are several important requirements for long-term wearing contact lens materials including high oxygen permeability, properly mechanical strength, good biocompatibility, anti-biofouling property and others which depend on specific situations. This chapter introduces different hydrogels and figures out one type, which obtains all the important requirements mentioned above. Biofouling is a serious problem for biomedical material especially for contact lens material [1]. This problem will not only limit the function of biomaterials but also cause adverse clinical problems. Surface modification is one of the most efficient ways to increase biomaterial's property. Existing chemical and physical methods for the surface treatment of commercial contact lens materials have been discussed here. Among them, matrix assisted pulsed laser evaporation (MAPLE) is a new contamination free surface modification system, which is especially suitable for biomaterials modification [2]. The mechanism and different parameters of MAPLE is also introduced in this chapter.

2.1 Hydrogel

Hydrogels are interconnected polymer chains, which can be formed from soluble monomers and/or multifunctional polymers (macromers) and connected together by crosslinkers. Hydrogels also consist of hydrophilic polymer chains to form three-dimensional (3D) networks, which have high water content (up to thousands of times their dry weight) [3]. As a result they have been extensively used as micro-device bases, tissue engineering scaffold, contact lens materials, etc.

Hydrogels have been used as contact lens material for about 50 years. During this period of time, different types of hydrogels have appeared. With the increasing demands for contact lens functions and comfort, new monomers and synthetic methods have been continuously discovered by scientists. There are several types of synthetic hydrogels, which have been used as contact lens materials in the past decades. Polymethylmethacrylate (PMMA) was the first commercial example used for contact lens in 1936 [4]. The monomer of PMMA hydrogel is shown in Figure 2.1(a). Poly-(2-Hydroxyethyl methacrylate) (PHEMA) hydrogel

was first introduced by Wichterle in 1960s and came into industry in 1970s, which made a huge improvement in the area of contact lens material. Figure 2.1(b) shows the main monomer (HEMA) of PHEMA hydrogel. PHEMA is a soft contact lens material that copolymerizes with other hydrophilic or non-hydrophilic monomers [5]. PHEMA is economical and very stable hydrogel with several excellent properties such as transparency, durability, sterilizability, hydrophilicity, and water-insolubility [6]. Therefore, PHEMA is one of the most popular hydrogels used for contact lens recently. But this hydrogel transmit gases (oxygen and carbon dioxide) through the aqueous phase, which limit this materials use for long-term wearing contact lens. Consequently, researchers are trying to add monomers or modify the surface of PHEMA hydrogel to improve the oxygen permeability [7]. However, modification cannot change the mechanism of oxygen transport in PHEMA and PMMA hydrogels, and it is difficult to increase the oxygen permeability substantially. Therefore, a more efficient way to overcome this challenge is developing a new material with a different gas transport mechanism.

2.2 Silicone hydrogel

The silicone hydrogel contact lens was first marketed in 1998 [8]. A different gas transport mechanism was introduced in this type of material. As we know, the gas permeability in polymer films and membranes are critical aspects in food packaging, protective coating, membrane separation processes and biomedical materials. For contact lenses, high oxygen permeability is a vital factor for long term wearing [9]. Silicone hydrogel has siloxane groups (Si-O-Si) that can carry large amounts of oxygen because oxygen is transported easier through the siloxane-phase than water phase [10]. Figure 2.1(c) shows the siloxane groups on the main monomer (TRIS) of silicone hydrogel. This new transport mechanism of silicone hydrogel results in higher oxygen transmissibility than conventional hydrogels.

Javier Pozuelo et al. [11] compared the oxygen permeability between conventional hydrogel and silicone hydrogel. The result showed that oxygen permeability of silicone hydrogel increased more than 10 times compared to conventional hydrogel that transport the oxygen though aqueous phase. The development of highly oxygen permeable silicone hydrogel contact lens materials has been a chief development in its vision correction. Meanwhile, silicone hydrogel also combine the softness and comfort of PHEMA based hydrogels, which

is one of the most important reasons why contact lens manufacturing changed focus from soft lens hydrogel to silicone hydrogel [9]. Contact lenses made from these materials satisfy the metabolic needs of the cornea, maintain its physiological health, and can be worn constantly for up to a month [12].

However, silicone hydrogel still requires modification to improve comfort and biocompatibility for long term wearing. There are two very important factors for long-term wearing experience of contact lenses. One is oxygen permeability, which has been introduced above, and the other is biofouling resistance property including protein fouling/ lipid fouling resistance and antimicrobial property. Silicone hydrogel is able to improve the oxygen permeability, but protein and lipid fouling is a very tough problem, as the tear film component is very complex with more than 400 types of proteins with a wide pH charge from 1 to 11 [13]. Even worse, the mechanism of interaction between protein in tear film and contact lenses are still not quite clear. Several reports show that the proteins adsorb on most biomaterials in a few seconds of their exposure, which will cause adverse clinical events due to inflammation and bacterial infection [8,14,15]. Consequently, the ability to control protein adsorption and bacterial infection is an important evaluation of this biomaterial [16].

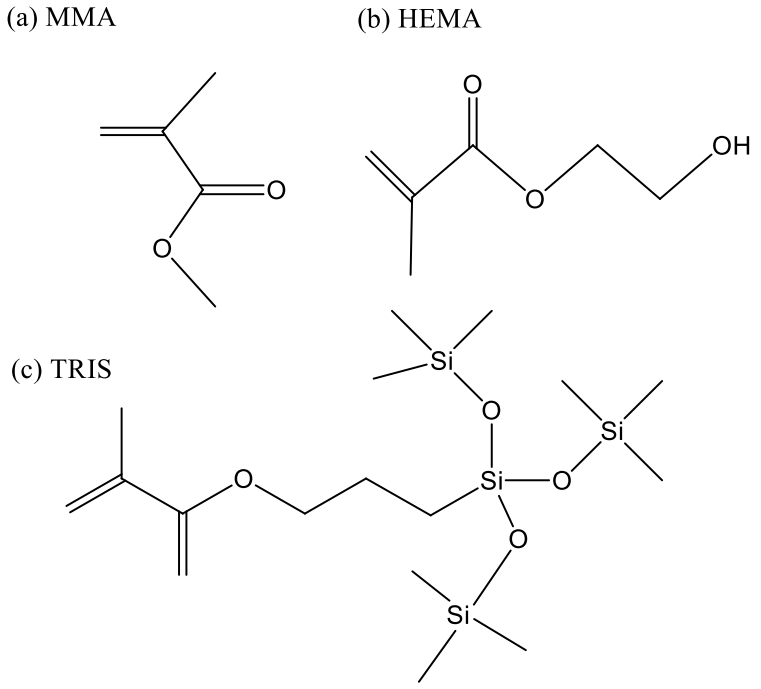

Figure 2.1 (a) monomer of PMMA hydrogel, (b) monomer of PHEMA hydrogel and (c)Monomer of Silicone hydrogel.

2.3 Biofouling mechanism, effects and solutions

Biofouling is the accumulation of proteins, cells and other biological materials on a surface, and biofouling is a great challenge for biomaterial applications, especially for biosensors, prosthetic devices and contact lenses [17]. The fouling is caused by the interaction between the membrane surfaces and the foulants that include biological substances in many different forms. Protein and bacteria are common foulants, which are extensively studied by researchers in biomedical field because protein fouling and bacteria adhesion will cause damage and limit the function of numerous biomedical devices and even cause adverse clinical events [18].

2.3.1 Protein fouling

Protein adsorbs onto the surface of biomedical device will reduce the efficiency and cause harmful side effects, such as stopping flow through separation and affinity columns and porous membranes, which will lead to thrombus formation or fibrosis and scar tissue formation [19–21]. Therefore, the use of protein resistant surfaces is an effective way to increase the performance of biomedical device [21]. Moreover, protein adsorption and the

subsequent protein layer formation will lead to microbial colonization and subsequent biofilm formation [1]. Figure 2.2 illustrates the protein fouling and bacteria adhesion process on biomaterial surface. The protein fouling on contact lenses easily causes several adverse clinical events such as microbial keratitis (MK), contact lens induced acute red eye(CLARE), asymptomatic infiltrative keratitis (AIK), asymptomatic infiltrates (AI), etc. [22] Therefore, low protein fouling is an essential requirement for long time wearing contact lenses.

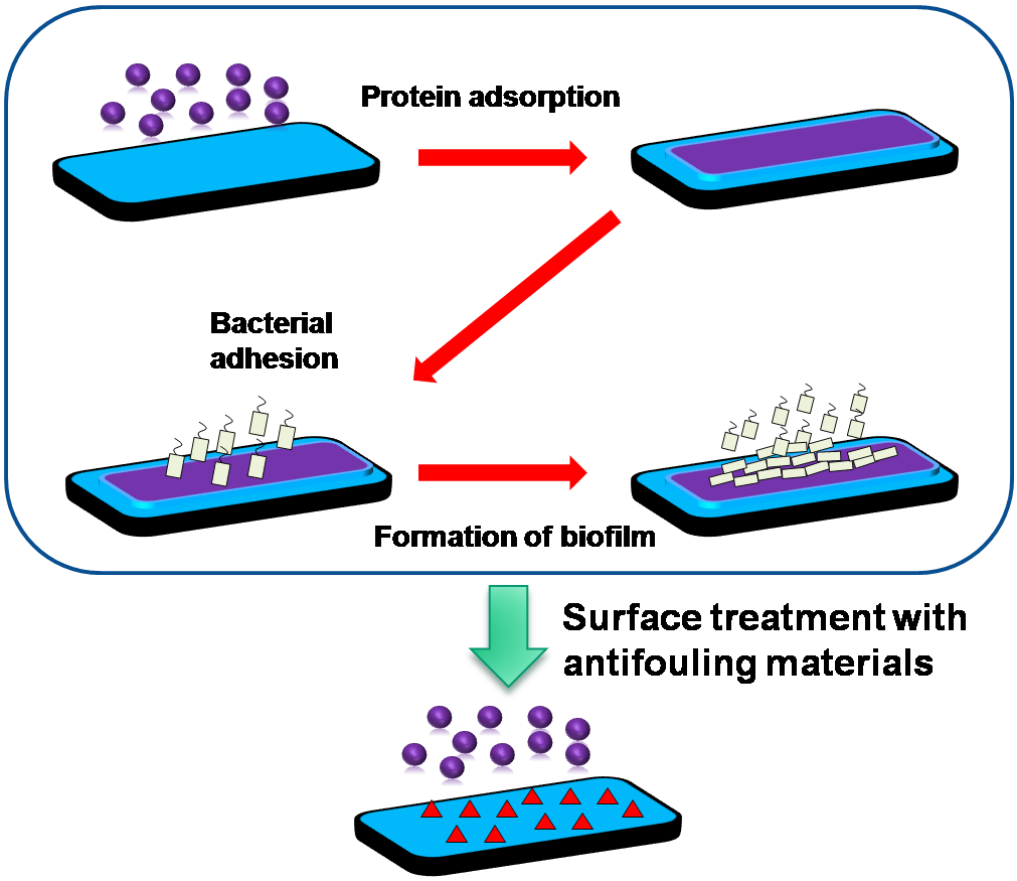

Figure 2.2 Mechanism of biofilm formation from protein adsorption.

Protein adsorption on contact lenses is mainly influenced by the lens material, the protein concentration, protein structure and charge of the proteins within the tear film [13]. Protein adsorption involves van der Waals force, hydrophobic and electrostatic interactions, and hydrogen bonding, which is a complex process and still not quite clear [23]. The surface property of material plays an important role in protein adsorption. The environmental surfaces that interact with protein can be divided into two categories. One is hydrophilic surface and the other is hydrophobic surface. Paul Roach et al. [24] analyzed the adsorption

behavior of bovine serum albumin (BSA) and fibrinogen on hydrophilic (OH) surface and hydrophobic (CH_3) surface separately. The results show that hydrophilic surface absorbs more protein than hydrophobic surface. However, hydrophobic surface causes irreversible protein adsorption, which threatens individuals' health.

Protein is folded in a three-dimensional structure that is metastable. When a protein adsorbs onto a solid surface, the hydrophobic (non-polar) amino acids will be protected inside of the protein molecule and hydrophilic(polar) amino acids side chain will be held outside to interact with their environment [13]. If the surface is hydrophobic, the protein molecules tend to rearrange the structure to reach a lower Gibbs energy [24,25]. The hydrophobic amino acids inside will interact with the hydrophobic surface of hydrogels, which will lead to the unfolding of the protein structure [13,26]. The unfolded proteins also known as denatured protein on hydrophobic surface is irreversible. These denatured proteins will also interact with other proteins, which may cause protein aggregation and cause adverse clinical events [8,15]. However, hydrophilic surface will not denature the protein structure. Consequently, hydrophilic surface modification will be an efficient way to prevent irreversible protein adsorption on biomedical materials.

2.3.1.1 Solutions of protein fouling

There are two methods to prevent irreversible protein adsorption on biomaterials. One is to provide a protein resistance surface (defense method), and the other is to coat protein degrading films (attack method) [1]. Polyethylene glycol (PEG) based polymers, polyvinylpyrrolidone (PVP), zwitterionic materials, carbohydrates and peptide-like polymers are common used polymers to modify the surface of biomaterials with a protein resistance surface.

Polyethylene glycol (PEG) is a polyether compound used in many industrial and biomedical applications. PEG has excellent properties including low toxicity, high hydrophilicity and low biodegradability [27]. Consequently, PEG is a very common used surface stabilizer and surface modification polymer. Although various materials have been reported to inhibit nonspecific adhesion of proteins, PEG and its derivatives are popular surface modification polymers [28]. Several techniques are chosen to immobilize PEG-based polymers, such as chemical adsorption, physical adsorption, covalent attachment, and graft copolymerization

[29]. Paul T. Charles et al. [30] incorporated three different PEG molecules into galactose-based polyarcylate hydrogels, and the result showed the non-specific protein adsorption was reduced. Benjamin S. Flavel et al. [31] grafted PEG onto an amine terminated silicon wafer. This method of attaching PEG proved to be an efficient way to reduce non-specific protein adsorption. Jiang Wu et al. [32] compared the interaction between protein and PEG/ poly(sulfobetaine methacrylate) (zwitterionic polymer). Both polymers have weak or undetectable interaction with proteins. According to its good biocompatibility and high protein resistance, PEG has been chosen as one of hydrophilic polymers to modify silicone hydrogel surface in my project.

Polyvinylpyrrolidone (PVP) is an important water soluble synthetic polymers, which has many ideal properties including low toxicity, chemical stability, and good biocompatibility [36], and has been extensively used in daily chemical industry, food, biomedical field, etc. [33] Therefore, PVP is another common used polymer to improve the hydrophilicity and antifouling properties of the hydrophobic polymer materials [34,35]. Louise Elizabeth Smith et al. [33] tested the direct and indirect contact between PVP and several types of cell from the human body, and results showed that PVP is generally tissue-compatible and non-irritating to skin, eye, and mucous membrane. Masato Matsuda et al. [37] hydrophilized dialysis membranes with PVP, which showed that the membranes after modification are able to inhibit the fibrinogen and human serum albumin adsorption. Currently, commercial PVP is treated as a prospective hydrophilic and antifouling surface modification reagent comparable to PEG.

The “attack” method to reduce irreversible protein adsorption is to incorporate proteases into coating. Proteases are enzymes, which are involved to digest long protein chains into shorter fragments by breaking down the peptide bonds that link amino acid residues. Prashanth Asuri et al. [38] incorporated serum protease onto single-walled carbon nanotubes to provide nanotube-enzyme composites film to resist protein adsorption, and the result showed that this film resisted up to 99% nonspecific protein adsorption.

2.3.2 Microbial contamination

Microbial contamination is a serious issue in health care, food industry and many other fields, so there have been considerable efforts over decades to find out solutions [39,40]. The

attachment of bacteria to a surface leads to subsequent colonization resulting in the formation of a biofilm [1]. Biofilms are matrix-enclosed microbial accretions that adhere to biological or non-biological surfaces, which represent an important and partial understood mode of bacteria growth [41]. Biofilms formation will cause more bacterial adhesion. Two types of interactions contribute to the bacteria adhesion on the surface of biomedical device. One is the formation of a protein layer and the other is nonspecific interaction. Biofilm formation on implant surfaces and subsequent infectious complications are also a frequent failure of many biomedical devices, such as total hip arthroplasties, indwelling voice prostheses, vascular or urinary catheters [42]. Recently, typically treatment method for this problem is replacing the contaminated device and antibiotic therapy at the same time, which cost additional health care [43]. The development of antimicrobial reagents and surface coatings has been attracting increasing attention in recent years.

Similar with the methods used to prevent protein adsorption, there are also two major approaches to inhibit bacteria growth on the surface of biomaterials. One is so called “attack”, and the other is “defend”. The attack approach is coating an antimicrobial material film onto the surface to kill bacteria, such as drugs, short peptides, cationic polymers, antibiotics, inorganic nanoparticles, etc. [44] Xiang Li et al. [45] immobilized two commercialized peptides (RK1 and RK2) onto a silicone surface, and the peptide-coated silicone surface performed outstanding microbial inhibiting activity towards bacteria and fungi in urine and PBS buffer.

The “defend” approach is to create a non-fouling coating, such as PEG, PVP, zwitterionic and their derivative polymers, to resist bacterial adhesion [44]. PEG is a well-known polymer, which is used to reduce protein adsorption and further avoid biofilm formation. Zwitterionic polymers involve anionic and cationic groups along with their chains, which allocate ultra-hydrophilicity and stay neutrally charged at the same time [46]. Consequently, zwitterionic polymers coating is an alternative way to decrease protein adsorption and inhibit bacteria attachment as well. Gang Cheng et al. [47] grafted zwitterionic poly (carboxybetaine methacrylate) via atom transfer radical polymerization onto glass surface for long-term bacterial resistance test. The results showed that after more than 100 hours, the bacteria attachment was reduced more than 90% compared to bare glass.

2.3.2.1 Silver-based materials

Silver nanoparticles (Ag NPs) have been studied over the past 120 years [48], because Ag NPs have extraordinary physico-chemical properties including high electrical and thermal conductivity, chemical stability, surface plasmon resonance, antimicrobial property, surface-enhanced Raman scattering, and catalytic activity [49]. In the field of antibacterial property, silver metal and silver ions were extensively used for ages [50]. Kshipra Naik et al. [51] used sol-gel method to coat AgCl-TiO_2 nanocomposite onto a glass surface for the aim of controlling biofilm formation, and the results showed the nanocomposite coated glass was able to inhibit the growth of Escherichia coli, Staphylococcus epidermidis and Pseudomonas aeruginosa growth. Siddhartha Shrivastava et al. [52] synthesized Ag NPs (around 10-15 nm), which showed potent antibacterial property and was tested by *E. coli*, ampicillin-resistant *E. coli*, multi-drug resistant *S. typhi* and *S. aureus.* Due to their antibacterial effect, Ag NPs have been used to coat numerous medical instruments and products [53].

There are several methods to synthesize Ag NPs, such as chemical, physical, photochemical and biological methods [54]. Different particle nanostructure can be synthesized by proper control of the nucleation, subsequent growth stages and corresponding selection stabilizer (chemical method), such as sphere, cube, tetrahedron, octahedron, bar, spheroid, right bipyramid, beam, decahedron, wire and rod, polygonal plates, branched structures and hollow structures [55]. Metal precursors, reducing reagents and stabilizing reagents are three main components of the reactions of chemical method [54]. Generally citrate, glucose, ethylene glycol, or sodium borohydride have been used as chemical reducing agents to reduce soluble silver salts into Ag NPs [56]. There are several types of polymeric stabilizer used to prevent synthesized Ag NPs form aggregation and control the particle size and shape, including polyvinylpyrrolidone (PVP), polyvinyl alcohol (PVA), polyethylene glycol (PEG) and sodium oleate [57]. The uniform size distribution of chemical method can be controlled by adjusting the reducing and stabilizing agents, trying to generate all nuclei at the same time and keeping the same subsequent growth. Dongjo Kim et al. [58] compared two different chemical methods and several parameters to synthesize size controllable and high mono-dispersible spherical Ag NPs.

Compared with chemical method, photochemical method has several advantages. First, it can be used to more easily control the formation process of nanoparticles due to the controllable photo irradiation time and energy. Second, the synthesis is a clean, convenient and environmentally-friendly process. Third, this method is able to synthesize nanoparticles under various mediums such as aqueous, emulsion, glasses, polymer films, and even cells [54]. Mansor Bin Ahmad et al. [59] chose chitosan and PEG as stabilizers and used photochemical method to synthesize Ag NPs in aqueous medium. Because they did not add any reducing reagent and hazard stabilizer, their synthesis process is an environmentally-friendly method. Therefore, we choose UV irradiation as reduction resource to synthesize Ag NPs in our project. The synthesis process is easy to control by changing different irradiation time, and also we add ethylene glycol as reducing agent, which speeds up the reaction. Moreover, the fabrication process is a gentle process, which happens under room temperature and atmosphere pressure.

2.3.2.2 Zinc-based materials

Zinc-based materials have shown an excellent resistance against corrosion and performed good antibacterial activity [60]. ZnO nanoparticles (NPs) and ZnO nanorods have been shown excellent performance to inhibit bacterial growth [40,61], but some papers showed that ZnO is toxic to host human cells at relatively high concentrations. Hopefully they are not expected to be toxic at very low concentration [62]. Nicole Jones et al. [63] proved that ZnO NPs can control the spreading of bacterial infections after testing the antibacterial property from a broad spectrum of microorganisms. As a common semiconductor, ZnO is one of the most broadly studied metal oxides for the use in solar cell, sensors, ultraviolet nanolaser and blue-light-emitting diodes (LEDs) [64]. Numerous methods have been applied to synthesize ZnO film, such as magnetron sputtering, chemical vapor deposition, pulsed-laser deposition (PLD), metal organic chemical-vapor deposition (MOCVD) and hydride or halide vapor-phase epitaxy (HVPE) [65,66]. Due to the above properties, ZnO NPs are ideal nanoparticles for silicone surface modification.

2.4 Surface modification methods for hydrogels

Surface modification is providing new physical, chemical or biological characteristics, which are different from the ones on the surface of original materials. Nonspecific protein

adsorption and bacterial infection of hydrogels are essential challenges for biomedical application. Hence, surface modification for hydrogels is a commonly used method to solve this problem. Different physical and chemical surface modification techniques have been used to add functional groups onto biomaterials by depositing complex polymers, nanomaterials and others, such as surface plasma treatment, wet chemical methods, spin coating, dip coating, and laser assisted surface coating techniques, etc.

Plasma treatment is a technique that is applied in order to add reactive functional groups to organic materials surface by using an inorganic gas radiofrequency [67]. Different controllable parameters of plasma treatment (such as gas composition and plasma conditions, ions, electrons, etc.) will lead to etching, activation and crosslinking of polymers [68]. Yingming Wang et al. [67] modified the surface of fluorosilicone acrylate contact lenses to improve hydrophilic property by plasma treatment. The hydrophilic surface will cause less proteins and lipids on its surface and reduce bacteria adhesion at the same time. Shantanu Bhattacharya et al. [69] also applied oxygen plasma treatment to convert the hydrophobic PDMS surface to hydrophilic. Plasma treatment can be used for large scale manufacturing. However, plasma treatment can not only add various functional groups under plasma exposure, but also cause aging problems which do not have long-time stability [68].

Surface grafting is a popular chemical surface modification method. End functionalized chains are necessary for grafting the polymer to the surface of solid materials by polymerization [70]. Susan J. Sofia et al. [71] grafted poly(ethylene oxide) (PEO) polymer to silicon with covalent bond. The PEO grafted surface was able to reduce three types of protein (cytochrome-c, albumin, and fibronectin) adsorption. Jing Jing Wang et al. [72] used poly(ethylene glycol) methyl ether acrylate (PEGMA) to modify the surface of silicone hydrogel to reduce protein adsorption by UV irradiation. The results showed that the PEGMA grafted silicone maintained its high oxygen permeability, transparency and mechanical property, and also efficiently changed the hydrophobic surface to hydrophilic. Although chemical method can provide more stable covalent bonding with the substrate, chemical reaction requires different type of chemicals which is toxic to human cells even at extremely low concentration. Meanwhile, there should be active groups on substrate surface or polymer chains. Therefore, these methods could only modify surfaces, which have specific active groups.

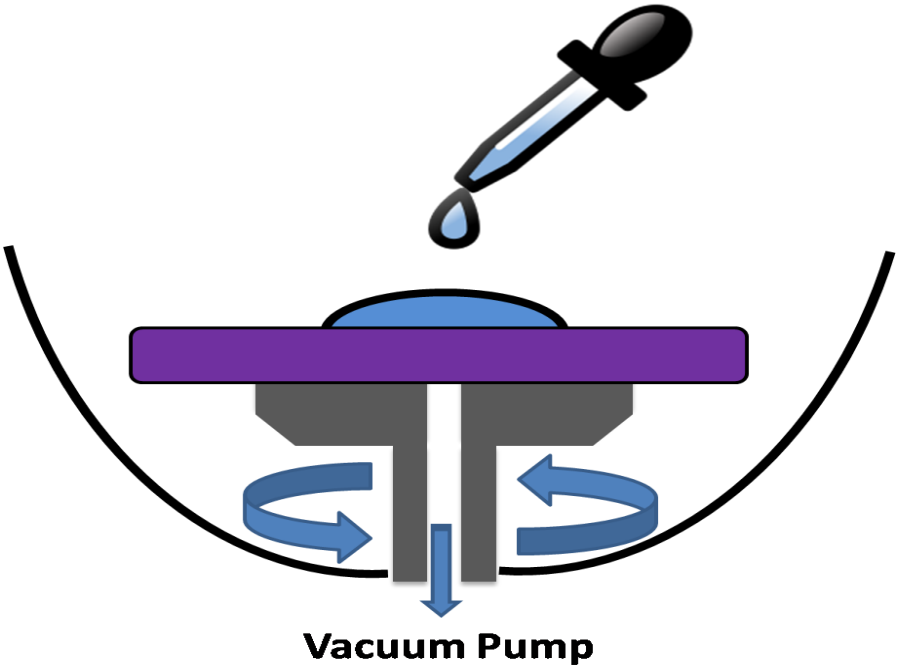

Figure 2.3 Schematic of spin coating.

Spin coating is usually applied to produce a thin film on a plate substrate. After adding some coating materials onto the center of the substrate, the substrate start to rotate at high speed to form a homogenous film by centrifugal force [73]. Figure 2.3 is the schematic of spin coating. Due to the large scale production property, spin coating is a popular physical coating method for deposition polymer films. Aline F. Dário et al. [74] used spin coating to deposit cellulose acetate butyrate (CAB) and poly (methylmethacrylate) onto Si wafers. The result showed the thickness of films was affected by the concentration of the polymer in solution, polymer molecular weight, spinning velocity and spinning time. Also they systematically investigated how the solvent composition used for polymer dissolution affects the porous structures of spin-coated polymers films. Typically only 2-5% of the material dispensed onto the substrate was efficiently used for spin coating, while the remaining 95-98 % is flung off in to the coating bowl and disposed [75]. Therefore, spin coating wastes too many coating materials.

Dip coating technique is also very attractive due to its simplicity, low cost, and high reproducibility [76]. The mechanism of dip coating is shown in Figure 2.4. The procedure of dip coating involves in inserting the objects, which need to be coated into the bath of coating solution, removing it, and then letting it air dry, so it is able to coat 3D objects. James Sibarani et al. [77] applied a simple dip coating method to modify the poly(dimethyl siloxane) (PDMS) surface with hydrophilic polymers such as poly(2-methacryloyloxylethyl phosphorylcholine(MPC)-co-n-butyl methacrylate) (PMB) and poly(MPC-co-2-ethylhexyl methacrylate-co-2-(N,N-dimethylamino)ethyl methacrylate) (PMED). The hydrophilicity of these polymers modified surface has been increased. Therefore they are able to reduce 56-90% protein adsorption compared with uncoated samples. D. Petti et al. [78] also used dip coating method to functionalize a gold surface with copolymer (copoly(DMA-NAS-MAPS)).

The methods mentioned above have their advantages and drawbacks. However, all the methods would make direct contact with solvents or other chemicals during modification. In addition, each of the methods only allows limited organic molecules to be coated or grafted on the surface of biomaterials. As a result, scientists focus on developing a new method,

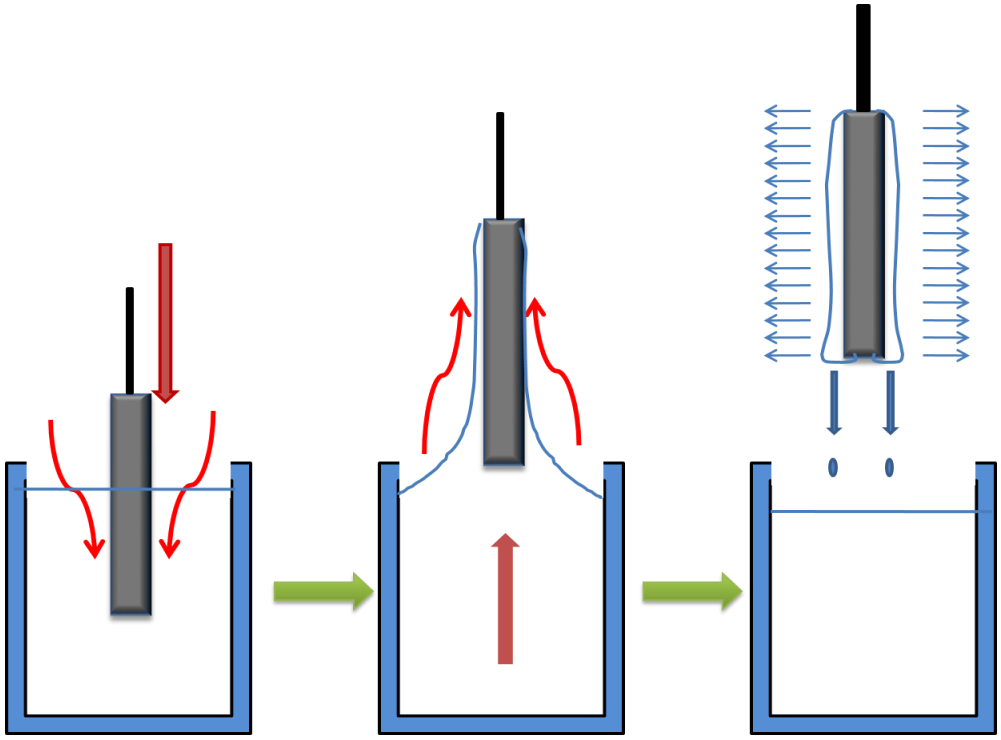

Figure 2.4 Schematic of dip coating.

which is able to modify surface with a wide range of molecules.

2.5 Laser assisted surface coating

Recently pulsed laser deposition (PLD) is extensively used for the production of thin films, and it shows numerous advantages compared to conventional deposition methods [79]. Figure 2.5 shows the schematic of the PLD system. PLD is able to make an accurate control of both the crystalline state of synthesized materials and their adherence to the substrate. PLD avoids contaminants during deposition process and provides various pressure in the chamber[80]. Further, the PLD process is a suitable method for the growth of oxide materials due to the energetic oxygen plasma created by the pulsed laser and controllable oxygen pressure [81]. Arun Aravind et al. [82] analyzed the surface morphology of ZnO film by SEM under different laser resource (KrF laser-248 nm and Nd:YAG laser-266 nm), substrate temperature (400 °C, 500 °C, 600 °C and 700 °C) and various oxygen pressure of the chamber (0.005mbar, 0.05 mbar and 0.5 mbar). According to characterization of XRD, FESEM, Raman scattering and PL, the authors concluded 500 °C (T_S) and 0.05 mbar (pO_2) is

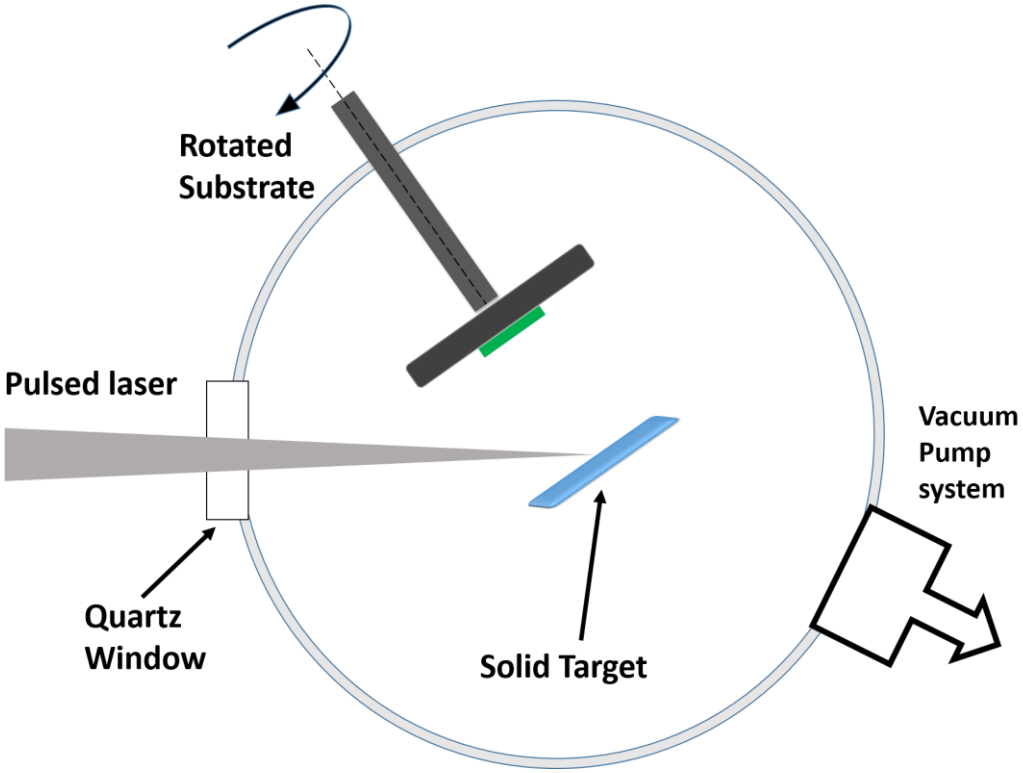

Figure 2.5 Schematic of PLD.

the optimized deposition condition. Therefore, various high-quality coatings have been produced by this method with the help of low temperature, controlled pressure and thickness.

Although PLD has lots of advantages for metals [83], semiconductors [84] and alloys [85], it is not suitable for organic materials because of the high energy, which will break the molecule structure. The matrix assisted pulsed laser evaporation (MAPLE) can be used to fulfill the requirements of depositing a wide range of complex organic materials, and also protect the structure of organic molecules. MAPLE is derived from pulsed laser deposition (PLD). The main difference between PLD and MAPLE is that MAPLE system contains the target preparation. Figure 2.6 shows the schematic MAPLE deposition chamber. In MAPLE process, the target material is embedded in a volatile solvent matrix to produce a frozen target [86]. Liquid nitrogen is used to freeze the target. After that, a laser beam is used to irradiate the frozen target. During the process, the energy is mainly absorbed by the solvent

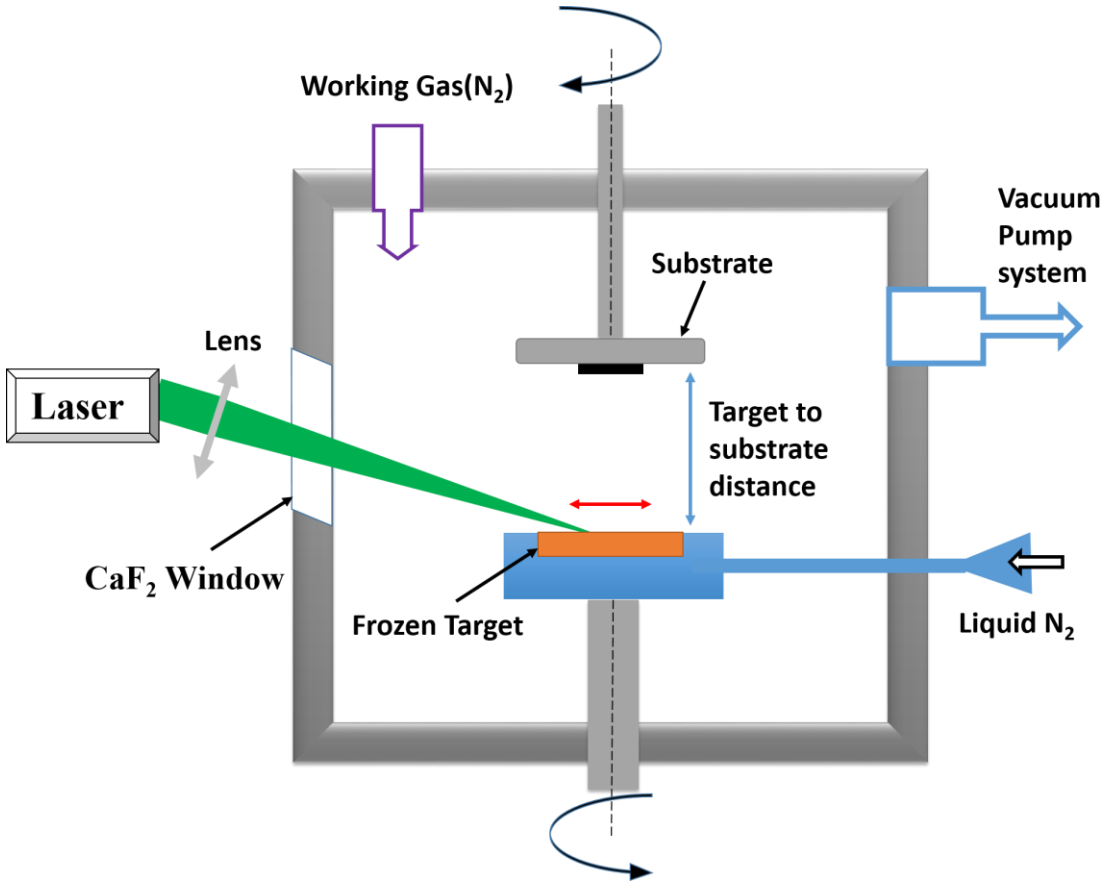

Figure 2.6 Schematic of MAPLE deposition.

and converted into thermal energy that allows the solvent to vaporize [87]. The solvent adsorbs thermal energy, which is vaporized and pumped away. The target polymer molecules or nanoparticles receive enough kinetic energy to be transferred in the gas phase and deposited as thin films on suitable substrates. Most of the laser energy is absorbed by the solvent of the matrix rather than target material, which helps to minimize their photochemical decomposition [88]. MAPLE causes nearly no damage to the target molecules but the target molecules can also be ejected from the target. Meanwhile, the chamber is under vacuum during MAPLE process, which protects the target materials from solvent and gas contamination. MAPLE process is able to achieve homogeneous, ultra-thin, well adherent coatings over large surfaces or preferred areas with accurate thickness control, and maintain the chemical structure and the physiochemical properties of the organic/ polymer molecules/ nanocomposite in the target [89,90]. The wavelength of the laser beam is an important parameter in MAPLE system. Up to now, depositions have been carried out with a wide range of wavelengths such as 193 nm, 248 nm, 266 nm, 355 nm, 532 nm and even IR range (table 2.1). The use of less energetic radiation, such as long wavelength, can decrease the photochemical decomposition of target polymer molecules, because long wavelength radiation is not energetic enough for electronic excitation [89]. Therefore, we chose Nd: YAG laser with wavelength (λ_{em}) at 532 nm for MAPLE deposition.

2.6 Materials used for MAPLE deposition

Many papers have demonstrated that a wide range of polymers, biomolecules and nanoparticles can be deposited to form thin films without significant damage of their chemical structure and function under appropriate laser wavelength, fluence, frequency, deposition time, target-to-substrate distance, target temperature, chamber pressure and type of solvent.

Polymer is extensively used in MAPLE process especially for biomaterial modification. L. Rusen et al. [91] deposited poly(ethylene glycol)-block-poly(ε-caprolactone) methyl ether copolymer, which was dissolved in chloroform (0.5-0.15 wt %). Nd: YAG laser with a wavelength of 266 nm, 6 ns pulse duration and 10 Hz repetition rate was used as irradiation resource. The results showed that the polymer films produced by MAPLE demonstrated a quite similar structure with the original copolymer. Irina Alexandra Paun et al. [92] focused

on depositing PEG with different molecular weights by MAPLE process. The different molecular weight PEG molecular were dissolved in water (1 wt %) and the laser resource is also 266nm and 10 Hz repetition rate. The results indicated that polymer molecular weight significantly affects the properties of the film deposited by MAPLE, so polymer molecular is needed to take into consideration for MAPLE deposition.

Protein is an essential functional biomolecule in biological system. However, it is hard to maintain its function after modification because of the fragile structure. Therefore, MAPLE was carried out to deposit protein and protect its function at the same time. B. R. Ringeisen et al. [93] was the first group to use MAPLE process to successfully deposit protein pattern onto substrate in 2001. They have deposited uniform thin films of insulin and horseradish peroxidase ranging from 10 nm to about 1 um. The result showed that the laser irradiation did not change the protein's mass but maintained its ability. C.A. Mateiand et al. [94] deposited lysozyme and myoglobin onto DTU Fotonik. They chose 355nm Nd:YAG laser and a pulse length of 6 ns to irradiate the water ice matrix and the target concentration was 1 wt %, and some fragmentation occurred. Valentina Dinca et al.[95] chose 266 nm with 5-7 ns pulse duration laser to deposit antitumor compounds (including lactoferrin and cisplatin) and biodegradable polycaprolactone (PCL) polymer onto the substrate (silicon and glass) without any significant chemical damage. They used a modified target system which can separate the above three different compounds. The PCL was dissolved in toluene (0.5 wt %), and two proteins were dissolved in water (1.5 wt %).

Nanoscale science and technology have appeared over the past decade as the leading edge of science and technology [96]. Due to the high surface to volume ratio, nanoscale material has been used in our daily life recently, especially the inorganic nanoparticles, which are able to withstand harsh process conditions [97]. For biomedical application, nanoparticles play an important role in the area of bioimaging, drug delivery, bacterial inhibition, etc. Daniel C. Mayo et al. [98] used resonant infrared MAPLE to deposit TiO_2 nanoparticle film onto Silicon wafer. Er:YAG laser (λ = 2.94 μm) energy can by adsorbed by -OH group. The authors used SEM to analyze the influence of different target concentration, solvent and laser fluence. The result indicated that tert-butanol and other butyl alcohol isomers provided more benefits than water. Angel Perez del Pino et al. [99] fabricated single well nanotubes thin film on glass substrate by MAPLE process. Surface morphology of nanotube film was

characterized by TEM and AFM depending on different fluence of laser resource. R. Cristescu et al. [100] have also deposited Fe_3O_4/oleic acid/ceftriaxone and Fe_3O_4/oleic acid/cefepime (core/shell/adsorption-shell) nanoparticles onto polishing silicon wafer using MAPLE technique with a KrF 248 nm laser. With the AFM image analyzing, they concluded that the roughness of Fe_3O_4 nanocomposite film was higher than drop-cast deposited film. Larger roughness means an extended active surface in biological systems. The structure of nanoparticles deposited by MAPLE process normally has small changes such as the size and the film roughness compared to drop-cast method, but it is similar to the original target material. The function is also maintained according to the recent reports. As a result, MAPLE is one of the most efficient ways to fabricate nanocomposite thin film onto biomaterials. Also some other experimental details about MAPLE deposition have been displayed in Table 2.1.

Table 2.1 Summary of Organic or Inorganic films deposited by MAPLE process.

Materials /Solvents	Substrate	Number of pulse	Fluence, (J/cm^2)	Laser frequency (Hz)	Wavelength (nm)	Pressure	Target (°C)
TiO_2 NPs/DDW (0.02 wt %) [88]	silica, alumina (Al_2O_3) slabs	6,500	0.55	10	193/248	10^{-3}-10^{-4}Pa	LNT
Poly(d,l-lactide)/ Ethyl Acetate (1wt % and 4 wt %) [101]	Polished Si substrate	30,000	0.5	10	248	7.5 Pa	-100
Fullerenes(C60)/Anisole (0.67 wt %) [102]	Si wafer	N.A.	0.5-4	N.A.	N.A.	10^{-4} -1 mbar	RT
PEG-block-PCL Me/chloroform(0.5–1.5 wt %) [103]	Glass coverslips	N.A.	0.2-0.9	10	266	2^{-3} x 10^{-3} Pa	LNT
SnO_2 NPs/toluene (0.2 wt %)[104]	Si wafer	6000	0.35	10	248	5×10^{-4} Pa	-160
PEG/ isopropanol (1 wt %)[105]	Quartz crystal microbalance	1800	2-10	2	355	10^{-6} mbar	LNT
PEG/ DDW (10 wt %) [106]	Si wafer	95,000	0.1	N.A.	355	$2x10^{-4}$ Pa	-170
Polythiophene /chloroform (0.56 wt %) [89]	Glass	20,000	0.094 /0.034 /0.115	N.A.	355/532 /1064	2.3 x 10^{-7} Torr	-187
Pure toluene[107]	PDMS	10,000	0.06-0.25	10	193	5 x 10^{-4} Pa	LNT
lysozyme /water (1 wt %) [108]	Si wafer	50-550	2	N.A.	355	5 $x10^{-5}$ mbar	LNT
Dendrimer precursor/ dichloromethane(0.5-1.5 wt %) [109]	Heated NaCl lens	1500-2500	7.5	1	11010	N.A.	LNT

2.7 Our contribution

MAPLE technique has been applied to modify the surface of biomaterials for about 15 years. Different types of polymers (natural and synthetic polymers) and nanomaterials (nanoparticles and nanorods) were chosen to customize surface properties in order to reduce specific defects of different materials. Non-specific protein adsorption and bacteria that attach on the surface of contact lens or other biomaterials will cause huge adverse clinical problems. As a result, lots of biomedical researchers try to avoid these drawbacks by testing different modification methods. However, there are not too many people focusing on reducing non-specific protein adsorption and inhibiting bacteria growth by MAPLE deposition, which is a contamination free system especially suitable for biomedical device surface modification.

According to the result of recent papers, some polymers have the ability to reduce non-specific protein adsorption such as PEG and PVP [30,37]. Chapter 4 focuses on the deposition of these polymers using MAPLE technique and studying the non-protein sticking property. Meanwhile, we are thinking about combining the nanotechnology with the MAPLE technique to create a multifunctional surface that can reduce non-specific protein adsorption and inhibit bacteria growth at the same time. It is well known that Ag NPs and ZnO NPs are able to eliminate different types of bacteria demonstrated by thousands of researchers. Therefore, we decided to use PEG and PVP as stabilizers to synthesize two types of hybrid nanoparticles (Ag-PVP NPs and ZnO-PEG NPs), and then use MAPLE to deposit nanocomposite film on silicone hydrogel. To our best knowledge, we are the first to deposit Ag-PVP NPs and ZnO-PEG NPs via MAPLE deposition for now.

2.8 Summary

Hydrogel is a commonly used material in biomedical application. PMMA, PHEMA and silicone are three typical hydrogels applied as commercial contact lens materials, but they both have advantages and disadvantages. Silicone hydrogel attracts lots of attention from contact lens industries due to its high oxygen permeability ability compared to other

types of hydrogel. However, silicone is easier to cause biofouling problems including irreversible protein adsorption and bacteria attachment because of its hydrophobic surface. Biofouling is a main drawback for long term wearing contact lenses. Hence, surface modification methods are carried out to modify it including chemical and physical methods. MAPLE technique has been reported as an efficient way to modify the biomaterial surface without gas, solvent or other chemical contamination during deposition process. Recently, MAPLE has been applied to fabricate polymer, biomolecule and nanocomposite thin films and maintain the original materials' properties at the same time. There are many parameters that can be used to control thin film formation during MAPLE process, such as laser wavelength, laser fluence, laser frequency, total pulses during deposition, chamber pressure, target temperature, substrate temperature, type of solvent, target concentration, target-substrate distance, target/ substrate rotate frequency, and deposition time. Surface modification with hydrophilic polymer is an efficient way to reduce irreversible protein adsorption. Silver and zinc based nanomaterials have been extensively used as antibacterial reagents. MAPLE is an ideal biomaterials modification system to deposit polymer and nanocomposite films with controllable thickness.

2.9 Reference

[1] Banerjee I, Pangule RC, Kane RS. Antifouling coatings: recent developments in the design of surfaces that prevent fouling by proteins, bacteria, and marine organisms. Adv Mater 2011;23:690–718.

[2] Rodrigo K, Czuba P, Toftmann B, Schou J, Pedrys R. Surface morphology of polyethylene glycol films produced by matrix-assisted pulsed laser evaporation (MAPLE): Dependence on substrate temperature. Appl Surf Sci 2006;252:4824–8.

[3] Annabi N, Tamayol A, Uquillas JA, Akbari M, Bertassoni LE, Cha C, et al. 25th Anniversary Article: Rational Design and Applications of Hydrogels in Regenerative Medicine. Adv Mater 2014;26:85–124.

[4] Kopeček J. HYDROGELS FROM SOFT CONTACT LENSES AND IMPLANTS TO SELF-ASSEMBLED NANOMATERIALS. J Polym Sci A Polym Chem 2009;47:5929–46.

[5] López-Alemany A, Compañ V, Refojo MF. Porous structure of Purevision versus Focus Night&Day and conventional hydrogel contact lenses. J Biomed Mater Res 2002;63:319–25.

[6] Baek C-H, Moon B-C, Lee W-E, Kwak G. Charge transfer dye-based PHEMA hydrogel sensor: its fluorescence responses to pH, metal ion, and humidity. Polym Bull 2012;70:71–9.

[7] Nicolson PC, Vogt J. Soft contact lens polymers: an evolution. Biomaterials 2001;22:3273–83.

[8] Kodjikian L, Casoli-bergeron E, Malet F, Janin-manificat H, Freney J, Burillon C, et al. Bacterial adhesion to conventional hydrogel and new silicone-hydrogel contact lens materials. Graefes Arch Clin Exp Ophthalmol 2008:267–73.

[9] Pozuelo J, Compañ V, González-Méijome JM, González M, Mollá S. Oxygen and ionic transport in hydrogel and silicone-hydrogel contact lens materials: An experimental and theoretical study. J Memb Sci 2014;452:62–72.

[10] Nicolson PC. Continuous wear contact lens surface chemistry and wearability. Eye Contact Lens 2003;29:S30–2; discussion S57–9, S192–4.

[11] Pozuelo J, Compan V, Gonzalez-Meijome JM, Gonzalez M, Molla S. Oxygen and ionic transport in hydrogel and silicone-hydrogel contact lens materials: An experimental and theoretical study. J Memb Sci 2014;452:62–72.

[12] Brennan N a, Coles MLC, Comstock TL, Levy B. A 1-year prospective clinical trial of balafilcon a (PureVision) silicone-hydrogel contact lenses used on a 30-day continuous wear schedule. Ophthalmology 2002;109:1172–7.

[13] Luensmann D, Jones L. Protein deposition on contact lenses: the past, the present, and the future. Cont Lens Anterior Eye 2012;35:53–64.

[14] Iskeleli G, Karakoc Y, Ozkok A, Arici C, Ozcan O, Ipcioglu O. Comparison of the effects of first and second generation silicone hydrogel contact lens wear on tear film osmolarity. Int J Ophthalmol 2013;6:666–70.

[15] Thissen H, Gengenbach T, du Toit R, Sweeney DF, Kingshott P, Griesser HJ, et al. Clinical observations of biofouling on PEO coated silicone hydrogel contact lenses. Biomaterials 2010;31:5510–9.

[16] Vandenbulcke K, Horvat L-IL, De Mil M, Slegers G, Beele H. Evaluation of the antibacterial activity and toxicity of 2 new hydrogels: a pilot study. Int J Low Extrem Wounds 2006;5:109–14.

[17] Wisniewski N, Reichert M. Methods for reducing biosensor membrane biofouling. Colloids Surfaces B Biointerfaces 2000;18:197–219.

[18] Rodriguez-Emmenegger C, Houska M, Alles AB, Brynda E. Surfaces resistant to fouling from biological fluids: towards bioactive surfaces for real applications. Macromol Biosci 2012;12:1413–22.

[19] Pop-Georgievski O, Rodriguez-Emmenegger C, Pereira ADLS, Proks V, Brynda E, Rypáček F. Biomimetic non-fouling surfaces: extending the concepts. J Mater Chem B 2013;1:2859.

[20] Rana D, Matsuura T. Surface modifications for antifouling membranes. Chem Rev 2010;110:2448–71.

[21] Hucknall A, Rangarajan S, Chilkoti A. In Pursuit of Zero: Polymer Brushes that Resist the Adsorption of Proteins. Adv Mater 2009;21:2441–6.

[22] Stapleton F, Stretton S, Papas E, Skotnitsky C, Sweeney DF. Silicone Hydrogel Contact Lenses and the Ocular Surface. Ocul Surf 2006;4:24–43.

[23] Mathé C, Devineau S, Aude J-C, Lagniel G, Chédin S, Legros V, et al. Structural determinants for protein adsorption/non-adsorption to silica surface. PLoS One 2013;8:e81346.

[24] Roach P, Farrar D, Perry CC. Interpretation of protein adsorption: surface-induced conformational changes. J Am Chem Soc 2005;127:8168–73.

[25] NORDE W. ENERGY AND ENTROPY OF PROTEIN ADSORPTION. J Dispers Sci Technol 1992;13:363–77.

[26] Bond H, Waals V Der, Waals D. Intermolecular and Surface Forces n.d.:1–18.

[27] Hamley IW, Krysmann MJ. Effect of PEG crystallization on the self-assembly of PEG/peptide copolymers containing amyloid peptide fragments. Langmuir 2008;24:8210–4.

[28] Huang R, Ferhan AR, Guo L, Qiu B, Lin Z, Kim D-H, et al. In situ synthesis of protein-resistant poly(oligo(ethylene glycol)methacrylate) films in capillary for protein separation. RSC Adv 2014;4:4883.

[29] Llanos GR, Sefton M V. Does polyethylene oxide possess a low thrombogenicity? J Biomater Sci Polym Ed 1993;4:381–400.

[30] Charles PT, Stubbs VR, Soto CM, Martin BD, White BJ, Taitt CR. Reduction of Non-Specific Protein Adsorption Using Poly(ethylene) Glycol (PEG) Modified Polyacrylate Hydrogels In Immunoassays for Staphylococcal Enterotoxin B Detection. Sensors (Basel) 2009;9:645–55.

[31] Flavel BS, Jasieniak M, Velleman L, Ciampi S, Luais E, Peterson JR, et al. Grafting of poly(ethylene glycol) on click chemistry modified Si(100) surfaces. Langmuir 2013;29:8355–62.

[32] Wu J, Zhao C, Hu R, Lin W, Wang Q, Zhao J, et al. Probing the weak interaction of proteins with neutral and zwitterionic antifouling polymers. Acta Biomater 2014;10:751–60.

[33] Smith LE, Rimmer S, MacNeil S. Examination of the effects of poly(N-vinylpyrrolidinone) hydrogels in direct and indirect contact with cells. Biomaterials 2006;27:2806–12.

[34] Jiang J, Zhu L, Zhu L, Zhang H, Zhu B, Xu Y. Antifouling and antimicrobial polymer membranes based on bioinspired polydopamine and strong hydrogen-bonded poly(N-vinyl pyrrolidone). ACS Appl Mater Interfaces 2013;5:12895–904.

[35] Wu Z, Chen H, Liu X, Zhang Y, Li D, Huang H. Protein adsorption on poly(N-vinylpyrrolidone)-modified silicon surfaces prepared by surface-initiated atom transfer radical polymerization. Langmuir 2009;25:2900–6.

[36] Liu X, Xu Y, Wu Z, Chen H. Poly(N-vinylpyrrolidone)-modified surfaces for biomedical applications. Macromol Biosci 2013;13:147–54.

[37] Matsuda M, Yamamoto K, Yakushiji T, Fukuda M, Miyasaka T, Sakai K. Nanotechnological evaluation of protein adsorption on dialysis membrane surface hydrophilized with polyvinylpyrrolidone. J Memb Sci 2008;310:219–28.

[38] Asuri P, Karajanagi SS, Kane RS, Dordick JS. Polymer-nanotube-enzyme composites as active antifouling films. Small 2007;3:50–3.

[39] Vasilev K, Griesser SS, Griesser HJ. Antibacterial Surfaces and Coatings Produced by Plasma Techniques. Plasma Process Polym 2011;8:1010–23.

[40] Tam KH, Djurišić a. B, Chan CMN, Xi YY, Tse CW, Leung YH, et al. Antibacterial activity of ZnO nanorods prepared by a hydrothermal method. Thin Solid Films 2008;516:6167–74.

[41] Hall-Stoodley L, Costerton JW, Stoodley P. Bacterial biofilms: from the natural environment to infectious diseases. Nat Rev Microbiol 2004;2:95–108.

[42] Roosjen A, van der Mei HC, Busscher HJ, Norde W. Microbial adhesion to poly(ethylene oxide) brushes: influence of polymer chain length and temperature. Langmuir 2004;20:10949–55.

[43] Lynch a S, Robertson GT. Bacterial and fungal biofilm infections. Annu Rev Med 2008;59:415–28.

[44] Cao Z, Mi L, Mendiola J, Ella-Menye J-R, Zhang L, Xue H, et al. Reversibly switching the function of a surface between attacking and defending against bacteria. Angew Chem Int Ed Engl 2012;51:2602–5.

[45] Li X, Li P, Saravanan R, Basu A, Mishra B, Lim SH, et al. Antimicrobial functionalization of silicone surfaces with engineered short peptides having broad spectrum antimicrobial and salt-resistant properties. Acta Biomater 2014;10:258–66.

[46] Mi L, Jiang S. Integrated antimicrobial and nonfouling zwitterionic polymers. Angew Chem Int Ed Engl 2014;53:1746–54.

[47] Cheng G, Li G, Xue H, Chen S, Bryers JD, Jiang S. Zwitterionic carboxybetaine polymer surfaces and their resistance to long-term biofilm formation. Biomaterials 2009;30:5234–40.

[48] Nowack B, Krug HF, Height M. 120 Years of Nanosilver History : Implications for Policy Makers 2011:1177–83.

[49] Krutyakov YA, Kudrinskiy AA, Olenin AY, Lisichkin G V. Synthesis and properties of silver nanoparticles: advances and prospects. Russ Chem Rev 2008;77:233–57.

[50] Yu H, Xu X, Chen X, Lu T, Zhang P, Jing X. Preparation and antibacterial effects of PVA-PVP hydrogels containing silver nanoparticles. J Appl Polym Sci 2007;103:125–33.

[51] Naik K, Kowshik M. Anti-biofilm efficacy of low temperature processed AgCl-TiO2 nanocomposite coating. Mater Sci Eng C Mater Biol Appl 2014;34:62–8.

[52] Shrivastava S, Bera T, Roy A, Singh G, Ramachandrarao P, Dash D. Characterization of enhanced antibacterial effects of novel silver nanoparticles. Nanotechnology 2007;18:225103.

[53] Eby DM, Luckarift HR, Johnson GR. Hybrid antimicrobial enzyme and silver nanoparticle coatings for medical instruments. ACS Appl Mater Interfaces 2009;1:1553–60.

[54] Tran QH, Nguyen VQ, Le A-T. Silver nanoparticles: synthesis, properties, toxicology, applications and perspectives. Adv Nat Sci Nanosci Nanotechnol 2013;4:033001.

[55] Rycenga M, Cobley CM, Zeng J, Li W, Moran CH, Zhang Q, et al. Controlling the synthesis and assembly of silver nanostructures for plasmonic applications. Chem Rev 2011;111:3669–712.

[56] Chernousova S, Epple M. Silver as antibacterial agent: ion, nanoparticle, and metal. Angew Chem Int Ed Engl 2013;52:1636–53.

[57] Lin J-J, Lin W-C, Li S-D, Lin C-Y, Hsu S-H. Correction to evaluation of the antibacterial activity and biocompatibility for silver nanoparticles immobilized on nano silicate platelets. ACS Appl Mater Interfaces 2013;5:2782.

[58] Kim D, Jeong S, Moon J. Synthesis of silver nanoparticles using the polyol process and the influence of precursor injection. Nanotechnology 2006;17:4019–24.

[59] Ahmad M Bin, Tay MY, Shameli K, Hussein MZ, Lim JJ. Green Synthesis and Characterization of Silver/Chitosan/Polyethylene Glycol Nanocomposites without any Reducing Agent. Int J Mol Sci 2011;12:4872–84.

[60] Siyanbola TO, Sasidhar K, Anjaneyulu B, Kumar KP, Rao BVSK, Narayan R, et al. Anti-microbial and anti-corrosive poly (ester amide urethane) siloxane modified ZnO hybrid coatings from Thevetia peruviana seed oil. J Mater Sci 2013;48:8215–27.

[61] Shafiq M, Yasin T, Rafiq MA. Structural , Thermal , and Antibacterial Properties of Chitosan / ZnO Composites. Polym Compos 2014;35.

[62] Roselli M, Finamore A, Garaguso I, Britti MS, Mengheri E. Biochemical and Molecular Actions of Nutrients Zinc Oxide Protects Cultured Enterocytes from the Damage Induced by Escherichia coli 1. Biochem Mol Actions Nutr Zinc 2003:4077–82.

[63] Jones N, Ray B, Ranjit KT, Manna AC. Antibacterial activity of ZnO nanoparticle suspensions on a broad spectrum of microorganisms. FEMS Microbiol Lett 2008;279:71–6.

[64] Sadeghi B. Preparation of ZnO/Ag nanocomposite and coating on polymers for anti-infection biomaterial application. Spectrochim Acta A Mol Biomol Spectrosc 2014;118:787–92.

[65] Özgür U, Alivov YI, Liu C, Teke A, Reshchikov MA, Doğan S, et al. A comprehensive review of ZnO materials and devices. J Appl Phys 2005;98:041301.

[66] Thirugnanam T. Effect of Polymers (PEG and PVP) on Sol-Gel Synthesis of Microsized Zinc Oxide. J Nanomater 2013;2013:1–7.

[67] Wang Y, Qian X, Zhang X, Xia W, Zhong L, Sun Z, et al. Plasma surface modification of rigid contact lenses decreases bacterial adhesion. Eye Contact Lens 2013;39:376–80.

[68] Hegemann D, Brunner H, Oehr C. Plasma treatment of polymers for surface and adhesion improvement. Nucl Instruments Methods Phys Res Sect B Beam Interact with Mater Atoms 2003;208:281–6.

[69] Bhattacharya S, Datta A, Berg JM, Gangopadhyay S. Studies on surface wettability of poly(dimethyl) siloxane (PDMS) and glass under oxygen-plasma treatment and correlation with bond strength. J Microelectromechanical Syst 2005;14:590–7.

[70] Stamm M. Polymer Surfaces and Interfaces. 1st ed. Springer; 2008.

[71] Sofia S, Premnath V, Merrill E. Poly(ethylene oxide) Grafted to Silicon Surfaces: Grafting Density and Protein Adsorption. Macromolecules 1998;31:5059–70.

[72] Wang JJ, Liu F. Imparting Antifouling Properties of Silicone Hydrogels by Grafting Poly (ethylene glycol) Methyl Ether Acrylate Initiated by UV Light 2011.

[73] Scriven LE. Physics and Applications of DIP Coating and Spin Coating. MRS Proc 2011;121:717.

[74] Dário AF, Macia HB, Petri DFS. Nanostructures on spin-coated polymer films controlled by solvent composition and polymer molecular weight. Thin Solid Films 2012;524:185–90.

[75] Sahu N, Parija B, Panigrahi S. Fundamental understanding and modeling of spin coating process: A review. Indian J Phys 2009;83:493–502.

[76] Yue L, Pu H, Li H, Pang S, Zhang Q. Dip-coated Al–In–Zn–O thin-film transistor with poly-methylmethacrylate gate dielectric. J Phys D Appl Phys 2013;46:445106.

[77] Sibarani J, Takai M, Ishihara K. Surface modification on microfluidic devices with 2-methacryloyloxyethyl phosphorylcholine polymers for reducing unfavorable protein adsorption. Colloids Surf B Biointerfaces 2007;54:88–93.

[78] Petti D, Torti a., Damin F, Sola L, Rusnati M, Albisetti E, et al. Functionalization of gold surfaces with copoly(DMA-NAS-MAPS) by dip coating: Surface characterization and hybridization tests. Sensors Actuators B Chem 2014;190:234–42.

[79] Lozovan a. a., Alexandrova SS, Mishnev M a., Prishepov SV. A study of the deposition process of multilayer coatings on the inner tube surface with the pulsed laser deposition technique. J Alloys Compd 2014;586:S387–S390.

[80] Vinodkumar R, Navas I, Porsezian K, Ganesan V, Unnikrishnan N V, Mahadevan Pillai VP. Structural, spectroscopic and electrical studies of nanostructured porous ZnO thin films prepared by pulsed laser deposition. Spectrochim Acta A Mol Biomol Spectrosc 2014;118:724–32.

[81] Ryu YR, Zhu S, Budai JD, Chandrasekhar HR, Miceli PF, White HW. Optical and structural properties of ZnO films deposited on GaAs by pulsed laser deposition. J Appl Phys 2000;88:201.

[82] Aravind A, Jayaraj MK, Kumar M, Chandra R. The dependence of structural and optical properties of PLD grown ZnO films on ablation parameters. Appl Surf Sci 2013;286:54–60.

[83] Gharbi M, Peyre P, Gorny C, Carin M, Morville S, Le Masson P, et al. Influence of a pulsed laser regime on surface finish induced by the direct metal deposition process on a Ti64 alloy. J Mater Process Technol 2014;214:485–95.

[84] Caricato a. P, Leggieri G, Luches a., Romano F, Barucca G, Mengucci P, et al. Morphological and structural characterizations of CrSi2 nanometric films deposited by laser ablation. Appl Surf Sci 2007;254:1224–7.

[85] Shibagaki K, Kawano K, Mori A. Synthesis and characterization of Ti–Ni shape memory alloy thin films by pulsed laser deposition. Appl Phys A 2012;110:805–8.

[86] Cristescu R, Mihaiescu D, Socol G, Stamatin I, Mihailescu IN, Chrisey DB. Deposition of biopolymer thin films by matrix assisted pulsed laser evaporation. Appl Phys A 2004;79:1023–6.

[87] Caricato a. P, Capone S, Epifani M, Lomascolo M, Luches A, Martino M, et al. Nanoparticle thin films deposited by MAPLE for sensor applications 2008;6985:69850H–69850H–13.

[88] Caricato a. P, Luches a., Leggieri G, Martino M, Rella R. Matrix-assisted pulsed laser deposition of polymer and nanoparticle films. Vacuum 2012;86:661–6.

[89] Bloisi F, Cassinese A, Papa R, Vicari L, Califano V. Matrix-Assisted Pulsed Laser Evaporation of polythiophene films. Thin Solid Films 2008;516:1594–8.

[90] Sima F, Davidson P, Pauthe E, Sima LE, Gallet O, Mihailescu IN, et al. Fibronectin layers by matrix-assisted pulsed laser evaporation from saline buffer-based cryogenic targets. Acta Biomater 2011;7:3780–8.

[91] Rusen L, Mustaciosu C, Mitu B, Filipescu M, Dinescu M, Dinca V. Protein-resistant polymer coatings obtained by matrix assisted pulsed laser evaporation. Appl Surf Sci 2013;278:198–202.

[92] Alexandra I, Valentin P, Dinescu CLM, Canulescu S, Schou J. In vitro studies of PEG thin films with different molecular weights deposited by MAPLE 2012:223–32.

[93] Ringeisen BR, Callahan J, Wu PK, Pique A, Spargo B, Mcgill RA, et al. Novel Laser-Based Deposition of Active Protein Thin Films 2001:3472–9.

[94] Matei a., Schou J, Constantinescu C, Kingshott P, Dinescu M. Growth of thin films of low molecular weight proteins by matrix assisted pulsed laser evaporation (MAPLE). Appl Phys A 2011;105:629–33.

[95] Dinca V, Florian PE, Sima LE. MAPLE-based method to obtain biodegradable hybrid polymeric thin films with embedded antitumoral agents 2014:11–21.

[96] Ahammed HAM, Jayakumar S, Vaideki K. Use of zinc oxide nano particles for production of antimicrobial textiles. Int J Eng Sci Technol 2010;2:202–8.

[97] Fu L, Liu Z, Liu Y, Han B, Hu P, Cao L, et al. Beaded Cobalt Oxide Nanoparticles along Carbon Nanotubes: Towards More Highly Integrated Electronic Devices. Adv Mater 2005;17:217–21.

[98] Mayo DC, Paul O, Airuoyo IJ, Pan Z, Schriver KE, Avanesyan SM, et al. Resonant infrared matrix-assisted pulsed laser evaporation of TiO2 nanoparticle films. Appl Phys A 2012;110:923–8.

[99] Tobias G. Deposition of functionalized single wall carbon nanotubes through matrix assisted pulsed laser evaporation 2012;0.

[100] Cristescu R, Popescu C, Socol G, Iordache I, Mihailescu IN, Mihaiescu DE, et al. Magnetic core/shell nanoparticle thin films deposited by MAPLE: Investigation by chemical, morphological and in vitro biological assays. Appl Surf Sci 2012;258:9250–5.

[101] Cristescu R, Popescu C, Dorcioman G, Miroiu FM, Socol G, Mihailescu IN, et al. Antimicrobial activity of biopolymer–antibiotic thin films fabricated by advanced pulsed laser methods. Appl Surf Sci 2013:3–5.

[102] Canulescu S, Schou J, Fæster S, Hansen K V., Conseil H. Deposition of matrix-free fullerene films with improved morphology by matrix-assisted pulsed laser evaporation (MAPLE). Chem Phys Lett 2013;588:119–23.

[103] Rusen L, Mustaciosu C, Mitu B, Filipescu M, Dinescu M, Dinca V. Protein-resistant polymer coatings obtained by matrix assisted pulsed laser evaporation. Appl Surf Sci 2013;278:198–202.

[104] Caricato a P, Epifani M, Martino M, Romano F, Rella R, Taurino a, et al. MAPLE deposition and characterization of SnO 2 colloidal nanoparticle thin films. J Phys D Appl Phys 2009;42:095105.

[105] Rodrigo K, Toftmann B, Schou J, Pedrys R. Laser Irradiation of Polymer-Doped Cryogenic Matrices. J Low Temp Phys 2005;139:683–92.

[106] Califano V, Bloisi F, Vicari LRM, Colombi P, Bontempi E, Depero LE. MAPLE deposition of biomaterial multilayers. Appl Surf Sci 2008;254:7143–8.

[107] Caricato a. P, Arima V, Cesaria M, Martino M, Tunno T, Rinaldi R, et al. Solvent-related effects in MAPLE mechanism. Appl Phys B 2013;113:463–71.

[108] Constantinescu C, Matei a., Schou J, Canulescu S, Dinescu M. Pulsed laser deposition of lysozyme: the dependence on shot numbers and the angular distribution. Appl Phys B 2013;113:367–71.

[109] Fajgar R, Novotn F. Applied Surface Science RIR MAPLE procedure for deposition of carbon rich Si / C / H films s Straˇ 2014;292:413–9.

Chapter 3

3 Experiment procedures

In this chapter, the experiment details of this project are introduced: (1) the synthesis of silicone hydrogel. (2) Ag-PVP nanoparticle and ZnO-PEG nanoparticle. (3) Polymers (PEG and PVP) and nanocomposites (Ag-PVP and ZnO-PEG) coatings produced by using MAPLE technique. (4) The characterization methods. (5) Protein adsorption and antimicrobial test.

3.1 Synthesis of silicone hydrogel

The silicone hydrogel was synthesized through photo-polymerization, which is developed by Kim et al. [1] 3 ml of 3-methacryloxypropy-tris(trimethylsiloxy)silane (TRIS), bis-alpha,omega-(methacryloxypropyl)polydimethylsiloxane (PDMS) and N,N-Dimethylacrylamide (DMA) was mixed by the volume ratio of 4:1:2 and then added 15 µl of ethylene glycol dimethacrylate (EGDMA) and 0.3 ml ethanol into the mixture. Nitrogen was purged into the mixture for 15 min before 8 mg of Diphenyl(2,4,6-trimethylbenzoyl)phosphine oxide (photo-initiator)was added and stirred for 5 min. Figure 3.1 shows the chemical structures of monomers, cross-linker, macromer, photo-initiator as well as produced silicone. After that the mixture was photo-polymerized under UV irradiation for 50 min to form complete crosslinking. 30% Ethanol was used to wash the hydrogel after photo-polymerization.

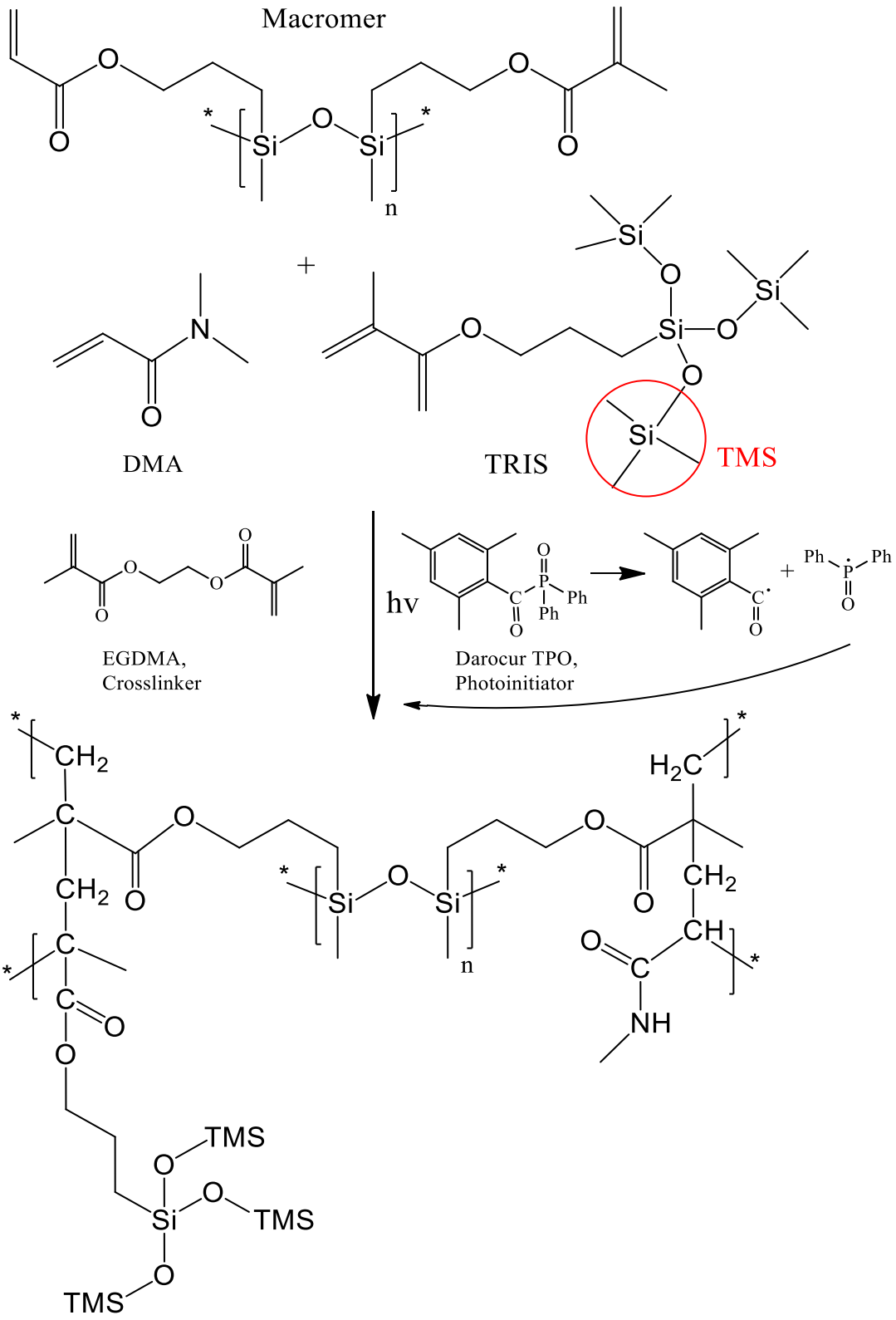

Figure 3.1 Schematic illustration of silicone photo initiated crosslinking reaction.

3.2 Synthesis of nanoparticles

3.2.1 Silver nanoparticles

Silver nanoparticles were synthesized from silver nitrate by photo reduction reaction. Polyvinylpyrrolidone (PVP), which molecular weight is 10000, was used as stabilizer during reduction reaction. To synthesize Ag-PVP NPs, it is necessary to keep the synthesis process from oxygen to prevent oxidation reactions during formation of Ag NPs. 100 ml ethylene glycol was added into 250 ml flask and then nitrogen gas used for 10 min to remove the oxygen in the ethylene glycol. Dissolve 1.5 g PVP in the ethylene glycol under stirring for 0.5 hour until it is fully dissolved. 1 gram of silver nitrate was added to the mixture solution. After silver nitrate was fully dissolved, keep the solution under irradiation of UV environment for 24 hours. The synthesis process of Ag NPs is shown in Figure 3.2. Centrifuge was used to get the Ag NPs out of reaction solution and wash Ag NPs with the mixture of ethanol and acetone solution [2,3].

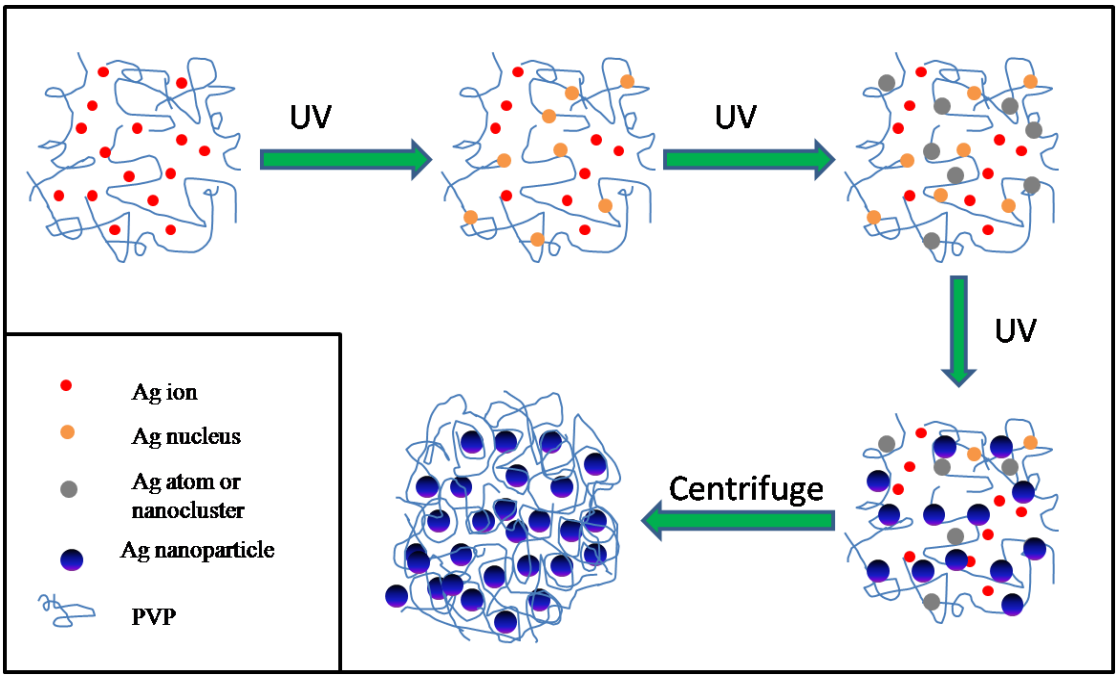

Figure 3.2 Schematic illustration of Ag-PVP nanoparticles synthesis.

3.2.2 Zinc oxide (ZnO) nanoparticle

PEG stabilizing ZnO nanoparticles (ZnO-PEG NPs) were prepared by a sol-gel method where precursor is zinc acetate dehydrate [Zn $(CH_3COOH)_2 \cdot 2H_2O$]. The brief experiment process is described here. 5.508 g of $Zn(CH_3COOH)_2 \cdot 2H_2O$ and PEG were dissolved in 300 ml of ethanol with a weight ratio of 10:1 (Zn: PEG). Mixture solution was stirred at 80 °C for 24 hours and then washed three to four times by methanol. Then it was calcined in the furnace at 150 °C for 2 h [4]. The synthesis equation is shown as Eq.3.1

$$Zn\,(CH_3COO)_2 + 2\,CH_3CH_2OH \rightarrow ZnO + 2\,CH_3COOCH_2CH_2 + H_2O$$

Eq.3.1

3.3 MAPLE parameters

MAPLE (PVD Products, Inc., USA) deposition is a contamination free surface modification system, which is able to protect the structure of organic target materials and create thickness controllable films. Figure 3.3 shows the MAPLE system and the

deposition chamber. For this project, MAPLE was applied to deposit polymers and inorganic nanoparticles.

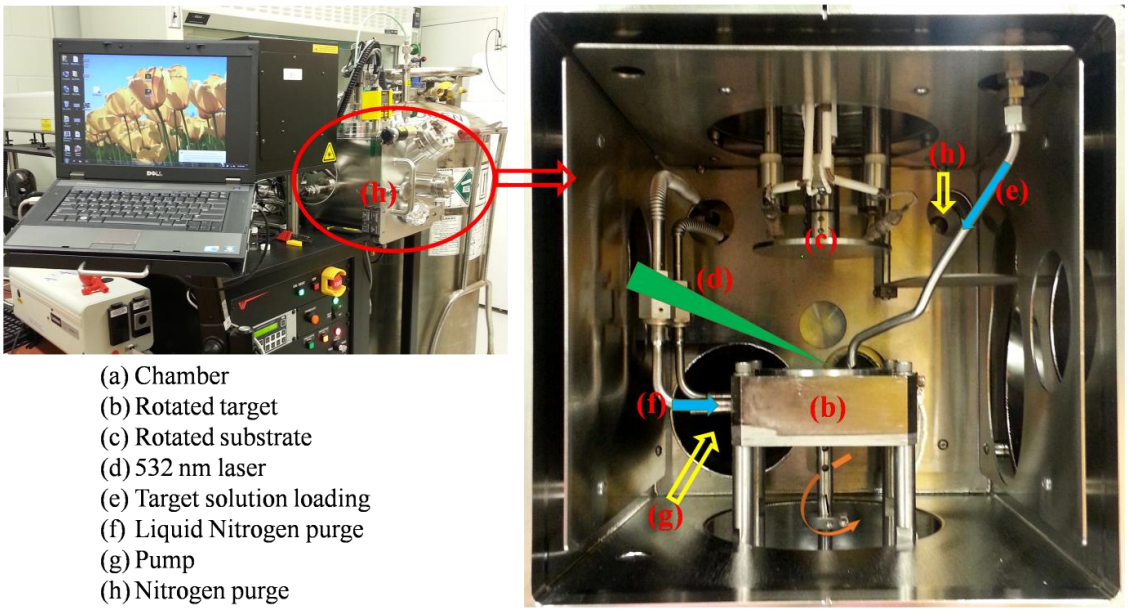

Figure 3.3 Illustration of MAPLE system and deposition chamber.

3.3.1 Polymer deposition

Thin film of polymer on the surface of silicone hydrogel was fabricated by MAPLE deposition. Polymers (PEG and PVP) were diluted in isopropanol with a concentration of 4 wt % and 1 wt % separately, and then liquid nitrogen was used to freeze the target solution. The laser used for deposition has the wavelength of 532 nm (λ_{em}), the frequency 10 Hz and the fluence about 1 J/cm^2. The temperature of the substrate is around 25 °C during the deposition. The depositions last for 2 hours and were conducted at a background pressure of 1×10^{-6} Torr with a substrate-to-target distance of 6 cm. Figure 3.4 shows the chemical structure of two polymers we used, one is PVP (10,000) and the other is PEG (200) [5].

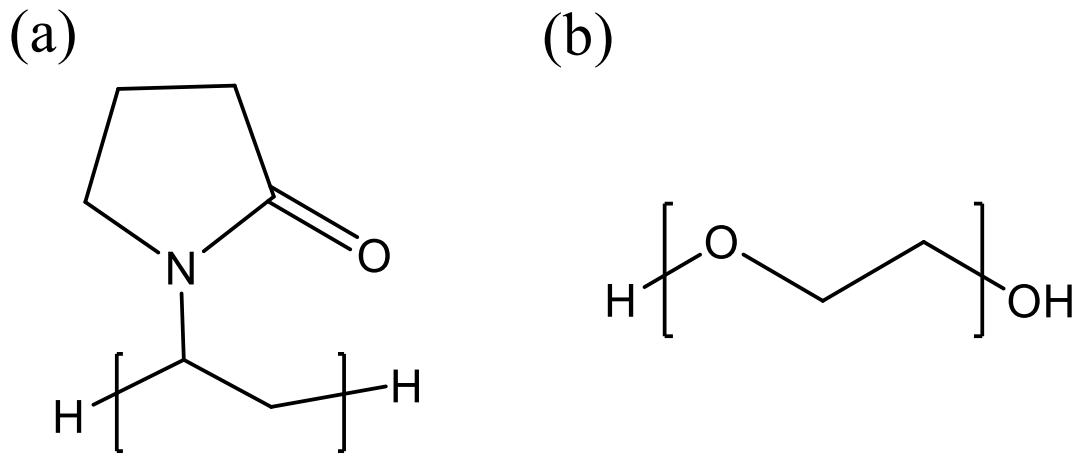

Figure 3.4 Chemical structures of (a) PVP and (b) PEG.

3.3.2 Nanoparticle deposition

Nanocomposite thin films (Ag-PVP and ZnO-PEG) on the surface of silicone hydrogel were fabricated by MAPLE deposition. Nanoparticles were diluted in isopropanol with a concentration of 0.5 wt %, after that liquid nitrogen was used to freeze the target solution. Nd: YAG laser at the wavelength 532 nm (λ_{em}) was used as the resource for MAPLE deposition. The ZnO-PEG NPs depositions lasted for 1 hour. The Ag-PVP NPs were deposited by different time (10 min, 20 min, 30 min and 60 min). All depositions were conducted at a background pressure of 1×10^{-6} Torr with a substrate-to-target distance of 6 cm.

3.4 Product characterization

The size and shape of nanoparticles before MAPLE and after MAPLE were observed by Transmission Electron Microscope (TEM, Philips CM10). The polymer films produce by MAPLE deposition was determined by Fourier Transform Infrared Spectroscopy (FTIR, Bruker FTIR-IFS 55) and Atomic Force Microscopy (AFM, Dimension 3100, Veeco Inc). The nanocomposite films after deposition was confirmed by UV-Visible Spectroscopy (UV-3600 Shimadzu, Japan), X-ray Diffraction (XRD, Rigaku RU-200BVH) and Energy-dispersive X-ray Spectroscopy (EDX, Hitachi 3400s), Photoluminescence Spectroscopy (PL, PTI QuantaMaster™ 40), Scanning Electron

Microscopy (SEM, Hitachi 3400s) and Atomic Force Microscope (AFM, Veeco Dimension 3100). Then Micro BCA assay (Thermo Scientific, U.S.A.) was carried out to measure the protein adsorption on each sample. The antibacterial property and mechanical strength were also measured. Last was the cytotoxicity test by MTT assay.

3.4.1 Transmission electron microscopy

Transmission electron microscopy (TEM) is a microscopy technique. A beam of electrons is transmitted through an ultra-thin specimen, and then interacts with the specimen as it passes through. An image is formed from the interaction of the electrons transmitted through the specimen; and the image is magnified and focused onto an imaging device or detected by a camera. The micrographs of Ag-PVP and ZnO-PEG NPs were examined by a Phillips CM10 TEM. The TEM samples, which used to characterize the nanoparticles before MAPLE deposition, were prepared by placing a drop of nanoparticles solution directly on a carbon coated copper grid (200 meshes). The samples were air dried before TEM examination. The samples after MAPLE deposition was prepared by placing the grid on the substrate during MAPLE process shown in Figure 3.5.

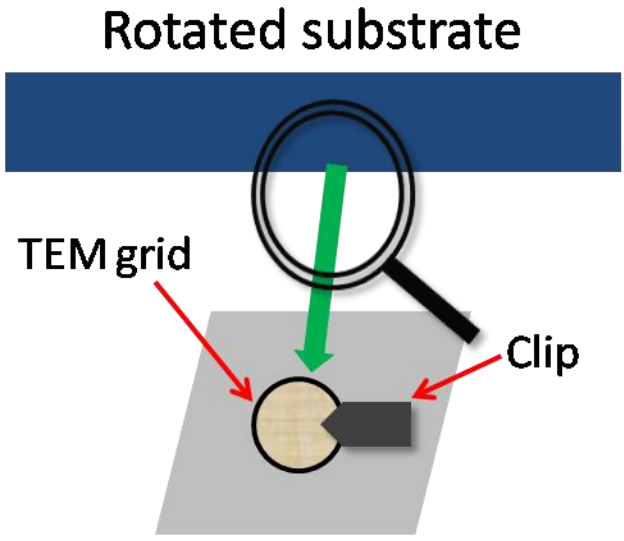

Figure 3.5 Preparation of copper grid for TEM observation after MAPLE deposition.

3.4.2 Fourier transform infrared spectroscopy

Fourier Transform Infrared spectroscopy (FTIR) is a technique, which is used to obtain an infrared spectrum of absorption, emission, photoconductivity or Raman scattering of a solid, liquid or gas. FTIR is based on the theory that each chemical group has characterized absorption infrared spectrum. In this project, FTIR was utilized to study the chemical structure of hydrogel and polymers, interaction of nanoparticles and surfactants, and the interaction between hydrogel and coating materials. And it is also used to confirm the presence of polymer films on silicone hydrogel produced by MAPLE process. The samples were scanned by FTIR in the range of 600–4000 cm^{-1} with a 1 cm^{-1} resolution. The instrument used air as background.

3.4.3 Ultraviolet–Visible spectroscopy

Ultraviolet–Visible Spectroscopy (UV-Vis) includes absorption spectroscopy and reflectance spectroscopy in the ultraviolet-visible spectral region, and it plays an important role in analytical chemistry. UV-Vis also has been extensively used in chemistry, physics and life sciences [6]. UV-Vis was carried out to confirm the surface plasmon resonance (SPR) of Ag-PVP NPs in solution and on the surface of silicone hydrogel. UV-Vis is also used to check the size and the shape of the synthesized Ag-PVP NPs. For antimicrobial test, UV-Vis is applied to measure the concentration of *E.coli* in PBS solution.

3.4.4 X-ray diffraction

Powder X-ray Diffraction (XRD) patterns were recorded by Rigaku RU-200BVH diffractometer employing a Co-Kα source (γ=1.7892 Å). XRD is able to measure the average spacings between layers or rows of atoms, determine the orientation of a single crystal or grain, find the crystal structure of an unknown material, and measure the size, shape and internal stress of small crystalline regions. For this project, the ZnO-PEG nanocomposite on silicone hydrogel was checked by XRD pattern compared to the standard reference (JCPDS no. 36-1451). The XRD patterns of ZnO-PEG NPs and ZnO-PEG nanocomposite film were compared in order to figure out if there is crystal damage after MAPLE deposition.

3.4.5 Scanning electron microscopy

Scanning Electron Microscopy (SEM) is a type of electron microscope, which generates images by scanning the surface of the samples with focused electron beam. When the electron beam interacts with the sample surface, the electron will be scattered and absorbed, which can be detected by specific detector. For sample preparation, specimens must be electrically conductive on the surface and also electrically grounded to prevent the accumulation of electrostatic charge. Therefore, organic samples need to coat conductive materials on the surface. In my project, bare silicone and ZnO-PEG coated silicone were coated with gold by HummerVI Sputter Coater. The surface morphology and Energy-dispersive X-ray spectroscopy (EDX) spectra were measured by SEM (Hitachi 3400s) at 10 kV.

3.4.6 Atomic force microscopy

Atomic Force Microscopy (AFM) is a high resolution scanning probe microscopy, which is able to observe the surface topography of a sample. It can be also used to measure thickness and roughness of the coating on the surface of substrate. All experiments were performed under tapping mode with atomic force microscope (AFM, Dimension 3100, Veeco Inc). A silicon nitride cantilever from Nanoscience with a nominal spring constant of 40 N/m and a tip radius of around 10 nm was used. When probe approaches the specimen surface, forces between probe and specimen may induce a deflection of the cantilever, which will be detected by a laser spot reflected from the top of cantilever into photodiode. In this project, the surface topography of PEG coated, PVP coated, Ag-PVP nanocomposite coated cover glass were examined by AFM. The film was scratched with a sharp tweezers to expose the glass substrate for thickness measurement.

3.4.7 Fluorescence spectroscopy

Fluorescence Spectroscopy is an instrument, which can be used to analyze the fluorescence from the samples, and it is also called as spectrofluorometer. It was used to measure the fluorescent property of ZnO-PEG nanoparticles solution and ZnO-PEG nanocomposite film on the surface of silicone. The equipment we use is QuantaMaster™ 40 Spectrofluorometer purchased from Photon Technology International Inc.

3.4.8 Mechanical test

A 1 x 1 cm sample of bare silicone hydrogel and target material coated silicone hydrogels were mounted in a BioTester 5000 test system (CellScale Biomaterials Testing, Waterloo, Ontario) by using the mounting system. The samples were stretched uniaxial with a loading of 0.2 N applied on the tensile test consistently. Meanwhile, the images of the deformation of the specimens were captured using a 1280x960 pixel charge coupled device CCD-camera. The stress and strain produced in order to understand the Stress-Strain curves of different samples and their Young's modulus (E), which is described as the Eq. 3.2 below. The slope of the Stress-strain curve is the Young's modulus (E) of the measured sample. Young's modulus is another way to display the stiffness property of a material.

$$\mathrm{E} = \frac{Stress}{Strain} = \frac{\sigma}{\varepsilon} = \frac{F/A}{\delta L/L_0}$$

Eq.3.2

Where E is the Young's modulus in Pascal (Pa), F the force applied in Newton (N), A the area perpendicular to the force vector (m^2), δL the displacement of the materials (m), and L_0 the original length of the materials (m).

3.4.9 Cell viability test

In vitro cell viability and cell proliferation is determined using the reduction of tetrazolium salt. It is now a widely accepted method of examining cell proliferation. Yellow tetrasolium MTT (3-(4, 5-dimethylthiazolyl-2)-2,5-diphenyltetrazolium bromide) is reduced by metabolically active cells. This is due in part to dehydrogenase enzymes generating intracellular purple formazan that can be solubilized and quantified by spectrophotometric means. 3T3 mouse fibroblast cells cultured in DMEM supplemented with 10% fetal bovine serum, and 1% penicillin and streptomycin. Cells were incubated under sterile conditions in 37 °C with 5% CO_2. Approximately 1×10^5 cells, determined by cell counting using a haemocytometer was seeded onto the bottom of 24 well plates and left to incubate overnight to ensure adhesion to the plate. Samples were added the

next day and left to incubate for 24 hours under sterile conditions. After 24 hours, the samples were removed and the media aspirated. 40 µl of 0.5% MTT solution, sterile filtered through 0.2um filter, was added to each well. Wells were made up to 500uL with cell media and left to incubate for 4 hours. The media was aspirated and rinsed twice with sterile PBS. Cells were lyzed and the formazan dissolved with 200 µl of DMSO. 150 µl from each well was pipetted into 96 cell plates for spectrophotometric analysis at 490nm.

3.5 Protein adsorption assay

Protein adsorption of artificial implants leads to protein fouling, which cause inflammatory response to human body, therefore the protein adsorption of hydrogels is another important index and was tested. Firstly, the samples (1cm × 1 cm) were immersed in PBS (phosphate buffer solution) for 24 hours, and then soaked in 0.5 mg/ml BSA-PBS solution for 3 hours at 37 °C. After that, PBS was used to rinse the samples 3 times to remove the non-absorbed BSA on the surface of hydrogel. After that the samples were immersed in 1 wt % SDS-PBS solution and sonicated for 20 minutes to completely detach BSA from hydrogel surface to the solution. Finally, the BCA protein assay kit (Micro BCA^{TM} Protein Assay Kit, Thermo Scientific, U.S.A.) was used to determine the protein concentration in SDS-PBS solution with a UV-Vis plate reader at the wavelength of 562 nm.

3.6 Thin film antimicrobial assay

The antibacterial activity of Ag-PVP and ZnO-PEG nanocomposite deposited silicone hydrogels obtained against the bacteria Escherichia coli (*E.coli*) was studied by the so-called antibacterial drop-test [7,8]. *E.coli* (strain W3110) were used as the experimental bacteria and cultured on the medium at 37°C for 18-24 h. Cultured bacteria were added in 10 ml PBS solution to reach the concentration of 10^8 CFU/ml approximately. The PBS bacteria solution was diluted to 10^6 CFU/ml for the ‘drop-test’ antibacterial experiments. Four groups of samples were prepared at the same area of 1 cm^2. UV light and PBS solution was used to sterilize and wash the samples. Sample groups are control (glass coverslip), bare silicone, Ag-PVP coated silicone and ZnO-PEG coated silicone. The samples were placed into sterilized 90 mm Petri dishes. Then 100 µl PBS solutions with

E.coli at a concentration of 10^6 CFU/ml were dropped onto the surface of each sample. The samples were laid at ambient temperature for a period of time (such as 1, 2, 4, 8, 12 hours). After each time period the bacteria containing drops were washed from the glass surfaces using 5 ml PBS in the sterilized Petri dish. Then 10 µl of each bacteria suspension was spread on the LB Agar plate. The number of surviving bacteria on the Petri dishes was counted after incubation for 24 h at 37°C. The relative numbers, which is the counted number of sample plate divided by the counted number of control plate, was used to show the results.

3.7 Reference

[1] Kim J, Conway A, Chauhan A. Extended delivery of ophthalmic drugs by silicone hydrogel contact lenses. Biomaterials 2008;29:2259–69.

[2] Ahmad M Bin, Tay MY, Shameli K, Hussein MZ, Lim JJ. Green Synthesis and Characterization of Silver/Chitosan/Polyethylene Glycol Nanocomposites without any Reducing Agent. Int J Mol Sci 2011;12:4872–84.

[3] Wei Q, Li B, Li C, Wang J, Wang W, Yang X. PVP-capped silver nanoparticles as catalysts for polymerization of alkylsilanes to siloxane composite microspheres. J Mater Chem 2006;16:3606.

[4] Tshabalala MA, Dejene BF, Swart HC. Synthesis and characterization of ZnO nanoparticles using polyethylene glycol (PEG). Phys B Condens Matter 2012;407:1668–71.

[5] Yin P, Engineering B, Studies P. Hydrogel-based Nanocomposites and Laser-assisted Surface Modification for Biomedical Application Hydrogel-based Nanocomposites and Laser-assisted Surface Modification for Biomedical Application 2012.

[6] Douglas A. Skoog. Principles of instrumental analysis. 4th ed. Toronto: Fort Worth; 1992.

[7] Sun S, Sun B, Zhang W, Wang D. Preparation and antibacterial activity of Ag – TiO 2 composite film by liquid phase deposition (LPD) method. Bull Mater Sci 2008;31:61–6.

[8] Trapalis CC, Keivanidis P, Kordas G, Zaharescu M, Crisan M, Szatvanyi A, et al. TiO 2 (Fe 3q) nanostructured thin films with antibacterial properties. Thin Solid Films 2003;433:186–90.

Chapter 4

4 Polymer films deposited by MAPLE process to reduce protein adsorption

Silicone hydrogel is a contact lens material used for long-term wearing because it has a different oxygen transport mechanism, which is transported through siloxane-phase rather than water [1]. However, silicone hydrogel still requires modification to improve comfort and biocompatibility for long term wearing. There are two important factors for long-term wearing experience of contact lenses. One is high oxygen permeability, which has been improved by the new transport mechanism of silicone, and the other is protein and lipid fouling resistance. As discussed in Chapter 2, hydrophobic surface will cause irreversible protein adsorption, which lead to numerous adverse clinical events [2,3]. Meanwhile, protein adsorption and the subsequent protein layer formation on the surface of biomedical implants will lead to microbial colonization and subsequent biofilm formation [4].

Due to the drawbacks of chemical structure, silicone hydrogel cannot keep the same level of hydrophilicity as PHEMA hydrogel [5]. Therefore, modification is needed for silicone hydrogel to reduce protein adsorption, which is caused by hydrophobic surfaces. Two main methods could be applied to modify silicone hydrogel. One is to incorporate hydrophilic monomers into the chemical structure, and the other is to modify the surface to improve the surface property. Surface modification is the most efficient way. There are many physical, chemical and even laser assisted surface modification methods. Among them, MAPLE deposition is one of the best choice for depositing polymers onto biomedical device without gas, solvent or other chemical contamination, and protecting the polymers' structure at the same time [6]. Consequently, MAPLE is an ideal surface modification method for silicone hydrogel modification in order to obtain a protein resistant surface, which is especially important property for long-term wearing contact lenses and other implant biological material.

4.1 Characterization of PEG deposited by MAPLE process

The mechanism of protein adsorption was introduced in chapter 2. Hydrophilic surface will lead to less irreversible protein adsorption. Therefore, the problem of nonspecific adsorption can be prevented by modify the substrate surface with a material that could reduce protein adsorption; such materials are typically hydrophilic and zwitterionic materials [7]. Poly (ethylene glycol) (PEG) is a biocompatible polyester compound, which is extensively used in our daily life from industrial products to medical application. Due to the C=O bond and -OH bond in PEG structure, it is a water solvable polymers. Therefore PEG has played an important role in reducing and eliminating protein adsorption to surfaces [8,9].

4.1.1 FTIR analysis of PEG on silicone hydrogel

FTIR was carried out to investigate chemical groups on bare silicone and the PEG thin

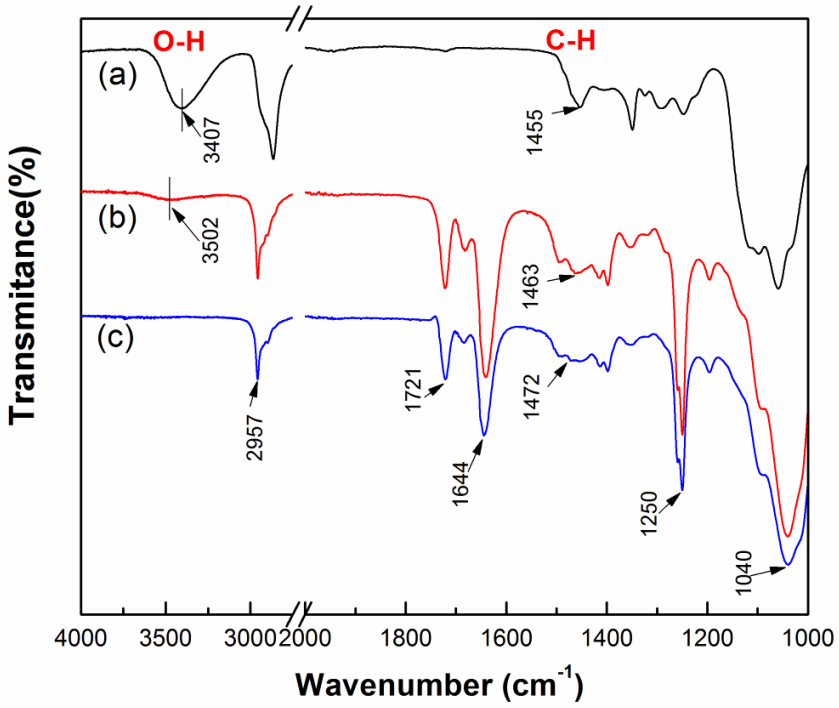

Figure 4.1 FTIR spectra of (a) bare PEG, (b) Silicone-PEG, and (c) bare silicone hydrogel.

film on the surface of silicone hydrogel. Figure 4.1 shows the FTIR spectra of bare PEG, PEG coated silicone hydrogel (Silicone-PEG) and bare silicone hydrogel. The bands at 1721 cm^{-1}, 1644 cm^{-1}, 1250 cm^{-1} and 1040 cm^{-1} all stand for the vibration of C=O group from silicone hydrogel shown in Figure 4.1(c). The band around 2957 cm^{-1} belongs to the stretching vibration of C-H from silicone. All these band introduced above are not affected by MAPLE deposition (Figure 4.1(b)). Compared Figure 4.1 (a) and (b), we can find out that PEG and PEG coated silicone have the band at 3407 cm^{-1} and 3502 cm^{-1} respectively, which represent stretching vibration of the O-H in PEG molecule [10]. There is no -OH group in bare silicone shown in Figure 4.1(c). All spectra in Figure 4.1 have the band between 1455 cm^{-1} and 1475 cm^{-1}, which indicates the C-H bending vibration from CH_2 group of PEG or silicone hydrogel [11]. Due to the overlap of Figure 4.1 (a) and (c), the C-H band shift from 1472 cm^{-1} to 1463 cm^{-1} shown in Figure 4.1(b). The appearance of O-H stretching vibration and the shift of C-H bending vibration from Figure 4.1 (b) confirm that PEG has been deposited onto the silicone hydrogel by MAPLE process.

4.1.2 AFM images of PEG thin film

AFM was applied to observe the surface morphology and measure the thickness and roughness of PEG thin film on glass coverslip produced by MAPLE deposition. Figure 4.2 shows 3D AFM image of PEG thin film. Before measurement we scratched the edge of the sample first, and then used the vertical distance between the surface of the film and the surface of glass coverslip to get the thickness. This 3D image also confirms the presence of PEG thin film. Figure 4.2 shows the thickness of this PEG film is around 155 nm after 2 hours deposition, which indicates MAPLE process is able to produce an ultra-thin (nano-level) film. Meanwhile the roughness of PEG film is only 10.6 nm, which confirms the PEG film is homogenous.

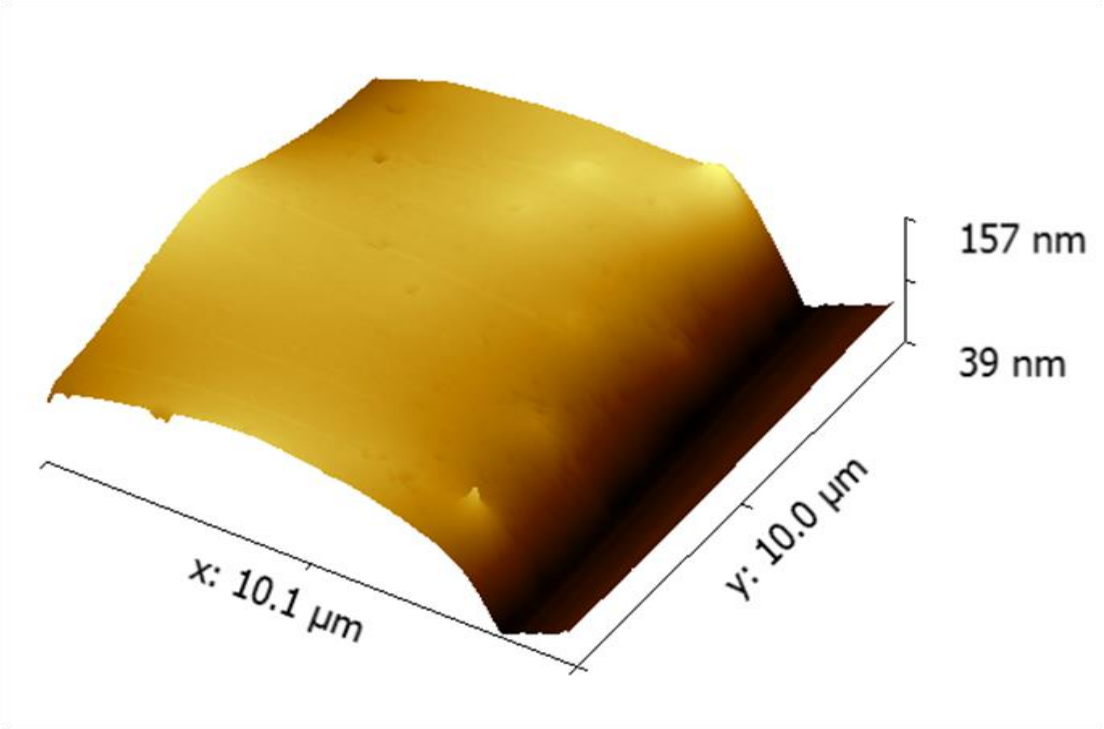

Figure 4.2 PEG film on the surface of cover glass measured by AFM.

4.2 Characterization of PVP deposited by MAPLE process

Polyvinylpyrrolidone (PVP) is a synthetic polymer, and has been extensively used in biomedical applications for a long time since it was first discovered in Germany in 1930 [12]. PVP has several beneficial properties, which make it suitable for biomedical applications such as high water solubility, chemical stability, good biocompatibility, and biological inertness [13,14]. Therefore, PVP is an ideal polymer for surface modification to reduce nonspecific protein adsorption [15].

4.2.1 FTIR analysis of PVP on silicone hydrogel

FTIR was used to study if PVP film deposited onto silicone hydrogel by MAPLE process. Figure 4.3 shows the FTIR spectra of bare PVP, PVP coated silicone (Silicone-PVP) as well as bare silicone. PVP can easily adsorb water from environment. Therefore, PVP has the peak around 3417cm^{-1}, which is O-H stretching vibration band as shown in Figure 4.3(a). Bare silicone hydrogel do not have any band between 3670 cm^{-1} and 3230 cm^{-1}, which demonstrate there is no -OH group on silicone hydrogel. Meanwhile, there is a band of C-H vibration at 1493cm^{-1} shown in Figure 4.3(a) [16], which is not presented in Figure 4.3(c). However, C-H (1494cm^{-1}) and O-H (3467cm^{-1}) vibration bands (come from PVP) show up in the spectrum of Silicone-PVP, which confirm that the PVP shows up on the surface of silicone after MAPLE deposition.

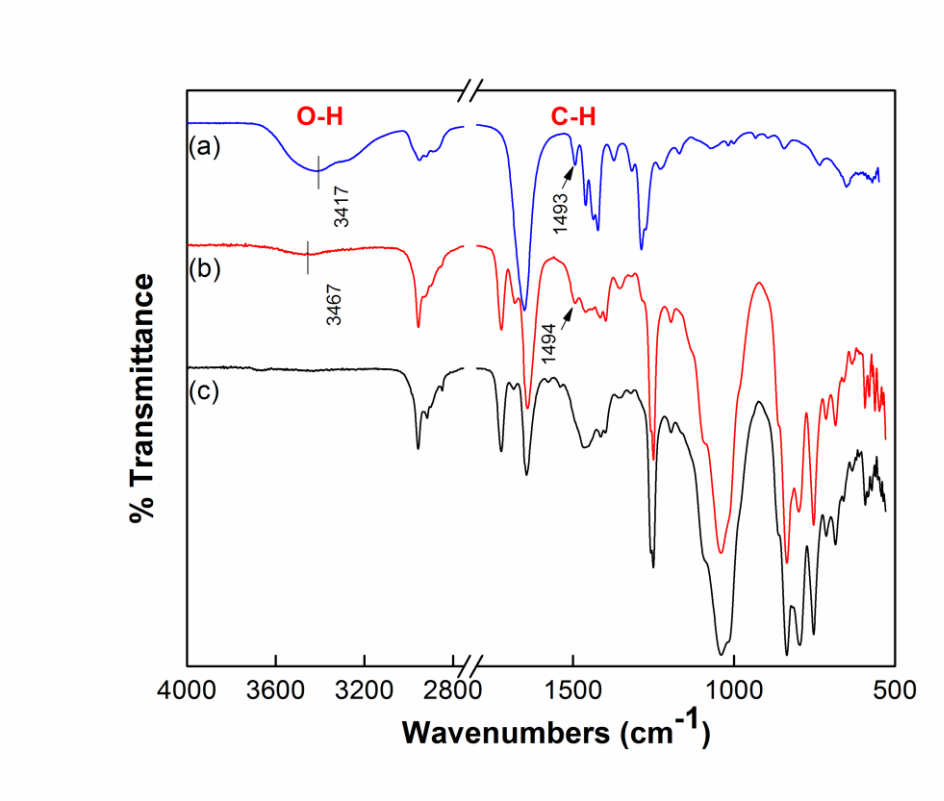

Figure 4.3 FTIR spectra of (a) PVP, (b) Silicone-PVP, and (c) bare silicone hydrogel.

4.2.2 AFM images of PVP thin film

In order to observe the surface morphology and measure the thickness and roughness of PEG thin film on glass coverslip produced by MAPLE deposition, AFM was carried out

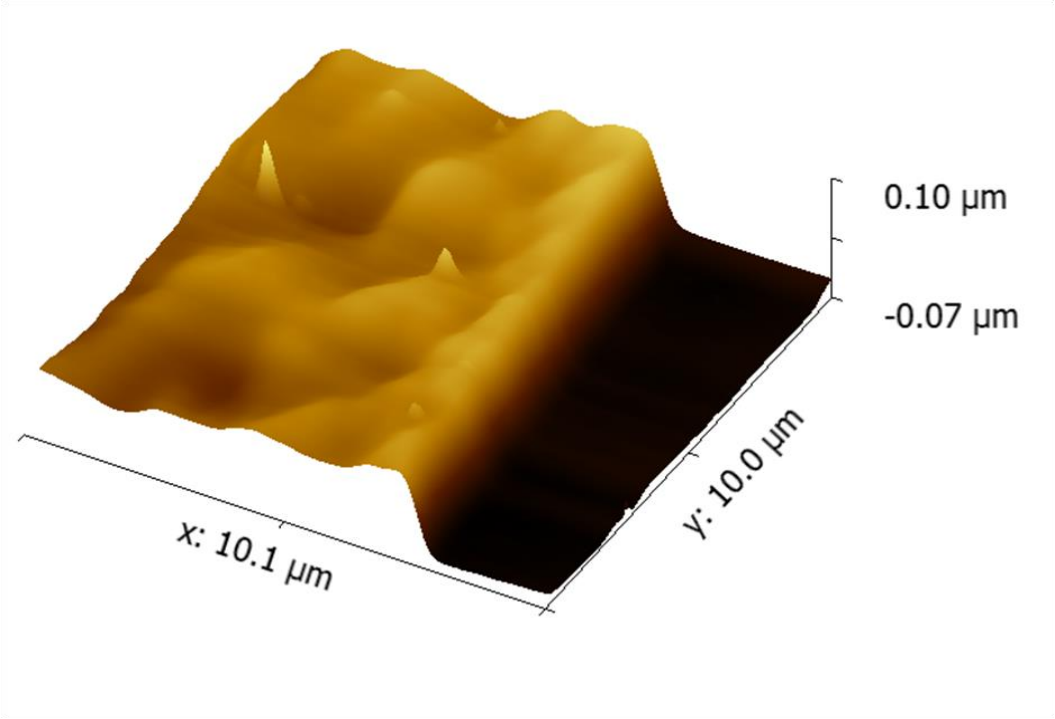

Figure 4.4 PVP film on the surface of cover glass measured by AFM.

to scan the surface of PVP coated surface after 2 hours deposition by MAPLE. Figure 4.4 shows 3D morphology of PVP thin film. After scratching the edge of the sample, we use the vertical distance between the surface of the film and the surface of glass coverslip to get the thickness. The thickness of this PVP film is around 45.4 nm, and the roughness of PEG film is 14.8 nm. This 3D image also helps to confirm the presence of homogenous PEG thin film produced by MAPLE.

4.3 Protein adsorption

Micro BCA method was used to measure the protein adsorption property of silicone and polymers coated silicone. Figure 4.5 shows BSA adsorption of bare silicone, PEG coated silicone and PVP coated silicone are 6.11µg/cm^2, 4.39 µg/cm^2, 4.97 µg/cm^{2}respectively.The BSA adsorbed on the surface of PEG thin film and PVP thin film decreases to 71.8% and 81.3% respectively after comparing with bare silicone. PEG and PVP have been demonstrated that they have the property to reduce non-specific protein adsorption [10,17]. PVP and PEG provided a more hydrophilic surface than bare silicone due to the C=O and -OH from their chains. It is well known that BSA is an globular

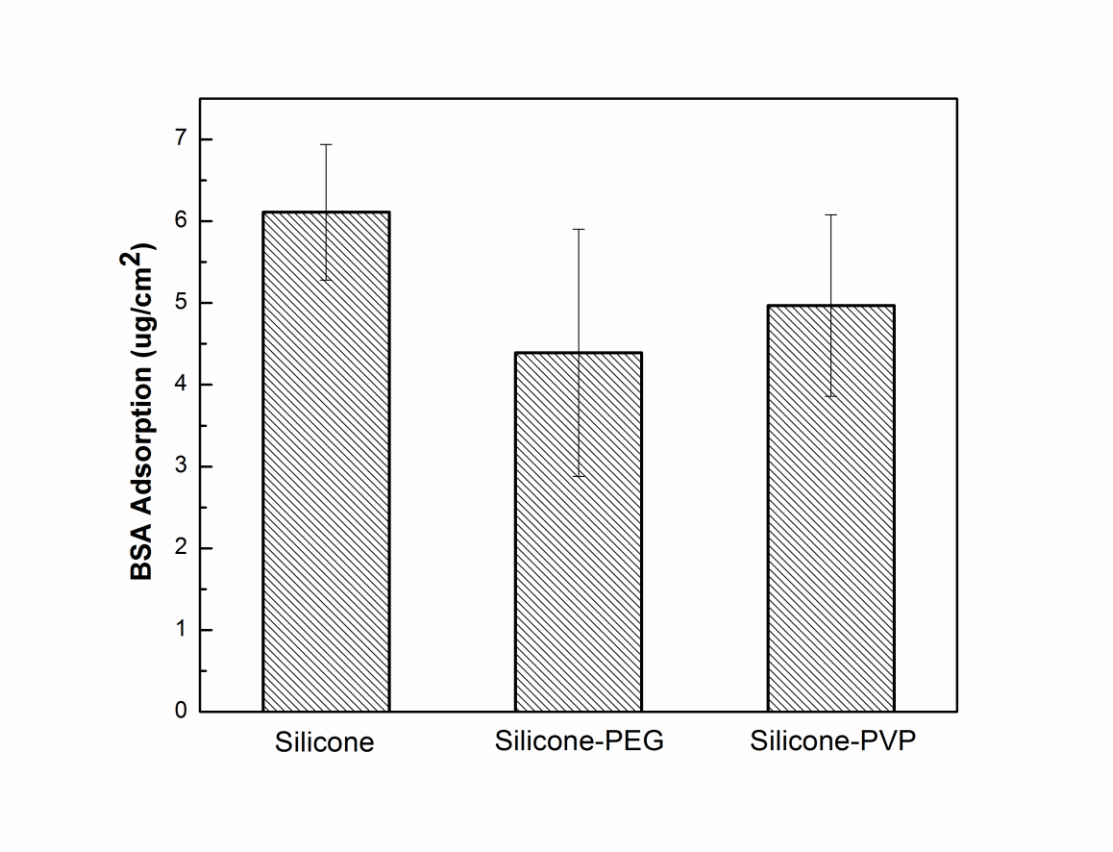

Figure 4.5 BSA adsorption of silicone, Silicone-PEG, and Silicone-PVP.

protein and its hydrophobic (non-polar) amino acids are protected inside of the protein molecule and hydrophilic(polar) amino acids side chain will be held outside to interact with their environment [2,10]. When the BSA interacts with hydrophobic surface, the protein core will try to interact with the hydrophobic surface in order to reach lower Gibbs energy, which will denature the protein structure. On the other side, when BSA interacts with hydrophilic surface, it will easily adsorb onto the surface without structure change, so it is not hard to wash the protein off. Consequently, polymer coated silicone will adsorb less protein than bare silicone hydrogel.

4.4 Young's modulus

The values of the Young's modulus (E) are shown in Table 4.1, which are obtained from the slope of Stress-Strain curves. Table 4.1 shows the Young's Modulus of silicone

hydrogel increases from 0.7083 MPa to 0.7668 MPa and 0.7236 MPa separately after coating PEG and PVP by MAPLE process, which means the stiffness of silicone hydrogel can be slightly increased by PEG and PVP thin film on the surface. According to previous research, the young's modulus range of human skin is between 0.42 MPa and 0.85 MPa depending on different ages[18]. Young's modulus of polymers coated silicone hydrogels still in this range after modification, which means it is suitable to be used as biological materials.

Table 4.1 Young's Modulus (E) of silicone and polymer coated silicone hydrogel.

	Silicone	Silicone-PEG	Silicone-PVP
E (MPa)	0.7083 ± 0.1640	0.7668 ± 0.1790	0.7236 ± 0.0796

4.5 Cell viability of hydrogels

It is known that modified silicone hydrogels are supposed to contact with cells as contact lens materials or other body implants. Therefore, the biocompatibility test of the silicone and polymer coated hydrogel is an important measurement. The cell response to silicone, Silicone-PEG and Silicone-PVP were investigated using NIH/3T3 mouse fibroblast cells. Samples were soaked into culture medium and incubated with cells for 24 h. Figure 4.6 indicates that the cell viability of silicone, Silicone-PEG and Silicone-PVP are 146.5%, 129.3% and 108.3% individually. Bare silicone has the highest number which is confirmed that silicone hydrogel is a biocompatible material. Meanwhile all the samples' cell viability reaches higher than 100%, which demonstrates that PEG and PVP coated silicone do not cause harmful effects to the cells.

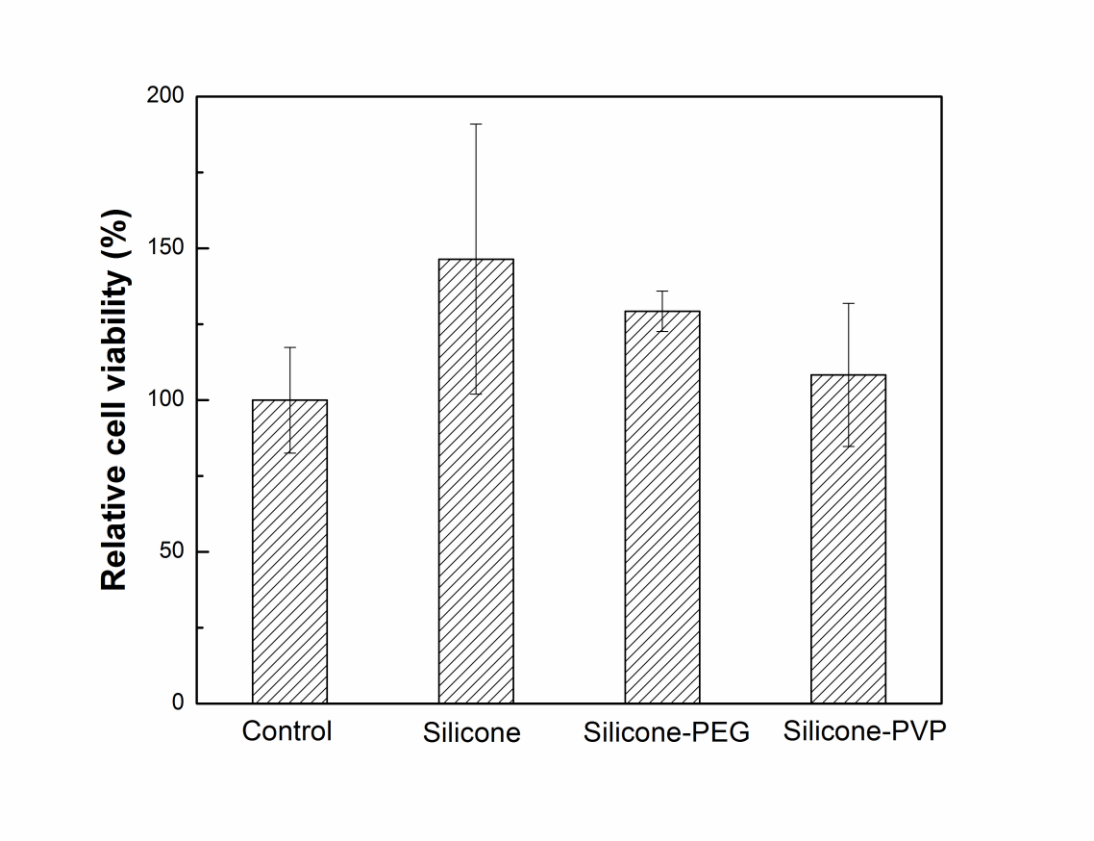

Figure 4.6 Cell viability of control, Silicone, Silicone-PEG and Silicone-PVP.

4.6 Conclusion

MAPLE technique is suitable for silicone hydrogel surface modification with PEG and PVP. The presence of polymers (PEG and PVP) on silicone hydrogel is confirmed by FTIR and AFM. According to result FTIR spectra, PEG and PVP polymers coated silicone have the –OH vibration band which demonstrate MAPLE produced polymer films is able to modify the surface to obtain hydrophilic property. AFM images indicate the polymers are homogenously spread (the roughness is around 10-15 nm) on the surface of silicone with the thickness of nanometer level. Followed by protein adsorption test, the polymer coated silicone show good protein resistance property, which can reduce 28.2% (PEG) and 18.7% (PVP) BSA adsorption compared to bare silicone. Moreover, The Young's modulus of polymer coated silicone hydrogels are increased from 0.7083 MPa to 0.7668 MPa (PEG coating) and 0.7236 MPa (PVP coating) separately. It is

expected that this PEG and PVP coated silicone hydrogel produced by MAPLE process can be used as a potential long-term wearing contact lens or other biological implants material due to its protein resistance.

4.7 Reference

[1] Nicolson PC. Continuous wear contact lens surface chemistry and wearability. Eye Contact Lens 2003;29:S30–2; discussion S57–9, S192–4.

[2] Luensmann D, Jones L. Protein deposition on contact lenses: the past, the present, and the future. Cont Lens Anterior Eye 2012;35:53–64.

[3] Bond H, Waals V Der, Waals D. Intermolecular and Surface Forces n.d.:1–18.

[4] Banerjee I, Pangule RC, Kane RS. Antifouling coatings: recent developments in the design of surfaces that prevent fouling by proteins, bacteria, and marine organisms. Adv Mater 2011;23:690–718.

[5] Vandenbulcke K, Horvat L-IL, De Mil M, Slegers G, Beele H. Evaluation of the antibacterial activity and toxicity of 2 new hydrogels: a pilot study. Int J Low Extrem Wounds 2006;5:109–14.

[6] Caricato a. P, Luches a., Leggieri G, Martino M, Rella R. Matrix-assisted pulsed laser deposition of polymer and nanoparticle films. Vacuum 2012;86:661–6.

[7] VandeVondele S, Vörös J, Hubbell J a. RGD-grafted poly-L-lysine-graft-(polyethylene glycol) copolymers block non-specific protein adsorption while promoting cell adhesion. Biotechnol Bioeng 2003;82:784–90.

[8] Michel R, Pasche S, Textor M, Castner DG. The Influence of PEG Architecture on Protein Adsorption and Conformation. Langmuir 2005;21:12327–32.

[9] Malmsten M, Emoto K, Van Alstine JM. Effect of Chain Density on Inhibition of Protein Adsorption by Poly(ethylene glycol) Based Coatings. J Colloid Interface Sci 1998;202:507–17.

[10] Yin P, Engineering B, Studies P. Hydrogel-based Nanocomposites and Laser-assisted Surface Modification for Biomedical Application Hydrogel-based

Nanocomposites and Laser-assisted Surface Modification for Biomedical Application 2012.

[11] Derrick MR. Infrared Spectroscopy in Conservation Science. Los Angeles: The Getty Conservation Institute; 1999.

[12] Wu Z, Chen H, Liu X, Zhang Y, Li D, Huang H. Protein adsorption on poly(N-vinylpyrrolidone)-modified silicon surfaces prepared by surface-initiated atom transfer radical polymerization. Langmuir 2009;25:2900–6.

[13] Liu X, Wu Z, Zhou F, Li D, Chen H. Poly(vinylpyrrolidone-b-styrene) block copolymers tethered surfaces for protein adsorption and cell adhesion regulation. Colloids Surf B Biointerfaces 2010;79:452–9.

[14] Liu X, Xu Y, Wu Z, Chen H. Poly(N-vinylpyrrolidone)-modified surfaces for biomedical applications. Macromol Biosci 2013;13:147–54.

[15] Gao B, Hu H, Guo J, Li Y. Preparation of polymethacrylic acid-grafted HEMA/PVP microspheres and preliminary study on basic protein adsorption. Colloids Surf B Biointerfaces 2010;77:206–13.

[16] Rapado Raneque M, Rodríguez Rodríguez A, Peniche Covas C. Hydrogel wound dressing preparation at the laboratory scale by using electron beam and gamma radiation. Nucleus 2013:24–31.

[17] Jiang J, Zhu L, Zhu L, Zhang H, Zhu B, Xu Y. Antifouling and antimicrobial polymer membranes based on bioinspired polydopamine and strong hydrogen-bonded poly(N-vinyl pyrrolidone). ACS Appl Mater Interfaces 2013;5:12895–904.

[18] Agache PG. Original Contributions. Arch Dermatol Res 1980;269:221–32.

Chapter 5

5 Nanocomposite film deposited by MAPLE process to reduce protein adsorption and inhibit bacteria growth

Nanomaterials have been extensively used in the past decade because of their distinctive physical and chemical properties. Nanocomposite is defined as a multiphase solid material where one of the phases has at least one dimension less than 100 nanometers(nm) [1]. Due to the different structures, compositions and properties of the constituents in a nanocomposite, it serves various functions. The products made from nanocomposite are usually multifunctional.

Silicone hydrogels are polymers with a backbone consisting entirely of silicon-oxygen bonds (siloxane), which is responsible for their high gas permeability, so silicone hydrogel can provide higher oxygen permeability than PHEMA based contact lens materials [2]. Therefore silicone hydrogel is especially suitable for continuous wear due to their higher oxygen permeability over conventional hydrogel lenses [3]. However some drawbacks still exist, such as bacterial attachment and protein adsorption on its surface.

Nanocomposite coating for silicone hydrogel can offer a multifunctional surface to lessen the drawbacks of bare silicone hydrogel. MAPLE process is able to deposit sensitive materials on the subtract surface to remain undamaged due to the low target material concentration and frozen matrix target provide by liquid nitrogen [4]. MAPLE has been used to successfully deposit a wide range of nanoparticle films, including thin-film carbon nanoparticle layers [5], SnO_2 nanoparticle layers [6] and TiO_2 nanoparticle/nanorod thin films [7], where fine control of deposited nanoparticle size was achieved [8].

5.1 Characterization of Ag-PVP nanoparticles and Ag-PVP nanocomposite thin film deposited by MAPLE process

Silver nanoparticles (Ag NPs) have emerged as one of the most popular research areas in the field of nanotechnology due to their well-known effectiveness in biomedical,

electronic, catalytic and optical applications [9]. Silver metal and silver ions have been known as effective antimicrobial reagents for a long time especially in the biomedical field, where they have been used for wound or burn dressings, catheters and bone cement [10]. Ag-PVP nanoparticles (Ag-PVP NPs) were used to modify the silicone hydrogel by MAPLE process to inhibit bacteria growth on silicone hydrogel surface. The antibacterial mechanism of Ag NPs is still not very clear. One of the most popular theories is that Ag NPs release silver ions, and silver ions are known to cause damages to bacterial DNA, proteins, enzymes, as well as the bacterial cell wall. The other is Ag NPs will interact with the cell wall and then destroy the metabolic response [11]. Although there are other theories, these two are the most extensively agreed upon. In order to synthesize Ag-PVP NPs, PVP was used as a stabilizer that will control the particle size, size distribution, shape, dispersion, etc. PVP is a also hydrophilic polymer, which will be unaffected by the changes in pH and ionic strength and will also help to provide a hydrophilic surface [12]. In this part, Ag-PVP NPs were used to modify the surface of silicone hydrogel to form an antimicrobial and hydrophilic surface. MAPLE deposition was carried out to prevent environment contamination during the coating process and create a homogenous film on silicone hydrogel.

5.1.1 TEM observation of Ag-PVP NPs

Figure 5.1 (a) shows the TEM micrograph of Ag-PVP NPs synthesized by UV-reduction. Figure 1 (b) is the TEM micrograph of Ag-PVP NPs deposited on Cu grid by MAPLE process. The scale is 100 nm. The insert small figures of Figure 5.1 (a) and (b) depict the size distribution. The average size of Ag-PVP NPs after MAPLE process is 11.61nm ± 3.58nm, which is bigger than Ag-PVP NPs that do not participate in MAPLE process (11.29 nm ± 1.88 nm). The size distribution is also broadened by MAPLE process at the same time. Surface Plasmon Resonance (SPR) property of Ag-PVP NPs is one of the most important reasons why the particle size of Ag-PVP NPs is changed by MAPLE process.

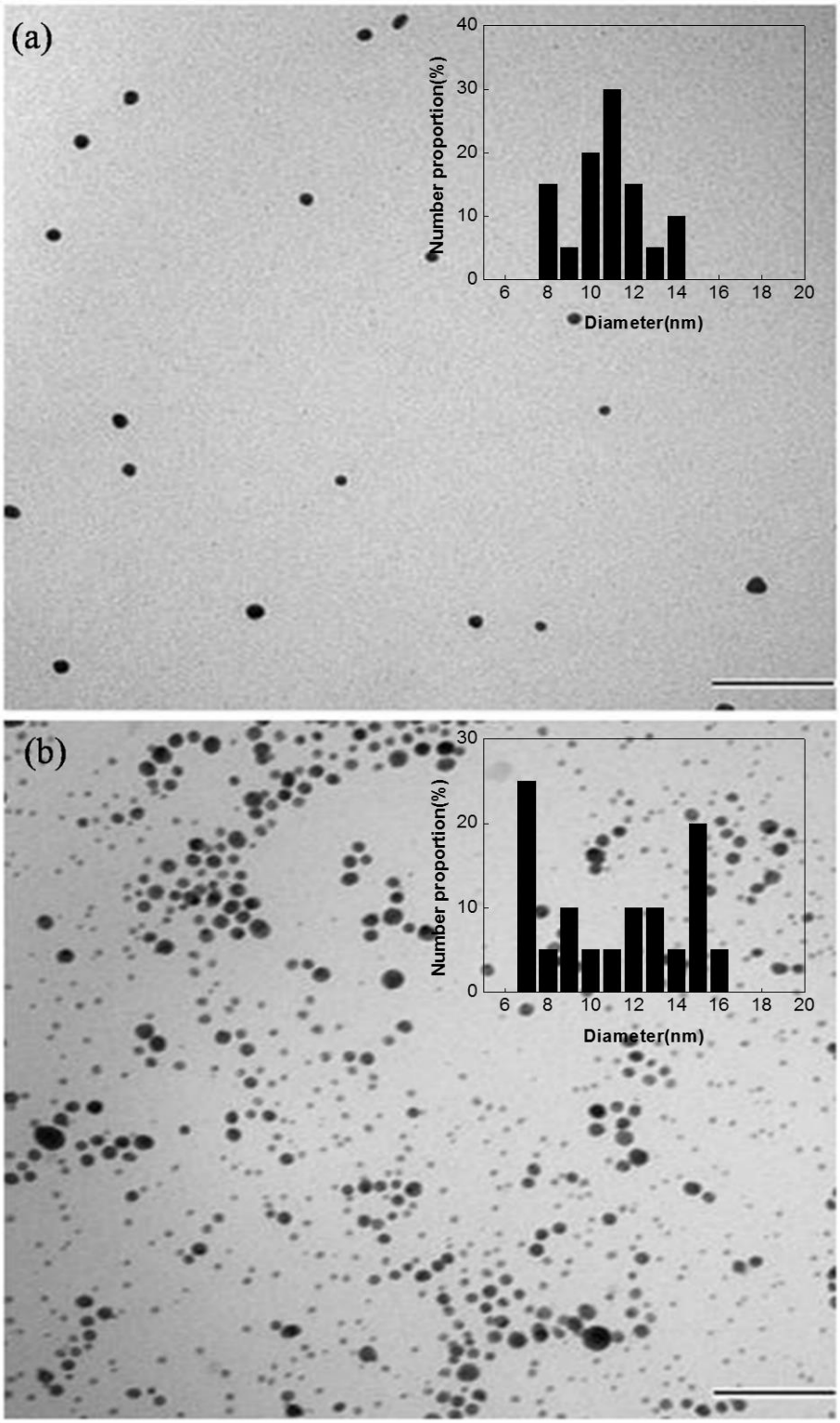

Figure 5.1 TEM micrograph of (a) Ag-PVP NPs, and (b) Ag-PVP NPs on substrate after MAPLE process.

When laser irradiates the frozen target, the isopropanol adsorbs the energy of 532nm laser and then starts to melt. After the isopropanol melts, the plasmon in the silver particles absorb photons from the 532nm laser and the electrons become excited, which produce a rapid temperature rise of Ag NPs. Due to less energy lost in the solution, the silver particle melts and becomes liquid[13]. When the temperature of the silver particles reaches the boiling point, atom sand/or small particles are ejected through vaporization into the surrounding solvent[14,15]. As a result, the reduction of particle size happened. However, the small particles are very unstable in the solution and they tend to aggregate onto the surface of other silver particles, which leads to the size of some silver particles to increase[13]. Therefore, the size of Ag-PVP NPs becomes non-uniform after MAPLE process.

5.1.2 FTIR analysis

The main chemical groups of pure PVP, Ag-PVP NPs, bare silicone and Ag-PVP

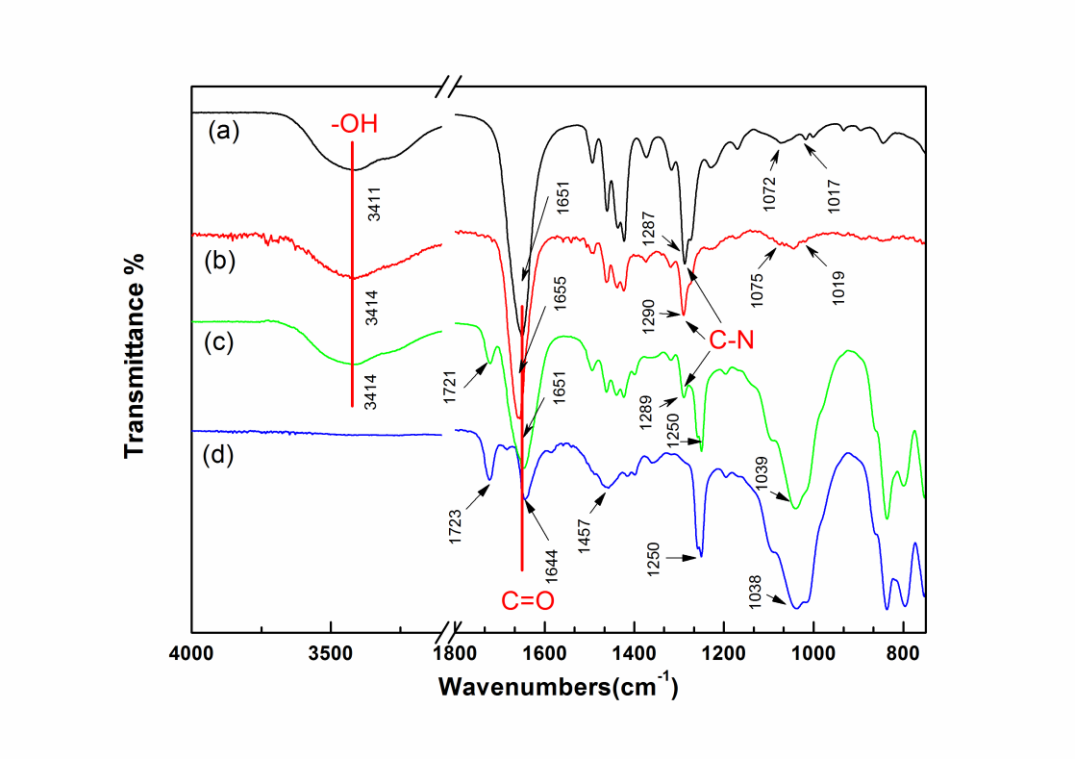

Figure 5.2 FTIR spectra of PVP, (b) Ag-PVP NPs, (c) Ag-PVP nanocomposite coated silicone, and (d) bare silicone hydrogel.

nanocomposite coated silicone hydrogel (Silicone-Ag-PVP) were examined by FTIR. Figure 5.2 (a) shows the FTIR spectrum of the pure PVP, and the bands of 1287 cm^{-1}, 1072cm^{-1} and 1017cm^{-1} indicates the C-N vibration band from PVP [16]. Figure 5.2 (b) is the FTIR spectrum of Ag-PVP NPs. C-N vibration band in Figure 5.2 (b) red shift to 1290 cm^{-1}, 1075 cm^{-1} and 1019 cm^{-1} compared with bare PVP, which confirm the silver atom is coordinated with N of the PVP [17]. The vibration band of C=O as shown in Figure 5.2 (b) is also red shifted from 1651 cm^{-1} to 1655 cm^{-1}, which indicates coordination band between silver atom and C unit from PVP [18].

Figure 5.2 (c) and (d) are the FTIR spectra of Silicone-Ag-PVP as well as bare silicone hydrogel. The bands at 1723 cm^{-1}, 1644 cm^{-1}, 1250 cm^{-1} and 1038 cm^{-1} are all stand for C=O vibration bands of silicone hydrogel shown in Figure 5.2 (d). After MAPLE process, most of the C=O vibration bands of silicone-Ag-PVP keep the same only the

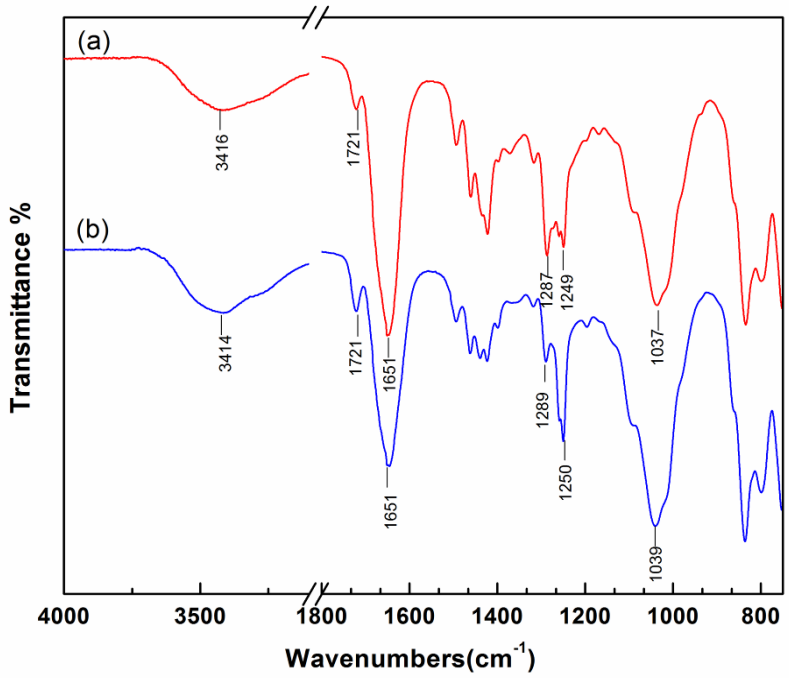

Figure 5.3 FTIR Spectra of (a) Silicone-Ag-PVP (MAPLE), and (b) Ag-PVP NPs coated silicone (Air dry).

band of 1644cm^{-1} shifted to 1651 cm^{-1} compared to Figure 2(d). The shift of C=O vibration band is because the overlap of C=O vibration from Ag-PVP NPs (1655 cm^{-1}) and bare silicone (1644 cm^{-1}). From Figure 5.2(c) we can find out that Silicone-Ag-PVP also has the C-N (1289 cm^{-1}) vibration band, which doesn't exist on bare silicone hydrogel (Figure 2(d)). Owing to the PVP's adsorption of water in the environment, PVP has the peak of 3411 which is O-H stretching vibration band as shown in Figure 5.2(a). Figure 5.2(c) shows silicone hydrogel after MAPLE process also has -OH group. The shift of C=O vibration and the presence of C-N vibration and O-H stretching vibration in Figure 5.2 (c) demonstrate the PVP from Ag-PVP NPs is deposited on silicone hydrogel. However, FTIR spectra cannot confirm whether Ag NPs were deposited on silicone together with PVP. Thus other characterization methods need to be applied to test Silicone-Ag-PVP.

Figure 5.3 (a) and (b) are the FTIR spectra of Ag-PVP NPs coated silicone hydrogel by the method of MAPLE process and Drop-Air-dry method separately. After comparing main vibrations from Figure 5.3 (a) and (b), there are no significant differences of the main bands, so Figure 5.3 indicates that MAPLE process does not break the chemical structure of PVP on the Ag-PVP nanocomposite.

5.1.3 EDX of Silicone-Ag-PVP

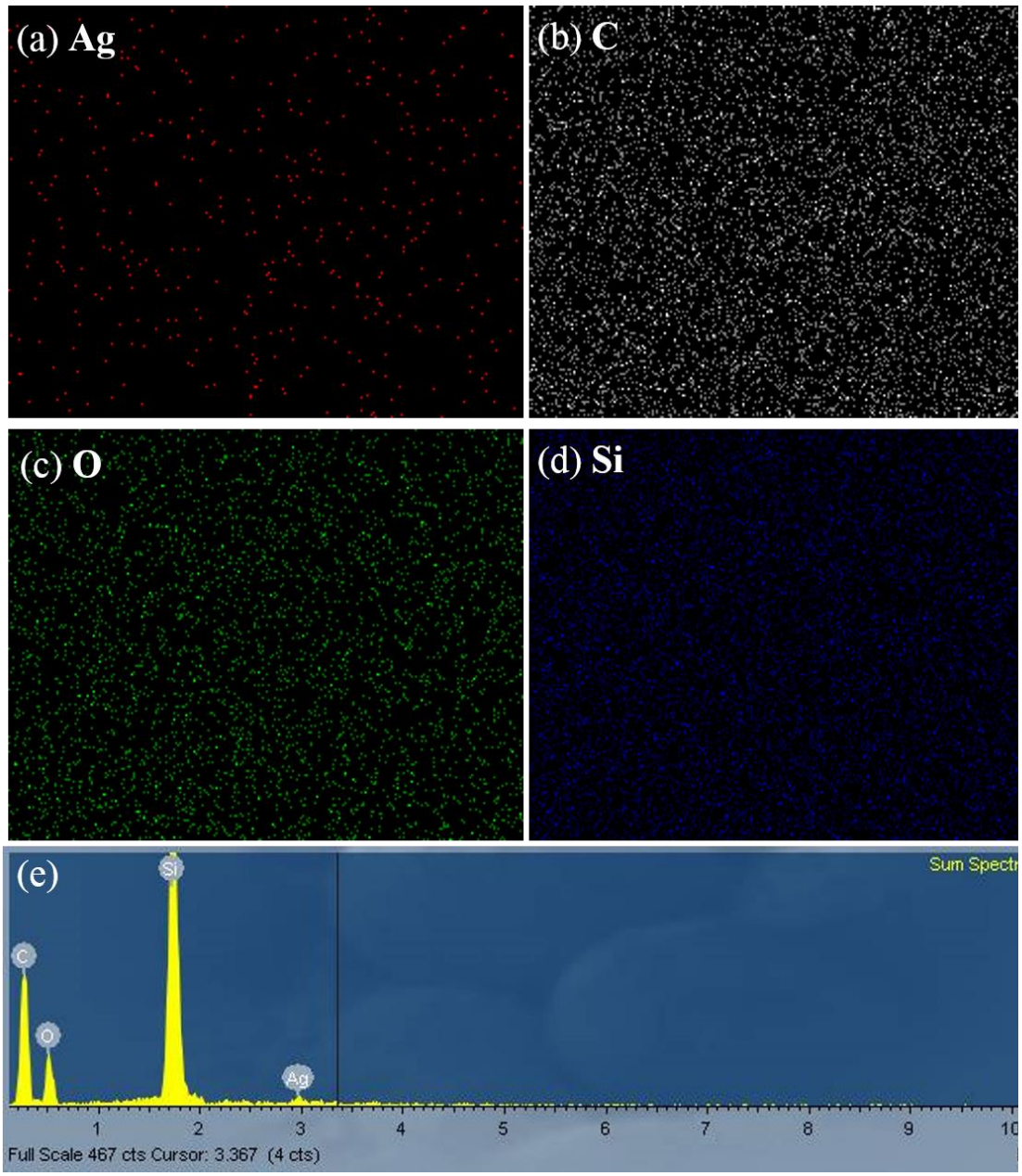

Figure 5.4 EDX mapping micrograph of (a) Ag, (b) C, (c) O and (d) Si; (e) EDX spectrum of Silicone-Ag-PVP.

Figure 5.4 includes the EDX mapping and EDX spectrum of the elements from Silicone-Ag-PVP produced by MAPLE. The dots of Figure 5.4 (a), (b), (c) and (d) are the elements of Ag, C, O and Si from silicone and PVP individually. Figure 5.4 (e) is the EDX spectrum of Silicone-Ag-PVP. The presence of silver element can be evidenced by

the EDX mapping and the EDX spectrum. Figure 5.4(a) also indicates that the Ag element on the silicone is homogenous distributed. However, EDX spectrum and mapping can only confirm the existence of Ag element on the surface of silicone.

5.1.4 Optical property of Ag-PVP NPs and Silicone-Ag-PVP

UV-visible spectroscopy was applied to characterize Ag-PVP NPs and Silicone-Ag-PVP, Ag-PVP NPs drop and air dried on silicone hydrogel as well as bare silicone hydrogel. Typically the UV adsorption peak which is the surface plasmon resonance (SPR) band was affected by the size, shape, dielectric environment of nanoparticles [19]. Figure 5.5 (a) shows the UV-Vis spectrum of Ag-PVP NPs which has SPR peak at 417 nm. Previous study shows that the Ag NPs will be spherical if the SPR band is around 400 nm[9]. Therefore, the shape of Ag-PVP NPs should be spherical as same as the result from TEM micrograph. Ag-PVP nanocomposite coated silicone hydrogel produced by MAPLE has

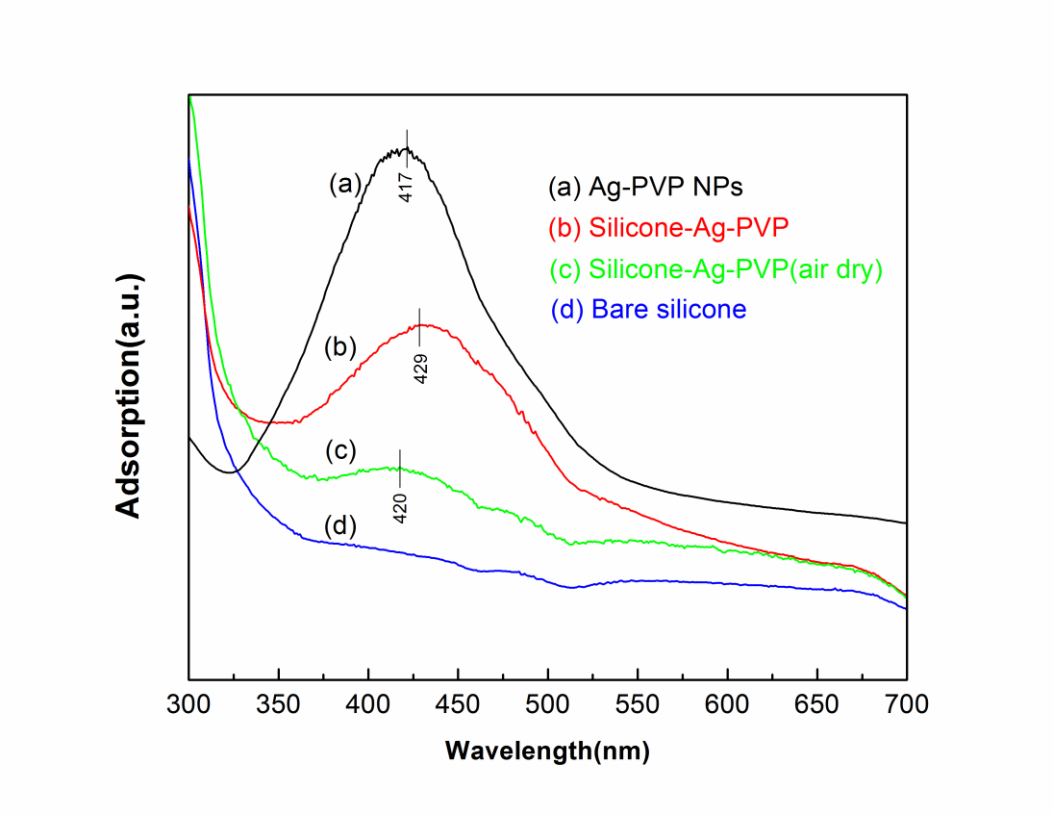

Figure 5.5 UV-Vis spectra of (a) Ag-PVP nanocomposite, (b) Silicone-Ag-PVP (MAPLE), (c) Silicone-Ag-PVP (drop and air dry) and (d) bare silicone.

SPR peak at 429 nm as shown in Figure 5.5(b). Figure 5.5 (d) is the UV-Vis spectrum of bare silicone which does not adsorption peaks between 400 nm and 500 nm. After comparing Figure 5.5 (b) and (d), the presence of Ag-PVP nanocomposite thin film on silicone is confirmed. Figure 5.5 (c) shows spectrum of Ag-PVP nanocomposite coated silicone produced by drop and air dry method, and there is also the SPR band (420 nm). However, the SRP peak of Silicone-Ag-PVP (MAPLE) shifts from 420 to 429nm compared with Silicone-Ag-PVP (Air dry). The red shift of SPR is attributed to the size increasing of Ag-PVP NPs, which is also confirmed by TEM micrographs [19].

5.1.5 AFM image of Ag-PVP nanocomposite film

AFM was used to observe the surface topography and measure the roughness and thickness of the Ag-PVP nanocomposite thin film on the surface of glass coverslip produced by MAPLE process. Before measurement we scratch the edge of the sample first, then use the vertical distance between the surface of the film and the surface of glass coverslip to get the thickness. Figure 5.6 is the AFM 3D images of Ag-PVP nanocomposite film on glass coverslip over different time. The thickness and roughness of this Ag-PVP nanocomposite film at different deposition time are shown in Table 5.1. Table 5.1 shows the Ag-PVP deposition is time dependent. Figure 5.7 presents the fitted linear line of thickness over time. During MAPLE deposition, all the parameters are fixed except deposition time. Therefore, the Ag-PVP nanocomposite deposition rate is 16.686 nm/min, which can be found from the slope of the fitted line in Figure 5.7.

Table 5.1 Thickness and roughness of Ag-PVP film over different deposition time.

Deposition time	Thickness	Roughness
10 min	58.5 nm	21 nm
20 min	178 nm	24.6 nm
30 min	341 nm	35 nm
60 min	877 nm	19 nm

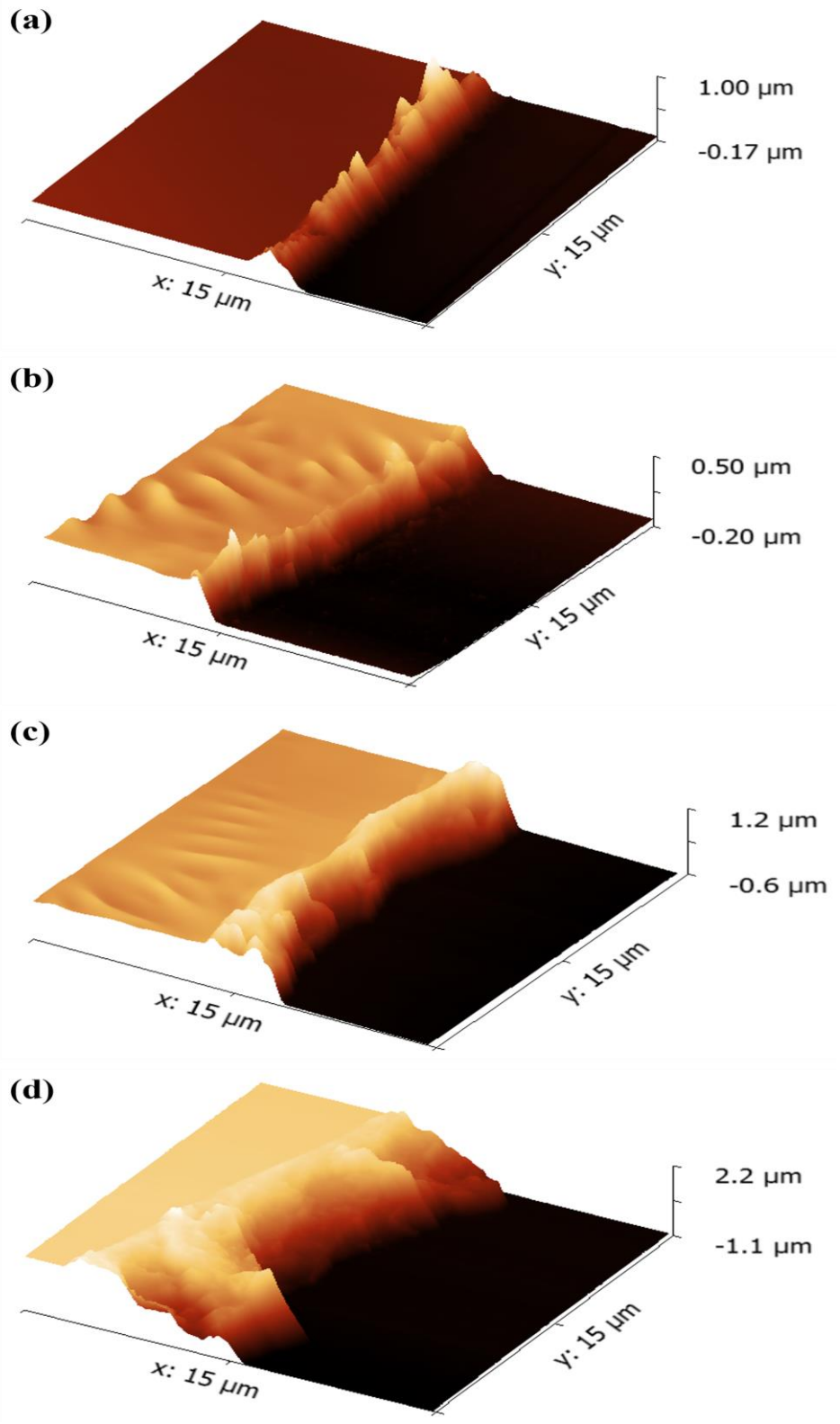

Figure 5.6 3D-AFM images of Ag-PVP film produce by MAPLE deposition in (a) 10 min, (b) 20 min, (c) 30 min, and (d) 60 min.

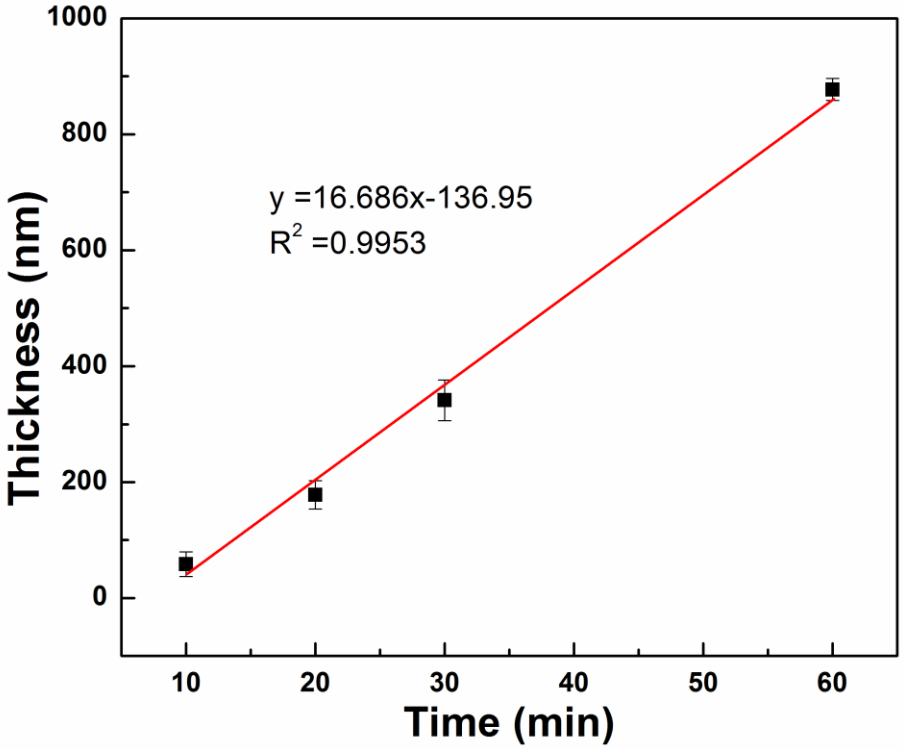

Figure 5.7 The thickness of Ag-PVP nanocomposite films over time.

5.2 Characterization of ZnO-PEG nanocomposite thin film deposited by MAPLE process

Zinc oxide (ZnO) is an inorganic compound extensively used in our daily life, such as piezoelectric transducers, optical waveguides, surface acoustic wave devices, phosphors, transparent conductive oxides, sensors, spin functional devices, UV-light emitters, and antimicrobial reagent [20]. ZnO nanoparticles exhibit strong antimicrobial properties over a wide range of bacteria [21]. However, the antimicrobial mechanism of ZnO nanoparticles is still not fully understood. The photo-catalytic generation of hydrogen peroxide was suggested to be one of the primary mechanisms [22]. ZnO is currently counted as a commonly recognized safe material by the Food and Drug Administration [23]. But the biocompatibility problem occurs when the size of ZnO nanoparticle is very small. Because the ultrafine ZnO particle will prefer to agglomerate in biological system [24]. As a result, Modify the ZnO surface to improve the biocompatibility property by polymer (such as PVP, PVA and PEG) is an efficient way. PEG is a well-known biocompatible polymer used in biomedical device and implant [25]. Moreover, PEG modified ZnO nanoparticles is easier to dissolve in isopropanol, which is used as the target solvent during MAPLE process. At the same time, ZnO-PEG nanocomposite can provide a hydrophilic surface. According to our previous study, hydrophilic surface will reduce the non-specific protein adsorption which is one type of biofouling.

5.2.1 TEM observation of ZnO-PEG nanoparticles

Figure 5.8 (a) is the TEM micrograph of PEG incorporated ZnO nanoparticles (ZnO-PEG NPs) synthesized by the sol-gel method. Figure 5.8 (b) is the TEM micrograph of ZnO-PEG NPs deposited on Cu grid by MAPLE process. The insert small figures of Figure 5.8 (a) and (b) depict the size distribution. The average size of ZnO-PEG NPs before (9.64 nm ±2.65 nm) and after (9.55 nm ± 2.49 nm) MAPLE indicate that MAPLE process do not interfere the formation of ZnO-PEG NPs in terms of particle shape and size. Meanwhile, Figure 5.8 (b) shows the ZnO-PEG on TEM grid was homogenous.

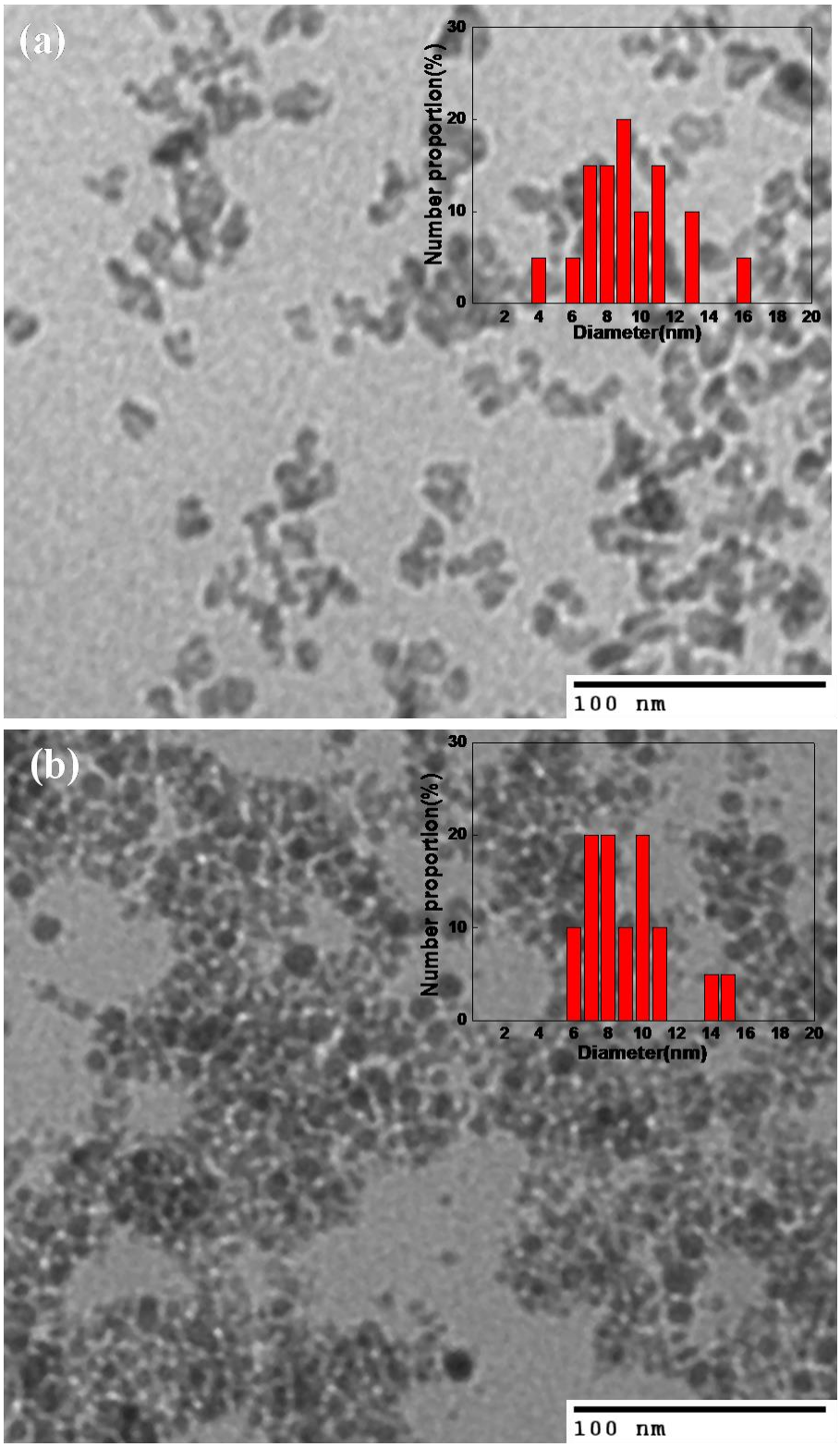

Figure 5.8 TEM micrographs of (a) ZnO-PEG NPs and (b) ZnO-PEG NPs on substrate after MAPLE process.

5.2.2 FTIR analysis

ZnO-PEG coated silicone hydrogel (Silicone-ZnO-PEG) was examined by FTIR in comparison with bare silicone and ZnO-PEG NPs. Figure 5.9 (a) shows the FTIR spectrum of ZnO-PEG NPs, which has the O-H stretching vibration band at 3344 cm^{-1}. Silicone hydrogel only have several significant C=O vibration band but no -OH group shown in Figure 5.9 (b). Figure 5.9 (c) is FTIR spectrum of the ZnO-PEG nanocomposite coated silicone produce by MAPLE. The O-H band at 3358 cm^{-1} in Figure 8 (c) is come from ZnO-PEG nanocomposite after compared with Figure 5.9 (a). Therefore, FTIR spectra confirm that PEG was deposited onto the surface of silicone hydrogel together with ZnO nanoparticle.

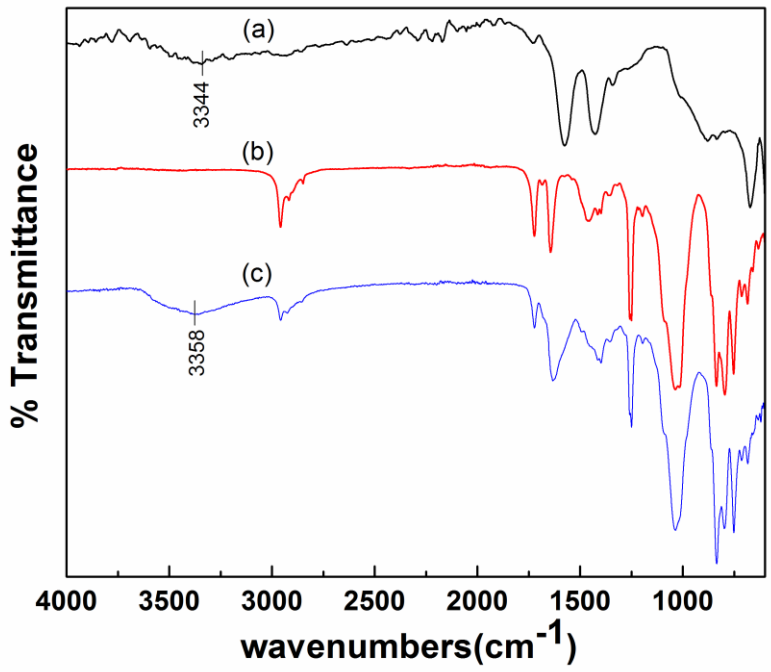

Figure 5.9 FTIR spectra of (a) ZnO-PEG NPs, (b) Silicone hydrogel, and (c) ZnO-PEG coated silicone hydrogel (Silicone-ZnO-PEG).

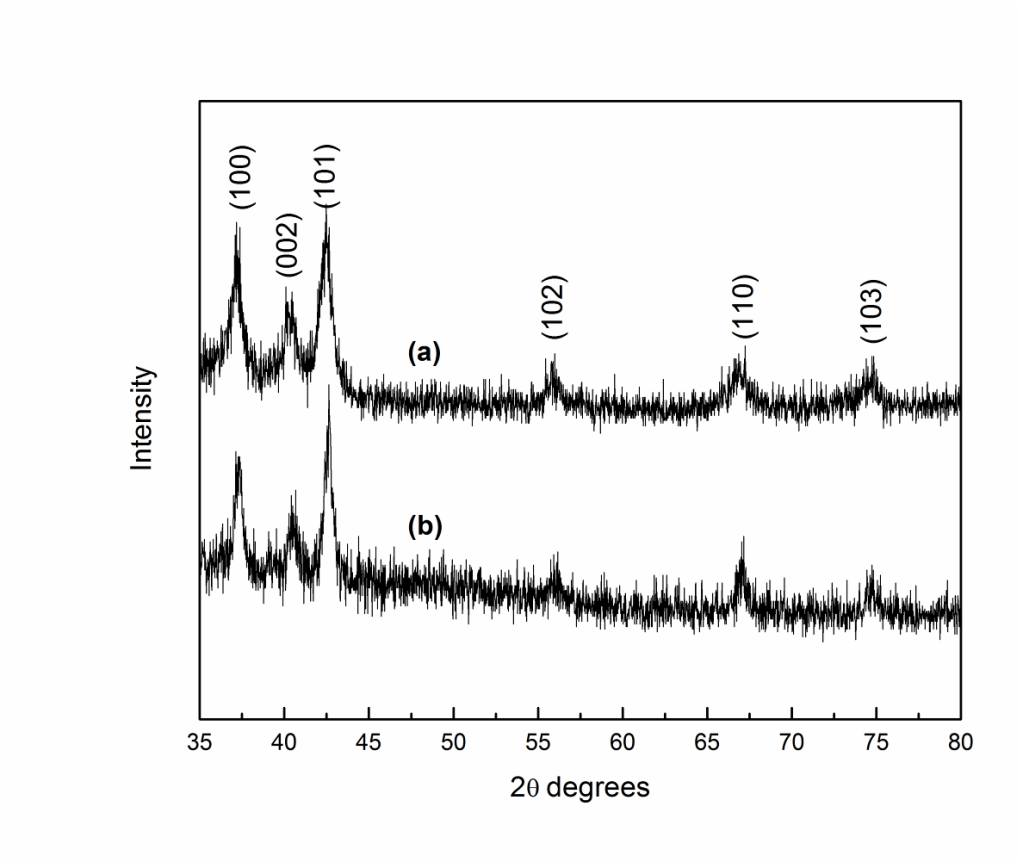

Figure 5.10 XRD patterns of (a) ZnO-PEG nanocomposite and (b) Silicone-ZnO-PEG.

5.2.3 X-ray diffraction

X-ray diffraction (XRD) was applied to measure the ZnO-PEG NPs made by sol-gel method, and Silicone-ZnO-PEG fabricated by MAPLE process. Figure 5.10 (a) shows the XRD profile of ZnO-PEG NPs made by sol-gel method. The typical diffraction peaks of ZnO structure (JCPDS no. 36-1451) indicate the synthesized ZnO-PEG NPs have the wurtzite structure [24]. Figure 5.10 (b) is XRD profile of Silicone-ZnO-PEG (MAPLE). After comparing the peaks of Figure 5.10 (a) and (b), we can conclude that MAPLE deposition do not change the structure of ZnO crystal.

5.2.4 SEM image and EDX spectrum

The surface morphology of silicone and Silicone-ZnO-PEG were examined by SEM. Figure 5.11 (a) is the bare silicone hydrogel surface morphology. Figure 5.11 (b) shows ZnO-PEG nanocomposite coated silicone hydrogel surface. The ZnO-PEG granular film is homogenously deposited on the surface of silicone hydrogel. The element of Zinc was certified by the EDX spectrum from Figure 5.11 (c).

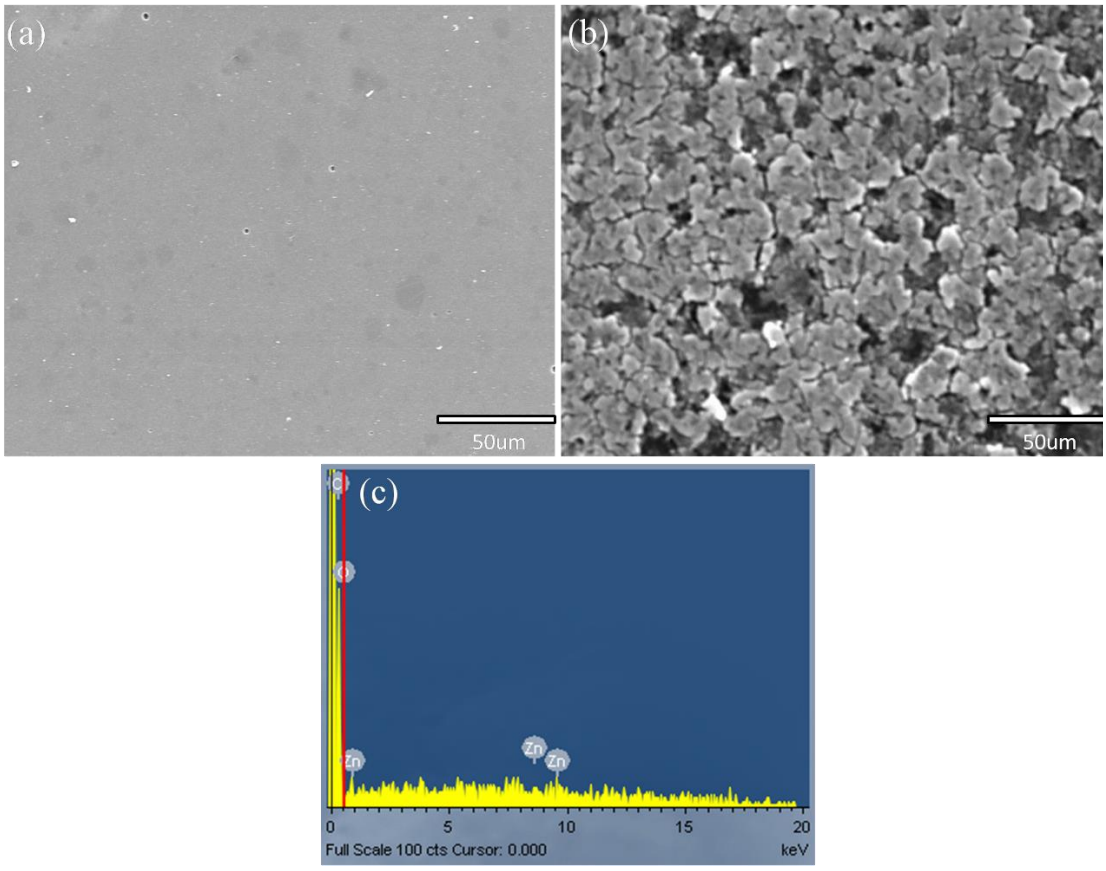

Figure 5.11 SEM images of (a) Silicone hydrogel and (b) ZnO-PEG coated silicone hydrogel; (c) EDX spectrum of Silicone-ZnO-PEG.

5.2.5 Fluorescent spectrum

The photoluminescence (PL) of the ZnO-PEG NPs made by sol-gel method, air dried ZnO-PEG NPs on silicone, Silicone-ZnO-PEG made by MAPLE as well as bare silicone are measured by fluorescence spectrometry under excitation of 320nm (λ_{ex}). Figure 5.12 (a) shows ZnO-PEG NPs made by the sol-gel method. The typical UV emission peaks (378 nm) of ZnO-PEG NPs is corresponding to near band-edge emission of ZnO, which demonstrates the ZnO-PEG is nanostructure [27]. Figure 5.12 (c) shows Silicone-ZnO-PEG also has emission peak at 388 nm however bare silicone (Figure 5.12(d)) has nothing at this wavelength. The comparison between Figure 5.12 (c) and (d) demonstrates that the ZnO-PEG NPs is successfully deposited by MAPLE. However the peak of ZnO-PEG has a slightly shift from 378nm to 388 nm after MAPLE composition.

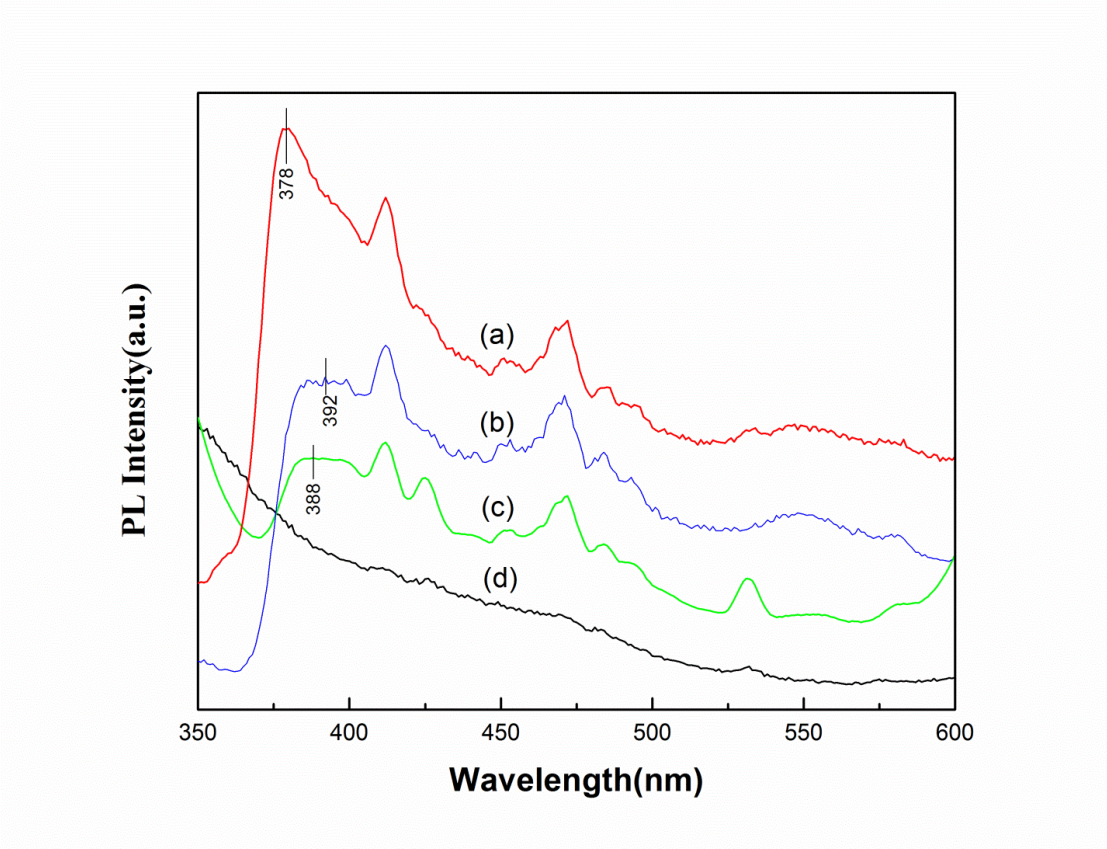

Figure 5.12 Fluorescent spectra of (a) ZnO-PEG NPs,(b) Air dried ZnO-PEG on silicone, (c) Silicone-ZnO-PEG (MAPLE) and (d) Bare silicone hydrogel.

5.3 Application of nanocomposite films deposited by MAPLE process

Silicone is a new contact lens material, which draws lots of researcher's attention due to its high oxygen permeability. This property makes long-term wearing possible. However, silicone has its own drawback, which is not as hydrophilic as conventional contact lens such as PHEMA. Thus, surface modification is carried out. From characterization parts of this chapter, we have confirmed two surface modification nanocomposites successfully deposited onto the silicone surface to promote surface properties. As we know, protein adsorption and bacterial contamination are the main drawbacks for long-term wearing contact lenses. Mechanical strength and cell viability are necessary for implants in the biological test. As a result, this part will focus on comparison between bare and modified silicone hydrogels.

5.3.1 Protein adsorption

Non-specific protein adsorption is a huge barrier for hydrogels used as implants especially for contact lens, such adsorption may reduce the efficacy of the implant and even cause adverse human body response [28]. The protein adsorption is influenced by the surface characteristics of hydrogels and the properties of proteins including molecular weight, protein structure, net charge and conformational stability [28,29]. Additionally, protein adsorption and the following formation of protein films on the surfaces of implants will lead to microbial colonization and consequent biofilm formation [30]. The protein adsorption property of silicone and nanocomposite coated silicone were tested by micro BCA method. Figure 5.13 shows the BSA adsorption of bare silicone, ZnO-PEG nanocomposite coated silicone and Ag-PVP nanocomposite coated silicone are 6.11 $\mu g/cm^2$, 4.28 $\mu g/cm^2$, 4.39 $\mu g/cm^2$ respectively. The protein adsorbed on the nanocomposite coated silicone hydrogels decreased 30% (ZnO-PEG coating) and 28.2% (Ag-PVP coating) separately compared to bare silicone hydrogel. We speculate the result is mainly influenced by the polymer from nanocomposite. After MAPLE deposition, the stabilizers of Ag NPs and ZnO NPs (PVP and PEG individually) have been successfully deposited onto the silicone hydrogel, which are confirmed by FTIR spectra. PEG and PVP have been demonstrated that they have the property to reduce non-specific protein

adsorption [28,31]. Because PVP and PEG provided a more hydrophilic surface which will cause less irreversible protein adsorption compared to bare silicone. Previous reports have demonstrate that BSA is an globular protein and its hydrophobic (non-polar) amino acids are protected inside of the protein molecule and hydrophilic (polar) amino acids side chain will be held outside to interact with their environment [28,29]. When the BSA interacts with hydrophobic surface, the protein core tries to interact with the hydrophobic surface in order to reach lower Gibbs energy, which will denature the protein structure. On the other side, when BSA interacts with hydrophilic surface, it will easily adsorb onto the surface without structure change, so it is not hard to wash the protein off. Therefore, nanocomposite coated silicone hydrogels cause less protein adsorption than bare silicone hydrogel.

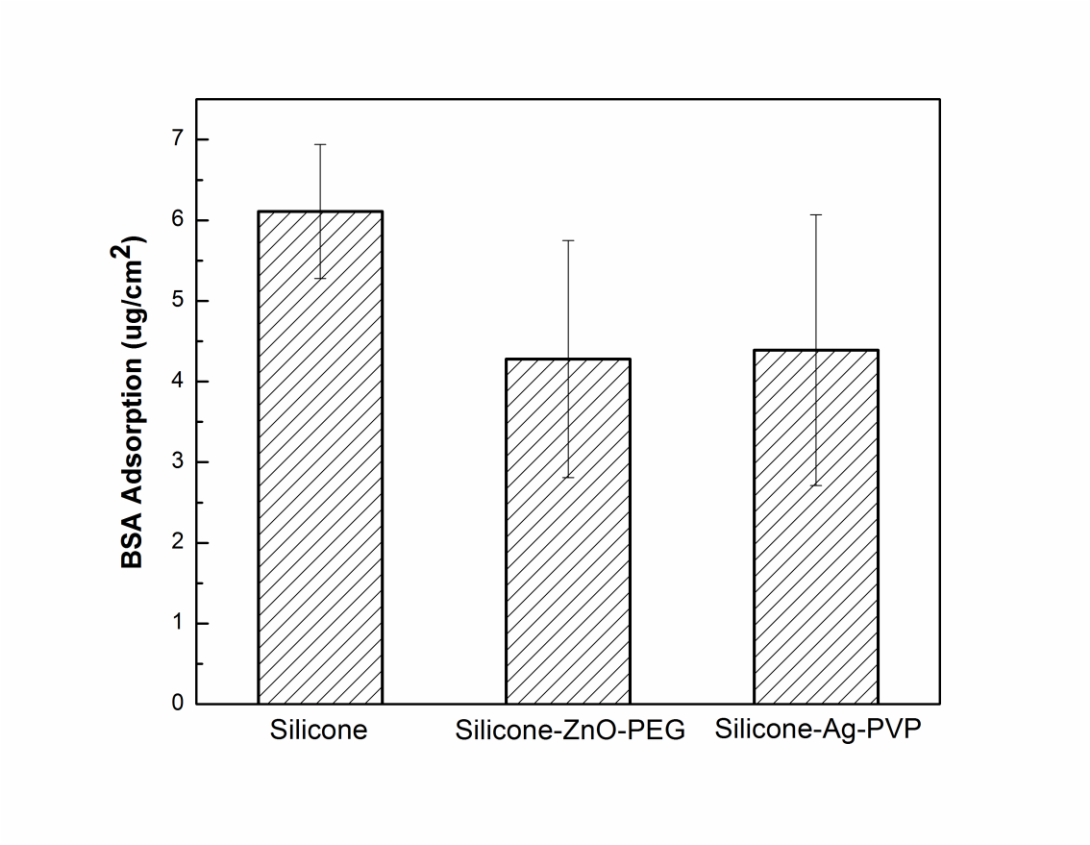

Figure 5.13 BSA Adsorption of bare silicone, ZnO-PEG coated silicone and Ag-PVP coated silicone.

5.3.2 Antibacterial property of hydrogels

Bacterial adhesion onto hydrogel surfaces and the subsequent formation of biofilm are tough problems for many biomedical implant or other biomaterials [32,33]. The formation of biofilm is also the reason of many persistent and chronic bacterial infections happened in biological system [34]. Silicone hydrogel provides a much better oxygen permeability compared to conventional hydrogel but the incorporation of TRIS and other monomers containing siloxane into hydrogel structure lead the decreasing of hydrophilicity, which could theoretically increase bacteria attachment [35]. Herein, Antimicrobial and non-fouling coatings are designed to prevent bacterial contamination of silicone hydrogel. Ag NPs and ZnO NPs that have been proved has the ability to inhibit bacterial growth were deposited onto the silicone surface by MAPLE deposition. The antibacterial effect of Ag-PVP and ZnO-PEG nanocomposite coated Silicone hydrogels against *E. coli* is evaluated by the method of film attachment.

Previous study has showed that releasing silver ions and the interaction between silver and bacterial cell are the typical antibacterial mechanism of Ag NPs [36]. Hence, Coating an ultrathin film on the surface of silicone hydrogel to provide an antibacterial silicone hydrogel is very prospective. Figure 5.14 (a) shows the survived bacteria colonies on agar plates, which obtain from control, bare silicone, and Silicone-Ag-PVP hydrogels on different culture time. Obviously there bacteria survived on silicone-Ag-PVP keep decreasing with time. Figure 5.14(b) presents different relative numbers of bacteria survived on bare silicone hydrogel and Silicone-Ag-PVP by MAPLE deposition in different culture time. As shown in Figure 5.14 (b), the relative survived number of *E.coli* on the bare silicone stays around 85% when the culture time increases, which means bare silicone hydrogel do not have the ability to inhibit bacteria growth. While the relative number of *E.coli* on Silicone-Ag-PVP keep decreasing as the incubation time increasing from 1 hour to 12 hours. After 8 hours, the Ag-PVP nanocomposite on silicone hydrogel eliminate almost all the bacteria (relative number declines to 0.2%). Consequently, it is a prospective way to coat a thin film of Ag-PVP nanocomposite by MAPLE process to prevent bacterial contamination for contact lens material.

Zinc-based materials have shown an excellent resistance against corrosion and performed good antibacterial activity [37]. From Figure 5.15 (a) and (b), we can conclude that the silicone coated with ZnO-PEG nanocomposite killed almost all the *E.coli* on its surface. However the bare silicone do not show any potential to inhibit bacterial growth. Figure 5.15 (c) presents the relative numbers of survived bacteria on silicone hydrogels before and after the deposition of ZnO-PEG nanocomposite through MAPLE deposition. As shown in Figure 5.15 (c), the relative survived number of *E.coli* on the bare silicone is increasing from 1.13 to 1.67 when the culture time increases from 1 hour to 12 hours. This means bare silicone hydrogel allows the growth of bacteria. This is one of the reasons why commercial silicone contact lens is not suitable for long-term wearing. While the relative number of *E.coli* on Silicone-ZnO-PEG keeps decreasing when the culture time increases from 1 hour to 12 hours. After 4 hours, the relative numbers of *E.coli* on the nanocomposite coated silicone hydrogel declines to 0.07 which is much lower than bare silicone hydrogel (1.12). The result indicates the ZnO-PEG coated silicone hydrogel could eliminate the growth of *E.coli* beyond 4 hours of culture time. Consequently, the MAPLE deposited ZnO-PEG coating has a strong antibacterial effect and may provide an efficient way to inhibit bacteria growth for contact lens material.

The nanocomposite coatings on silicone hydrogels produced by MAPLE process show the significant antibacterial property. Both Ag-PVP and ZnO-PEG nanocomposite films can eliminate almost all the *E.coli* on the surface of the samples. Consequently, the nanocomposite coated silicone is expected for long-term wearing contact lens or other implant biological materials due to its antimicrobial property.

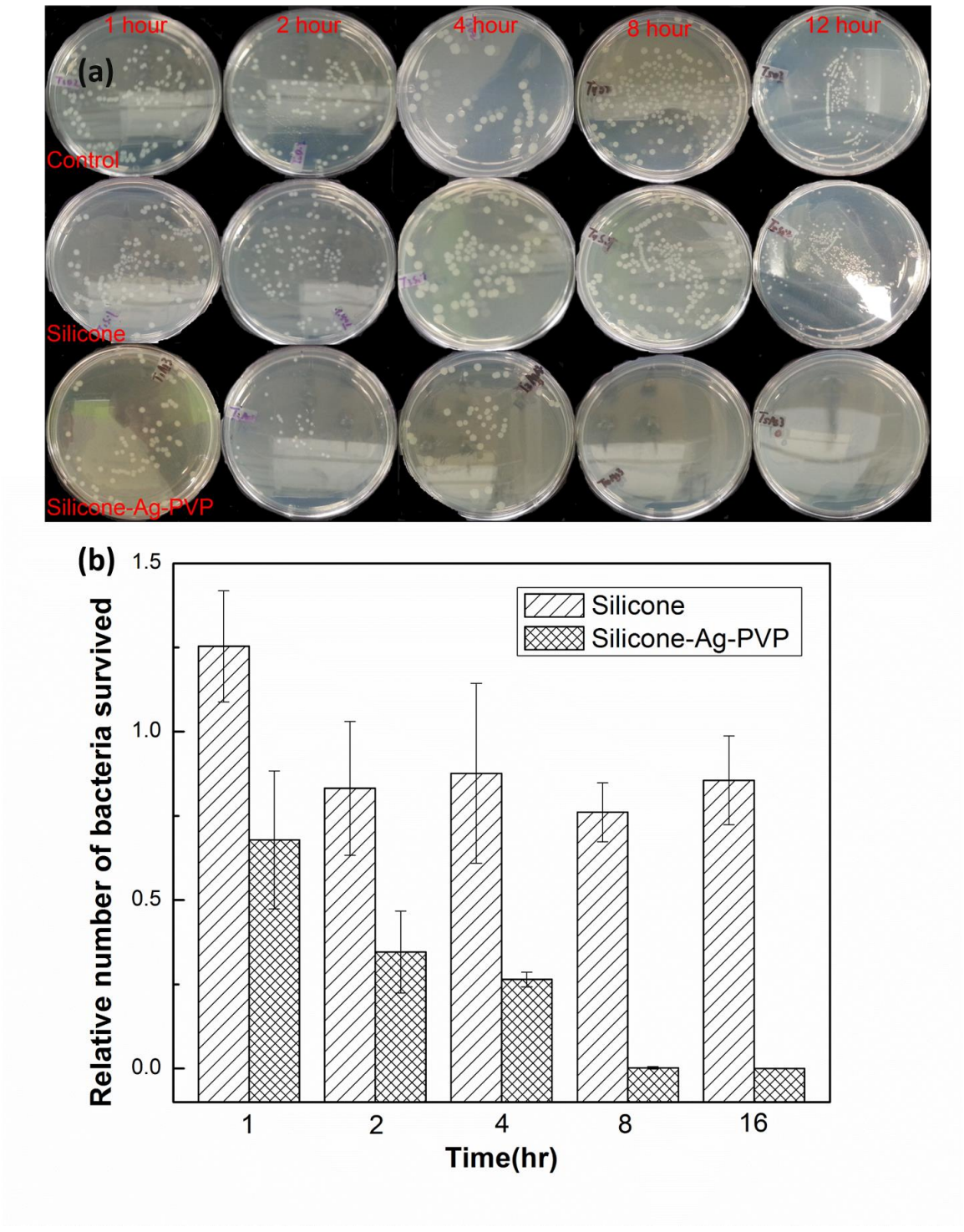

Figure 5.14 Plate counting of E.coli from Silicone hydrogel and Silicone-Ag-PVP hydrogel; (b) Antibacterial test of silicone hydrogel and Silicone-Ag-PVP.

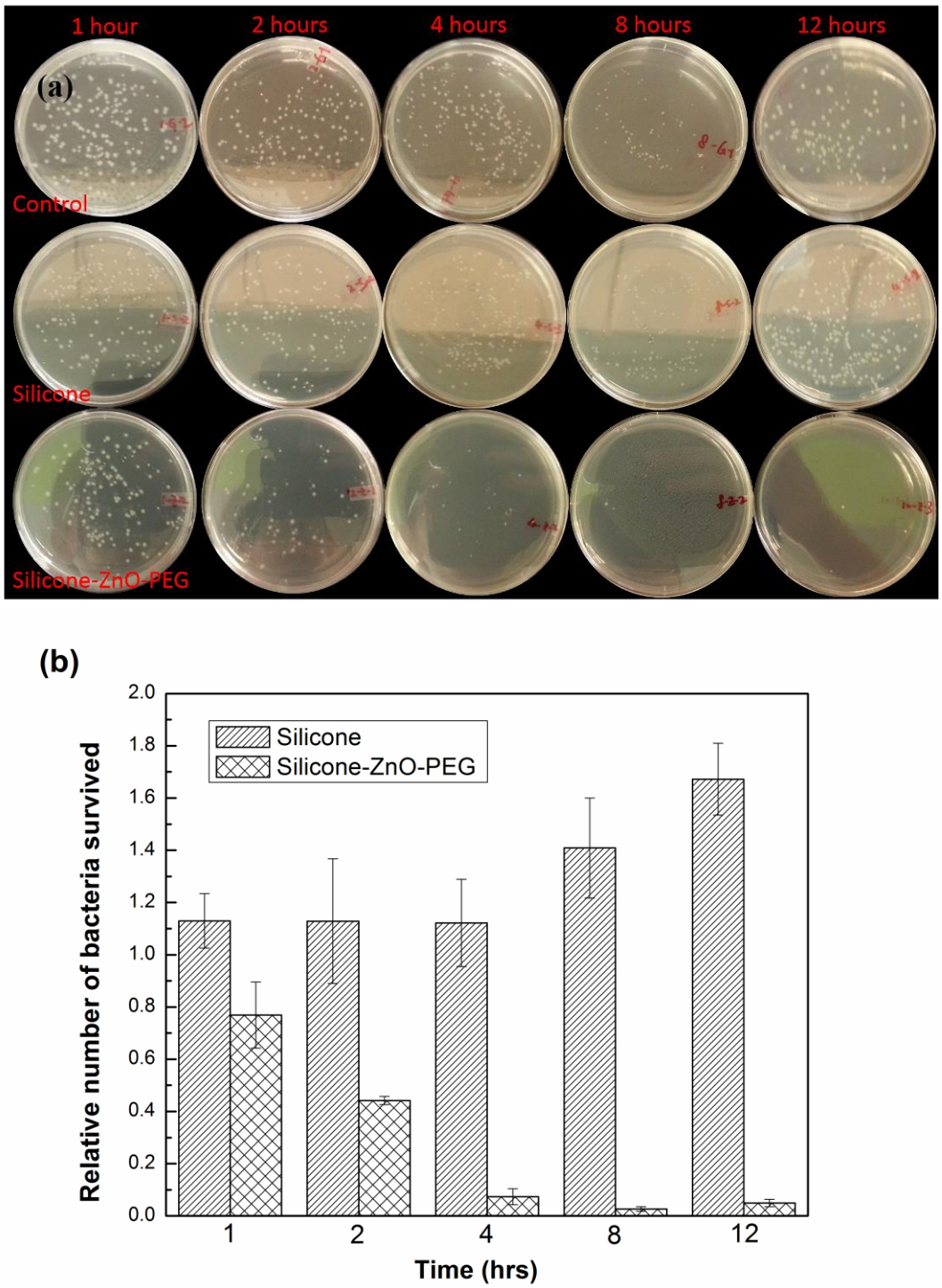

Figure 5.15 (a) Plate counting of E.coli from Silicone hydrogel and Silicone-ZnO-PEG; (b) Antibacterial test of silicone and Silicone-ZnO-PEG.

5.3.3 Mechanical property test

Young's modulus indicates the stiffness of measured material. As we know, silicone hydrogel has been used as contact lens material due to its high oxygen permeability and also it has the potential to replace the soft lens materials in the future. Proper mechanical strength is an important requirement for biomaterials, so it is necessary to measure the mechanical property of silicone hydrogel. Different body implants require different mechanical strength. Most of the hydrogels are elastic materials, their stiffness are measured by tensile modulus, also known as Young's modulus. The tensile modulus of silicone hydrogel and nanocomposite coated were measured through the uniaxial tensile test [28]. Table 5.2 shows that the Young's modulus of silicone hydrogel increased from 0.7083 MPa to 0.8109 MPa and 0.8145 separately after coating Ag-PVP and ZnO-PEG nanocomposites by MAPLE deposition. According to previous research, the young's modulus of human skin range is between 0.42 MPa and 0.85 MPa depending on different ages [38]. Young's modulus of silicone hydrogel and nanocomposite coated silicone hydrogels are similar with human skin, which is an important factor need to take into consideration before it is applied as body implants and contact lenses.

Table 5.2 Young Modulus (E) of bare silicone, Ag-PVP coated silicone and ZnO-PEG coated silicone.

	Bare silicone	Silicone-Ag-PVP	Silicone-ZnO-PEG
E (MPa)	0.7083 ± 0.1640	0.8109 ± 0.1249	0.8145 ± 0.1244

5.4 Cell viability of hydrogels

Good biocompatibility of the silicone and nanocomposite coated hydrogel is critical to be able to be used as contact lens materials and/or other body implants. NIH/3T3 mouse fibroblast cells were used for cell viability test. Samples were soaked into culture medium and incubated with cells for 24 h. Figure 5.16 indicates that the cell viability of silicone, Silicone-Ag-PVP and Silicone-ZnO-PEG are 146.5%, 81.1% and 103.1% separately. Bare silicone has the highest which is confirmed that silicone hydrogel is a biocompatible material. Meanwhile all the samples' cell viability reaches higher than 80%, which

confirm that Ag-PVP and ZnO-PEG coated silicone do not impose toxic effect to the cells.

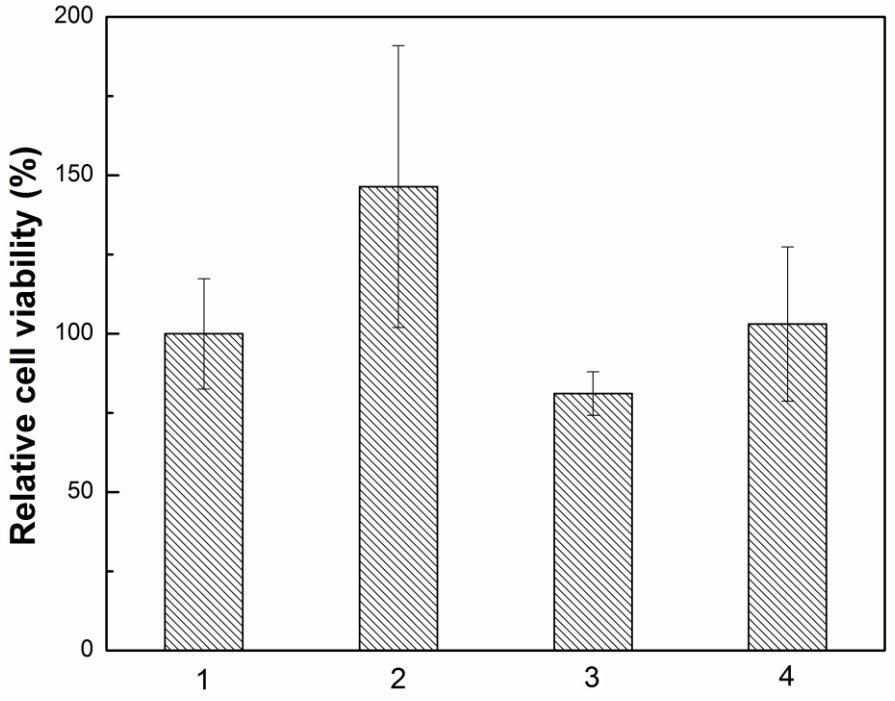

Figure 5.16 Cell viability of 1 control, 2 Silicone, 3 Silicone-Ag-PVP and 4 Silicone-ZnO-PEG.

5.5 Conclusions

MAPLE technique is suitable for silicone hydrogel surface modification with Ag-PVPNPs and ZnO-PEG NPs. The Ag-PVP nanocomposite film is confirmed by FTIR, UV-Vis, EDX and AFM. The TEM micrographs show size increasing (from 11.29 nm to 11.61 nm) and the broadened size distribution of Ag-PVP NPs on silicone produced by MAPLE. The red shift of SPR peak from UV-Vis also indicates the size increasing and the shape of Ag-PVP NPs. The AFM images show the homogeneous Ag-PVP nanocomposite film as well as thickness and roughness on different deposition time. Meanwhile, the thickness of Ag-PVP film is linearly increased over time, and the deposition rate is 16.686 nm/min. ZnO-PEG nanocomposites have been successfully coated on silicone hydrogel by MAPLE process. The ZnO nanoparticles (average diameter = 9.5 ± 2.5 nm) maintain their shape and crystal structures after MAPLE deposition. A slight change in terms of size and size distribution of the ZnO nanoparticles is observed comparing them before and after the MAPLE deposition. In addition, the PEG-ZnO nanocomposites coated on silicone hydrogel have been investigated by FTIR, EDX, XRD, PL spectra, and SEM. The ZnO-PEG nanocomposite is homogenously deposited on the surface of silicone. MAPLE process does not influence the polymer (PEG) structure. In addition, the nanocomposites coated silicone show significant protein resistance property, which can reduce about 28.2 % (Ag-PVP coating) and 30 % (ZnO-PEG coating) BSA adsorption compared to bare silicone. Antimicrobial test assay further demonstrates that Ag-PVP and ZnO-PEG nanocomposites coated silicone have the ability to inhibit bacteria growth. After 4 hours incubation, ZnO-PEG coating can eliminate most of the bacteria on Silicone-ZnO-PEG surface (only 7% left), but *E.coli* keeps growing on bare silicone. Ag-PVP coating can kill all the bacterial on the hydrogel surface after 8 hours incubation. Moreover, both Ag-PVP and ZnO-PEG coatings can increase Young's modulus from 0.7083 MPa to 0.8109 MPa (Ag-PVP) and 0.8145 MPa (ZnO-PEG) individually The nanocomposites coated silicone hydrogels and bare silicone are biocompatible material according to the cell viability result. Therefore, it is expected this silicone nanocomposites (Silicone-Ag-PVP & Silicone-ZnO-PEG) produced by MAPLE process could be used as a potential long-term wearing contact lenses or other biological implants material due to their protein resistance and antimicrobial properties.

5.6 Reference

[1] Ajayan PM, Schadler LS, Braun P V. Nanocomposite Science and Technology (Google eBook). John Wiley & Sons; 2006.

[2] Pozuelo J, Compan V, Gonzalez-Meijome JM, Gonzalez M, Molla S. Oxygen and ionic transport in hydrogel and silicone-hydrogel contact lens materials: An experimental and theoretical study. J Memb Sci 2014;452:62–72.

[3] Yesilirmak N, Altınors DD. A silicone hydrogel contact lens after 7 years of continuous wear. Cont Lens Anterior Eye 2013;36:204–6.

[4] Mihaiescu DE, Cristescu R, Dorcioman G, Popescu CE, Nita C, Socol G, et al. Functionalized magnetite silica thin films fabricated by MAPLE with antibiofilm properties. Biofabrication 2013;5:015007.

[5] Hunter CN, Check MH, Muratore C, Voevodin a. a. Electrostatic quadrupole plasma mass spectrometer measurements during thin film depositions using simultaneous matrix assisted pulsed laser evaporation and magnetron sputtering. J Vac Sci Technol A Vacuum, Surfaces, Film 2010;28:419.

[6] Caricato a. P, Capone S, Epifani M, Lomascolo M, Luches A, Martino M, et al. Nanoparticle thin films deposited by MAPLE for sensor applications 2008;6985:69850H–69850H–13.

[7] Caricato a. P, Luches a., Leggieri G, Martino M, Rella R. Matrix-assisted pulsed laser deposition of polymer and nanoparticle films. Vacuum 2012;86:661–6.

[8] Mayo DC, Paul O, Airuoyo IJ, Pan Z, Schriver KE, Avanesyan SM, et al. Resonant infrared matrix-assisted pulsed laser evaporation of TiO2 nanoparticle films. Appl Phys A 2012;110:923–8.

[9] Ahmad M Bin, Tay MY, Shameli K, Hussein MZ, Lim JJ. Green Synthesis and Characterization of Silver/Chitosan/Polyethylene Glycol Nanocomposites without any Reducing Agent. Int J Mol Sci 2011;12:4872–84.

[10] Yu H, Xu X, Chen X, Lu T, Zhang P, Jing X. Preparation and antibacterial effects of PVA-PVP hydrogels containing silver nanoparticles. J Appl Polym Sci 2007;103:125–33.

[11] Lin J-J, Lin W-C, Li S-D, Lin C-Y, Hsu S-H. Correction to evaluation of the antibacterial activity and biocompatibility for silver nanoparticles immobilized on nano silicate platelets. ACS Appl Mater Interfaces 2013;5:2782.

[12] Hitchman A, Smith GHS, Ju-Nam Y, Sterling M, Lead JR. The effect of environmentally relevant conditions on PVP stabilised gold nanoparticles. Chemosphere 2013;90:410–6.

[13] Kurita H, Takami A, Koda S. Size reduction of gold particles in aqueous solution by pulsed laser irradiation. Appl Phys Lett 1998;72:789.

[14] Takami A, Kurita H, Koda S. Laser-Induced Size Reduction of Noble Metal Particles. J Phys Chem B 1999;103:1226–32.

[15] Mafune F, Kohno J, Takeda Y, Kondow T. Formation and Size Control of Silver Nanoparticles by Laser Ablation in Aqueous Solution. J Phys Chem B 2000;104:9111–7.

[16] Wang H, Qiao X, Chen J, Wang X, Ding S. Mechanisms of PVP in the preparation of silver nanoparticles. Mater Chem Phys 2005;94:449–53.

[17] Soltani N, Saion E, Hussein MZ, Erfani M, Rezaee K, Bahmanrokh G. Phase Controlled Monodispersed CdS Nanocrystals Synthesized in Polymer Solution Using Microwave Irradiation. J Inorg Organomet Polym Mater 2011;22:830–6.

[18] Bryaskova R, Pencheva D, Nikolov S, Kantardjiev T. Synthesis and comparative study on the antimicrobial activity of hybrid materials based on silver nanoparticles (AgNps) stabilized by polyvinylpyrrolidone (PVP). J Chem Biol 2011;4:185–91.

[19] Kelly KL, Coronado E, Zhao LL, Schatz GC. The Optical Properties of Metal Nanoparticles: The Influence of Size, Shape, and Dielectric Environment. JPhysChem 2003;107:668–77.

[20] Djurisić AB, Leung YH. Optical properties of ZnO nanostructures. Small 2006;2:944–61.

[21] Li Q, Mahendra S, Lyon DY, Brunet L, Liga M V, Li D, et al. Antimicrobial nanomaterials for water disinfection and microbial control: potential applications and implications. Water Res 2008;42:4591–602.

[22] Sawai J. Quantitative evaluation of antibacterial activities of metallic oxide powders (ZnO, MgO and CaO) by conductimetric assay. J Microbiol Methods 2003;54:177–82.

[23] Espitia PJP, Soares N de FF, Coimbra JS dos R, Andrade NJ, Cruz RS, Medeiros EAA. Zinc Oxide Nanoparticles: Synthesis, Antimicrobial Activity and Food Packaging Applications. Food Bioprocess Technol 2012;5:1447–64.

[24] Sudha M, Senthilkumar S, Hariharan R, Suganthi a., Rajarajan M. Synthesis, characterization and study of photocatalytic activity of surface modified ZnO nanoparticles by PEG capping. J Sol-Gel Sci Technol 2012;65:301–10.

[25] Jiang G, Sun J, Ding F. PEG-g-chitosan thermosensitive hydrogel for implant drug delivery: cytotoxicity, in vivo degradation and drug release. J Biomater Sci Polym Ed 2014;25:241–56.

[26] Mu A and. Nanowires Science and Technology. InTech; 2010.

[27] Yu ZB, Xie YP, Liu G, Lu GQ (Max), Ma XL, Cheng H-M. Self-assembled CdS/Au/ZnO heterostructure induced by surface polar charges for efficient photocatalytic hydrogen evolution. J Mater Chem A 2013;1:2773.

[28] Yin P, Engineering B, Studies P. Hydrogel-based Nanocomposites and Laser-assisted Surface Modification for Biomedical Application Hydrogel-based

Nanocomposites and Laser-assisted Surface Modification for Biomedical Application 2012.

[29] Luensmann D, Jones L. Protein deposition on contact lenses: the past, the present, and the future. Cont Lens Anterior Eye 2012;35:53–64.

[30] Banerjee I, Pangule RC, Kane RS. Antifouling coatings: recent developments in the design of surfaces that prevent fouling by proteins, bacteria, and marine organisms. Adv Mater 2011;23:690–718.

[31] Jiang J, Zhu L, Zhu L, Zhang H, Zhu B, Xu Y. Antifouling and antimicrobial polymer membranes based on bioinspired polydopamine and strong hydrogen-bonded poly(N-vinyl pyrrolidone). ACS Appl Mater Interfaces 2013;5:12895–904.

[32] Hall-Stoodley L, Costerton JW, Stoodley P. Bacterial biofilms: from the natural environment to infectious diseases. Nat Rev Microbiol 2004;2:95–108.

[33] Donlan RM, Costerton JW. Biofilms : Survival Mechanisms of Clinically Relevant Microorganisms Biofilms : Survival Mechanisms of Clinically Relevant Microorganisms 2002;15.

[34] Costerton JW. Bacterial Biofilms: A Common Cause of Persistent Infections. Science (80-) 1999;284:1318–22.

[35] Kodjikian L, Casoli-bergeron E, Malet F, Janin-manificat H, Freney J, Burillon C, et al. Bacterial adhesion to conventional hydrogel and new silicone-hydrogel contact lens materials. Graefes Arch Clin Exp Ophthalmol 2008:267–73.

[36] Eckhardt S, Brunetto PS, Gagnon J, Priebe M, Giese B, Fromm KM. Nanobio silver: its interactions with peptides and bacteria, and its uses in medicine. Chem Rev 2013;113:4708–54.

[37] Siyanbola TO, Sasidhar K, Anjaneyulu B, Kumar KP, Rao BVSK, Narayan R, et al. Anti-microbial and anti-corrosive poly (ester amide urethane) siloxane modified

ZnO hybrid coatings from Thevetia peruviana seed oil. J Mater Sci 2013;48:8215–27.

[38] Agache PG. Original Contributions. Arch Dermatol Res 1980;269:221–32.

Chapter 6

6 Summary and future work

6.1 Summary

Compared to conventional hydrogels such as PMMA and PHEMA-based hydrogels, silicone hydrogels show higher oxygen permeability due to the different gas transport mechanism, which significantly extend the wearing period of contact lens, and improve the comfortability level to people who wear the contact lenses. However, the surface of silicone hydrogels is less hydrophilic due to the siloxane group in the structure of silicone. Irreversible protein adsorption and biofilm formation are two major issues hinder the further clinical applications of silicone hydrogels. One of the most efficient solutions is to create a hydrophilic surface of silicone hydrogels.

In this study, MAPLE technique was used to modify the silicone surface to reduce the protein adsorption and inhibit the growth of bacteria. PEG and PVP are the hydrophilic and biocompatible polymers to modify the silicone surface by MAPLE system. FTIR and AFM were used to characterize the polymer films. The roughness of PEG and PVP films is around 10-15 nm, which confirms the MAPLE deposited polymer films are homogeneous. In addition, micro BCA method was applied to measure the protein adsorption, and the results indicate the protein adsorption decreases to 71.8% (PEG coating), and 81.3% (PVP coating), respectively. The Young's modulus of polymer coated silicone hydrogels are increased from 0.7083 MPa to 0.7668 MPa (PEG coating) and 0.7236 MPa (PVP coating) separately. In addition, the relative cell viabilities of different samples were carried out by using T3T cell line. No toxic effect is observed in the cultured cell line treated by polymer coated silicone hydrogels.

PEG and PVP are not only suitable hydrophilic surface modification polymers but also commonly used stabilizers for nanoparticles, nanorods or other types of nanomaterials. Ag NPs and ZnO NPs have shown anti-microbial properties. Consequently, Ag NPs stabilized by PVP (Ag-PVP NPs) were synthesized through a photochemical method. The ZnO NPs stabilized by PEG (ZnO-PEG NPs) were produced from zinc acetate.

Furthermore, the two types of nanoparticles, Ag-PVP NPs and ZnO-PEG NPs, were deposited on silicone hydrogels by MAPLE process to minimize the microbial contamination of silicone hydrogel. The presence of PVP from Ag-PVP nanocomposite film produced by MAPLE process is confirmed by FTIR spectra. Ag NPs on silicone are confirmed by EDX and UV-Vis spectra. The size of Ag-PVP NPs changes from 11.29 nm ± 1.88 nm to 11.61 nm ± 3.58 nm due to the SPR property of Ag NPs. The surface morphology of Ag-PVP nanocomposite film is observed by AFM, which indicates that the thickness over time is linear (deposition rate of 16.686 nm/min), and the nanocomposite film is homogenous (the roughness is around 20-35 nm).The presence of ZnO-PEG nanocomposite on silicone hydrogel is confirmed by FTIR, EDX, XRD, PL spectra, and SEM. According to results of TEM micrographs, XRD profiles and PL spectra, MAPLE process does not influence the size, shape, crystal structure and PL property of ZnO-PEG NPs. The size of ZnO-PEG is approximately 9.5 ± 2.5 nm. The SEM images indicate that the ZnO-PEG nanocomposite is homogenously deposited on the surface of silicone. In addition, the Ag-PVP and ZnO-PEG nanocomposite coated silicone hydrogels show significant protein resistance property, which can reduce about 28.2 % and 30 % BSA adsorption compared to bare silicone. Antimicrobial test assay further demonstrates that Ag-PVP and ZnO-PEG nanocomposite coated silicone have the ability to inhibit bacteria growth. After 4 hours' incubation, ZnO-PEG coating can eliminate most of the bacteria on Silicone-ZnO-PEG surface (only 7% left), while *E.coli* keeps growing on bare silicone when culturing time increases as the same time period. Ag-PVP coating can kill all the bacteria on the hydrogel surface after 8 hours incubation. Moreover, both Ag-PVP and ZnO-PEG coatings can increase Young's modulus from 0.7083 MPa to 0.8109 MPa (Ag-PVP) and 0.8145 MPa (ZnO-PEG) individually. The nanocomposite coated silicone hydrogels and bare silicone are biocompatible materials according to the cell viability results.

This study indicate the MAPLE technique is a suitable surface coating system that can produce homogeneous polymer and nanocomposite films without significantly damaging the polymers. It is expected that these polymer and nanocomposite coated silicone hydrogels fabricated by MAPLE process could be used as potential long-term wearing

contact lenses or other biological implants materials due to their protein resistant and antimicrobial property.

6.2 Future work

Further research works to efficiently apply MAPLE process in surface modification are discussed as follows.

- We have used the photochemical method to synthesize Ag-PVP NPs and then deposited the nanoparticles by MAPLE system, which is a two steps method. It may be possible to use laser as a resource to synthesize and deposit Ag-PVP NPs at the same time. The effects of MAPLE process on nanomaterials in terms of size and size distribution will be studied.

- There is a limit for our MAPLE technique, which is only able to deposit one type of target material at one time, so my future work will try to design a new target, which can deposit several materials at one time without opening the chamber. This modification will save energy and time.

- Our MAPLE system is recently installed an OPO which is able to allow us to change the wavelength to the NIR and/or IR range. Further studies will be needed to find out the effects of wavelength on different polymer and nanocomposite depositions.

Curriculum Vitae

Name:	Guobang Huang
Post-secondary Education and Degrees:	Zhejiang Sci-Tech University Hangzhou, Zhejiang, China 2008-2012 B.Eng. The University of Western Ontario London, Ontario, Canada 2012-2014 M.E.Sc.
Related Work Experience	Teaching Assistant The University of Western Ontario 2013-2014

Publications:

G. Huang, Y. Chen and J. Zhang, Nanocomposite Coating produced by Laser-assisted Process to Prevent Bacterial Contamination and Protein Fouling, Submitted.

G. Huang, Q. Guo and J. Zhang, Ag-PVP Nanocomposite Coating produced by Laser-assisted Process to Prevent Bacterial Contamination and Protein Fouling, in preparing.

L. Chen, A. Siemiarczuk, H. Hai, Y. Chen, G. Huang, and J. Zhang, Development of Biocompatible and Proton-Resistant Quantum Dots Assembled on Gelatin Nanospheres, Langmuir 2014, 30(7), 1893–9.

Y. Pei, G. Huang, W, Tse, and J. Zhang, Laser-assisted modification of silicone nanocomposites to inhibit protein adsorption, in preparing.